



LUND UNIVERSITY

Dynamics of the glomerular filtration barrier - Physiological and pathophysiological aspects

Axelsson, Josefin

2011

[Link to publication](#)

Citation for published version (APA):

Axelsson, J. (2011). *Dynamics of the glomerular filtration barrier - Physiological and pathophysiological aspects*. [Doctoral Thesis (compilation), Nephrology]. Department of Nephrology, Lund University.

Total number of authors:

1

General rights

Unless other specific re-use rights are stated the following general rights apply:

Copyright and moral rights for the publications made accessible in the public portal are retained by the authors and/or other copyright owners and it is a condition of accessing publications that users recognise and abide by the legal requirements associated with these rights.

- Users may download and print one copy of any publication from the public portal for the purpose of private study or research.
- You may not further distribute the material or use it for any profit-making activity or commercial gain
- You may freely distribute the URL identifying the publication in the public portal

Read more about Creative commons licenses: <https://creativecommons.org/licenses/>

Take down policy

If you believe that this document breaches copyright please contact us providing details, and we will remove access to the work immediately and investigate your claim.

LUND UNIVERSITY

PO Box 117
221 00 Lund
+46 46-222 00 00

Dynamics of the glomerular filtration barrier

Physiological and pathophysiological aspects

Josefin Axelsson
Clinical Sciences, Lund
Department of Nephrology



LUND UNIVERSITY
Faculty of Medicine

Lund 2011

AKADEMISK AVHANDLING

som med vederbörligt tillstånd av Medicinska Fakulteten vid Lunds Universitet
för avläggande av doktorsexamen i medicinsk vetenskap kommer att
offentligen försvaras i Segerfalksalen, BMC Hus A, Lund
fredagen den 17 juni 2011, kl 9.00

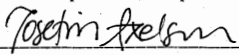
FAKULTETSOPPONENT

Professor A. Erik G. Persson, Uppsala University,
Uppsala, Sweden

Organization LUND UNIVERSITY Clinical Sciences, Lund Department of Nephrology Author(s) Josefín Axelsson	Document name DOCTORAL DISSERTATION	
	Date of issue 2011-06-17	
	Sponsoring organization Lund University	
Title and subtitle Dynamics of the glomerular filtration barrier - Physiological and pathophysiological aspects		
Abstract <p>The dynamic properties of the glomerular filtration barrier (GFB) are of fundamental importance for the understanding of the physiology and pathophysiology of microalbuminuria and proteinuric diseases. In the studies of this doctoral thesis the properties of the rat glomerular filtration barrier were investigated under resting conditions and following a number of challenges using highly sensitive gel filtration chromatography (HPSEC) detection of FITC-Ficoll in serum and urine. This permeability model is extremely sensitive, and by using HPSEC, it was possible to measure extremely low concentrations of Ficoll molecules in the urine. Under resting conditions the sieving coefficient (θ; filtrate-to-plasma concentration ratio) for Ficoll 70Å was approximately 0.00001, and θ for albumin was found to be low, 0.0003 (or less). During increases in glomerular permeability θ for albumin and θ for Ficoll 50-80Å increased in parallel, conceivably reflecting an increase in the number of large pores in the GFB. In study I, lipopolysaccharide (LPS) induced sepsis produced increases in θ for albumin and θ for Ficoll 50-80Å, at 120 min after LPS injection. In anaphylaxis there was a rapid permeability response already after 5 min which was reversed within 40 min. In study II, laparotomy, with or without muscle crush trauma, induced an increase in glomerular permeability after 5 min, which was to a large extent sustained after 60 min. Hyperglycemia (study III) induced an increase in θ for Ficoll 50-80Å after 20 min, but not at 5 min, and after 60 min glomerular permeability was back to normal. The permeability increase seen after hyperglycemia at 20 min was totally abolished by a Rho-kinase inhibitor, indicating that the cytoskeleton of endothelial cells and/or podocytes may be involved. In study IV, high or low doses of ANP induced an increase in glomerular permeability for Ficoll 50-80Å, reaching its maximum at 5 and 15 min. During ANP infusion (cf. congestive heart failure) there was a bimodal response, with a dip after 30 min, after which θ for Ficoll 50-80Å again tended to increase. In this thesis the novel concept of a rapidly dynamic glomerular filtration barrier is introduced. During different challenges the size-selectivity of the GFB, rather than its charge-selectivity, was found to be subject to rapid and reversible alterations.</p>		
Key words: Glomerular filtration barrier, Glomerular permeability, Microalbuminuria, Albumin, Ficoll, Sieving Coefficient (θ), Rats		
Classification system and/or index terms (if any):		
Supplementary bibliographical information:	Language English	
ISSN and key title: 1652-8220	ISBN 978-91-86871-08-6	
Recipient's notes	Number of pages 110	Price
	Security classification	

Distribution by (name and address) Josefín Axelsson, e-mail: josefin.axelsson@med.lu.se

I, the undersigned, being the copyright owner of the abstract of the above-mentioned dissertation, hereby grant to all reference sources permission to publish and disseminate the abstract of the above-mentioned dissertation.

Signature 

Date 2011-05-03

Dynamics of the glomerular filtration barrier

Physiological and pathophysiological aspects

Josefin Axelsson



LUND UNIVERSITY
Faculty of Medicine

Lund 2011

Clinical Sciences, Lund
Department of Nephrology

Copyright © Josefin Axelsson
Clinical Sciences, Lund
Department of Nephrology
Lund University 2011

Lund University, Faculty of Medicine Doctoral Dissertation Series 2011:59
ISBN 978-91-86871-08-6
ISSN 1652-8220

Typesetting: Ilgot Liljedahl

Printed by **Media-Tryck**, Lund University, Sweden 2011

**CLIMATE
COMPENSATED
PAPER**



To mom and dad

Table of contents

Abstract	9
Original papers	11
Abbreviations	13
Aims of the thesis	15
Background	17
The kidneys and their structure	17
The glomerular filtration barrier	18
Structure	18
Properties of the GFB in some disease states	19
Tubular handling of proteins	20
Proteinuria	21
Molecular probes	22
Models of glomerular membrane permselectivity	23
Solute and solvent flux across membranes	24
Two-pore model of glomerular permselectivity	25
Some pathophysiological conditions provoking microalbuminuria	26
Sepsis	26
Anaphylactic shock	26
Trauma	26
Hyperglycemia	27
Congestive heart failure	27
Material and methods	29
Animals	29
Surgery	29
Molecular probes	29
Experimental procedures	30
Paper I	30
Paper II	30
Paper III	31
Paper IV	31
High pressure size exclusion chromatography (HPSEC). Ficoll _{50-80Å} serve as probes for the large pore equivalent	32

Radioactivity measurements	33
Tissue-uptake technique	33
Transmission electron microscopy (TEM)	34
Two-pore analysis	35
Statistics	35
Results	37
Endotoxemia and anaphylaxis alter glomerular permeability (study I)	37
Effects of trauma on glomerular permselectivity (study II)	39
Rapid, reversible increases in glomerular permeability due to hyperglycemia.	
Inhibition by a Rho-kinase inhibitor (study III)	41
ANP induced rapid, cyclic alterations in glomerular permselectivity (study IV)	43
Discussion	45
Glomerular permeability under normal conditions	45
The GFB as a dynamic barrier	45
Microalbuminuria	47
Fundamental behavior of the two-pore model	48
Possible mechanisms of increased glomerular permeability	49
Hyperglycemia	49
Rho-kinase and glomerular hyperpermeability during hyperglycemia	50
Hemodynamic parameters	51
Conclusions	55
Populärvetenskaplig sammanfattning (Swedish summary)	57
Grants	61
Acknowledgements	63
References	65
Appendix – Study I-IV	71

Abstract

The dynamic properties of the glomerular filtration barrier (GFB) are of fundamental importance for the understanding of the physiology and pathophysiology of microalbuminuria and proteinuric diseases. In the studies of this doctoral thesis the properties of the rat GFB were investigated under resting conditions and following a number of challenges using highly sensitive gel filtration chromatography (HPSEC) detection of FITC-Ficoll in serum and urine. This permeability model is extremely sensitive, and by using HPSEC, it was possible to measure extremely low concentrations of Ficoll molecules in the urine. Under resting conditions the sieving coefficient (θ ; filtrate-to-plasma concentration ratio) for Ficoll_{70Å} was approximately 10^{-5} , and θ_{alb} was found to be low, 3×10^{-4} (or less). During increases in glomerular permeability θ_{alb} and θ for Ficoll_{50-80Å} increased in parallel, conceivably reflecting an increase in the number of large pores in the GFB. In study I, lipopolysaccharide (LPS) induced sepsis produced increases in θ_{alb} and θ for Ficoll_{50-80Å} at 120 min after LPS injection. In anaphylaxis there was a rapid permeability response already after 5 min which was reversed within 40 min. In study II, laparotomy, with or without muscle crush trauma, induced an increase in glomerular permeability after 5 min, which was to a large extent sustained after 60 min. Hyperglycemia (study III) induced an increase in θ for Ficoll_{50-80Å} after 20 min, but not at 5 min, and after 60 min glomerular permeability was back to normal. The permeability increase seen after hyperglycemia at 20 min was totally abolished by a Rho-kinase inhibitor, indicating that the cytoskeleton of endothelial cells and/or podocytes may be involved. In study IV, high or low doses of ANP induced an increase in glomerular permeability for Ficoll_{50-80Å}, reaching its maximum at 5 and 15 min. During ANP infusion (cf. congestive heart failure) there was a bimodal response, with a dip after 30 min, after which θ for Ficoll_{50-80Å} again tended to increase. In this thesis the novel concept of a rapidly dynamic glomerular filtration barrier is introduced. During different challenges the size-selectivity of the GFB, rather than its charge-selectivity, was found to be subject to rapid and reversible alterations.

Original papers

This thesis is based on the studies reported in the following papers, referred to in the text by Roman numerals (I-IV):

Axelsson J, Rippe A, Venturoli D, Swärd P, and Rippe B.
Effects of early endotoxemia and dextran-induced anaphylaxis on the size-selectivity of the glomerular filtration barrier in rats. *Am J Physiol Renal Physiol*. 2009, 296(2): F242–F248.

Axelsson J, Mahmutovic I, Rippe A and Rippe B.
Loss of size-selectivity of the glomerular filtration barrier in rats following laparotomy and muscle trauma. *Am J Physiol Renal Physiol*. 2009, 297(3): F577–F582.

Axelsson J, Rippe A and Rippe B.
Acute hyperglycemia induces rapid, reversible increases in glomerular permeability in non-diabetic rats. *Am J Physiol Renal Physiol*. 2010, 298(6): F1306–F1312.

Axelsson J, Rippe A and Rippe B.
Transient and sustained increases in glomerular permeability following ANP infusion in rats. *Am J Physiol Renal Physiol*. 2011, 300(1):F24–F30.

Papers are reprinted with permission of the journal/publisher.

Abbreviations

A/A_0	Diffusional restriction factor
$A_0/\Delta X$	Unrestricted pore area over unit diffusion path length
a_e	Stokes-Einstein radius
a_s	Radius of a solid sphere
Cl	Clearance
CPM	Counts per minute
Da	Dalton
E. coli	Escherichia coli
FITC	Fluorescein Iso-thiocyanate
GBM	Glomerular basement membrane
GFB	Glomerular filtration barrier
GFR	Glomerular filtration rate
IgG	Immunoglobulin G
IgM	Immunoglobulin M
J_s	Solute flux
J_v	Fluid flux
J_{v_L}/GFR	Fractional fluid flow through the large pores
K_{av}	Distribution coefficient
LDL	Low density lipoprotein
LMW	Low molecular weight
LPS	Lipopolysaccharide
$L_p S$	Hydraulic conductance
MW	Molecular weight
nm	Nanometer
P_c	Capillary hydrostatic pressure
Pe	Peclet number ($J_v(1-\sigma)/PS$)
P_i	Interstitial hydrostatic pressure
ΔP	$P_c - P_i$

PKC	Protein kinase C
PS	Permeability-surface area product
PSD	Podocyte slit diaphragm
PTR	Proximal tubular reabsorption
r_L	Large pore radius
r_p	Pore radius
r_s	Small pore radius
TLR	Toll-like receptor
UAER	Urinary albumin excretion rate
Å	Ångström
θ	Sieving coefficient
α_L	Hydraulic conductance accounted for by the large pores
λ	a_e / r_p
σ	Reflection coefficient
π_c	Osmotic pressure of capillary fluid
π_i	Osmotic pressure of interstitial fluid
$\Delta\pi$	$\pi_c - \pi_{Bow}$
$1-\sigma$	Restriction coefficient to convection

Aims of the thesis

The overall aim of the present thesis was to gain further insight into the functions of the glomerular filtration barrier (GFB) in order to shed light on the mechanisms of microalbuminuria. How does the barrier behave during different pathological conditions and how does the permeability of the barrier change? The specific aims of the studies were:

- Study I To investigate how the GFB is affected by systemic inflammation, induced by bacterial LPS, and to compare these changes with those occurring during acute anaphylaxis.
- Study II To investigate the functional behavior of the GFB following acute trauma, i.e. in response to laparotomy, with or without skin dissection, and with or without muscle crush injury.
- Study III To investigate the impact of acute hyperglycemia on the GFB and to elucidate if hypertonic mannitol or NaCl can affect the glomerular barrier. In addition, to investigate if a Rho-kinase inhibitor, by affecting the assembly of F-actin stress fibers in podocytes or endothelium, can impact upon the glomerular permeability during acute hyperglycemia.
- Study IV To study the functional behavior of the GFB following infusion of ANP and hence to investigate if ANP can be responsible for the microalbuminuria seen during volume overload, such as in congestive heart failure.

Background

The kidneys and their structure

The kidneys are bean-shaped structures lying behind the peritoneum on each side of the lumbar vertebral column. The kidneys serve different essential functions, such as functioning as a plasma filter, thereby removing metabolic waste products and toxins, regulating the body fluid composition, regulating the acid-base and electrolyte balance and producing different hormones. The two kidneys comprise less than 0.5 % of the total body weight in man (300 g compared to 70 kg), but despite their low weight, receive approximately 20 % of the cardiac output.

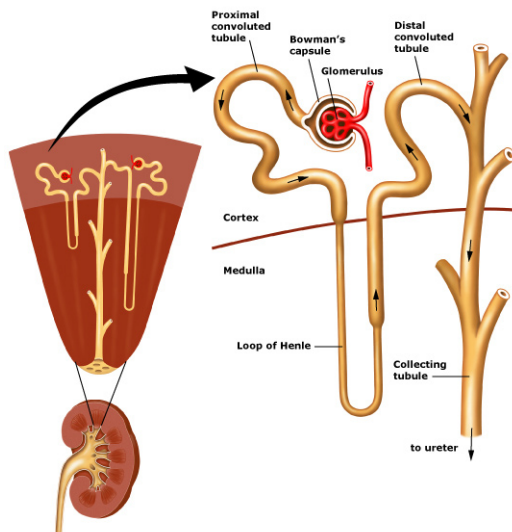


Figure 1. The structure of the kidney¹.

The functional unit in the kidney is the nephron. Each kidney consists of approximately one million nephrons in man. A nephron consists of a glomerulus and tubular system, ending up in a collecting duct (Fig. 1). The glomerulus is a capillary tuft that is invaginated into and surrounded by the Bowman's capsule, containing the Bowman's space, into which an ultrafiltrate of plasma is produced *via* the glomerular filtration bar-

rier (GFB), by plasma sieving. A healthy adult filters roughly 180 L of plasma, so-called primary urine, every 24 hours across the GFB of its two kidneys. The filtrate is largely devoid of proteins, but otherwise has a composition similar to that of plasma (but affected by the Donnan equilibrium). From Bowman's capsule the nephron continues with the tubule system. To maintain extracellular volume, electrolyte and acid-base homeostasis the tubules reabsorb (and control) the primary urine so that a final urine volume of roughly 1.5 L is excreted daily.

The glomerular filtration barrier

Structure

The glomerular filtration barrier is made up of three sequential layers; the glomerular endothelial cells, the glomerular basement membrane (GBM) and the podocytes with their foot processes² (Fig. 2).

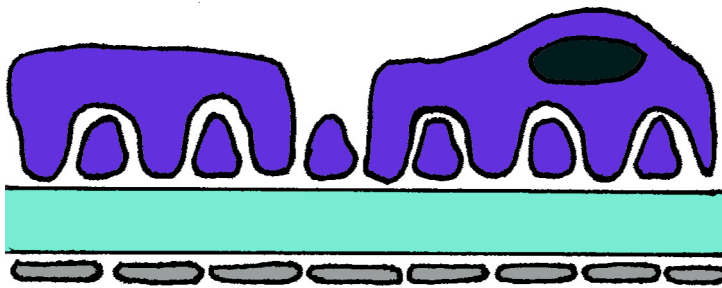


Figure 2. Schematic picture of the glomerular barrier. Endothelial cells in grey, glomerular basement membrane in green and podocytes with their foot processes in blue.

The endothelial cells are the cells closest to the plasma side and on the abluminal (urinary) side lined by the GBM and the podocytes. They contain large fenestrations (diameter $\sim 60\text{--}80\text{ nm}$)³, holes that provide no restriction to the movement of water and small solutes but restrict blood cells. Endothelial cells are coated, on the plasma side, by a negatively charged glycocalyx⁴⁻⁵ consisting of glycosaminoglycans and proteoglycans. This layer may, by virtue of its negative charge, be important in restricting albumin and other negatively charged molecules from entering the GBM. The basement membrane, ($0.3\text{ }\mu\text{m}$ thick) separates the endothelial layer from the epithelial layer. The GBM is basically a matrix of type IV collagen and laminin, crosslinked with negatively charged, sulphated glycoproteins and proteoglycans, such as agrin, perlecan and nidogen/en-

tactin⁶⁻⁷. The outermost layer of the glomerular filtration barrier is represented by the podocytes with their foot processes, enwrapping the glomerular capillaries. Foot processes have a contractile apparatus composed of F-actin filaments and non-muscle myosin, and the cell body is rich in microtubules and intermediate filaments⁸. Between the foot processes are the filtration slits, which are interconnected by a thin structure, the slit diaphragm. The podocyte slit diaphragm (PSD) was first described by Rodewald and Karnovsky⁹ and its presence has been confirmed by recent studies using modern techniques. A number of different proteins are known to span the filtration slits, such as nephrin, P-cadherin, podocin and Neph 1¹⁰⁻¹¹. Of these, nephrin is the most important¹²⁻¹³. The proteins in the PSD play a critical role in coordinating podocyte structure and function¹⁴ by inter-linking the F-actin cytoskeleton between individual foot processes. Conceivably this is important, because the cytoskeleton of the podocytes seem to maintain the function of the entire barrier. Glycoproteins with negative charges cover the podocytes, filtration slits and slit diaphragms¹⁵.

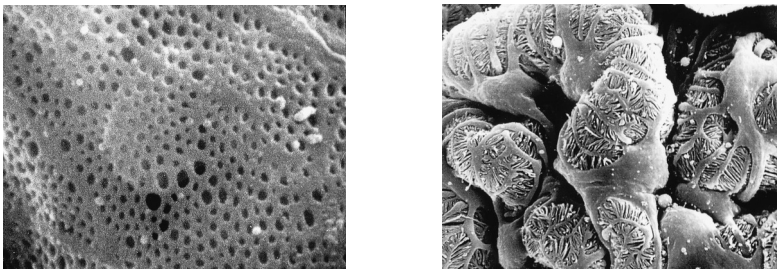


Figure 3. A view of the glomerular barrier. In the left image a view from the inside of a fenestrated endothelium, and in the right image a view of the podocytes¹⁶.

Properties of the GFB in some disease states

Ever since the discovery that a mutation in the gene coding for nephrin¹⁷ can cause massive proteinuria (the congenital nephrotic syndrome of Finnish type), the podocyte slit diaphragm has been postulated to be the ultimate barrier for protein leakage. Many researchers are convinced that the PSD *per se* is an efficient sieve for macromolecules. However, the opinion that podocyte foot processes and the intervening slit diaphragm represent a scaffolding structure, which when damaged, causes the barrier (including the endothelium and the GBM) to lose its normal architecture and become leaky, is now gaining support. Studies using Angiotensin II on cultured podocytes has proposed that podocytes contract during this stimulation¹⁸⁻¹⁹. Because the actin-based cytoskeletal network in podocyte foot processes is linked to the basement membrane and slit diaphragm *via* various linker molecules, changes in the F-actin cytoskeleton in the foot processes may thus affect the structure and function of the entire glomerular barrier¹⁸. A study using Angiotensin II and ANP¹⁹ on cultured podocytes indicated contraction of podocytes after Angiotensin II, and podocyte relaxation after ANP, suggesting that ei-

ther change in the podocyte structure (contraction or relaxation) may cause changes in the glomerular barrier. Defects in any of the PSD proteins, with the possible exception of P-cadherin, can lead to the nephrotic syndrome including foot process effacement. For example, mutations in the gene encoding for α -actinin-4 can cause an inherited form of FSGS (FSGS type I) which leads to the nephrotic syndrome, and eventually, to renal failure. During this mutation, an abnormal assembly of actin is seen in the podocytes²⁰. Mutations in the type IV collagen gene, the backbone (together with laminin) of the GBM, may result in Alport's syndrome or, in its heterozygous form, the more benignant "thin membrane disease" (benign familial hematuria)^{6, 11}. However, the collagen network alone does not seem to be crucial for the size and charge selectivity of the barrier, since patients with Alport's syndrome only suffer from mild proteinuria, besides having hematuria. Laminin may be of greater importance, since laminin β 2 knockout mice display a severe nephrotic syndrome, without initial podocyte changes²¹. During preeclampsia, the endothelial cells (GBM and podocytes are at least initially intact) have been postulated to be the culprit for the proteinuria as indicated by swelling of the endothelial cells, eventually leading to disruption of the barrier²². It seems that any alteration, of at least one of the three layers of the barrier^{15, 23-25}, may cause a non-functional GFB, eventually resulting in proteinuria, and that normal function of the glomerular barrier requires the presence of three intact layers. The endothelial glycocalyx may represent the major charge barrier of GFB^{4, 15, 26}, since there is evidence that the negative charges of the GBM is of minor importance for charge selectivity of the glomerular filter²⁷. A previous study²⁶ suggests that enzymatic removal of the endothelial glycocalyx, with e.g. hyaluronidase, markedly reduced the selectivity of the GFB to albumin, indicative of an effect of the charge barrier. However, unpublished (own) data indicate that there is an increase in the number of the large pores of the GFB after infusing hyaluronidase in rats, without any primary changes in the charge selectivity.

Tubular handling of proteins

Polypeptides and proteins are categorized in four different groups with respect to their size (i.e. molecular weight, MW): polypeptides of MW < 10 kDa, proteins of low molecular weight (LMW) (10–44 kDa), proteins of intermediate MW (44–90 kDa) and high MW (>90 kDa). The kidney is mainly responsible for the metabolic clearance of circulating LMW proteins that are extensively filtered in the glomerulus and fully reabsorbed and catabolized by the proximal tubular cells and returned to the circulation as amino acids. With increasing protein size there is a steep decrease in their filterability, and for large proteins (albumin ($a_e \sim 36 \text{ \AA}$), orosumucoid ($a_e \sim 30 \text{ \AA}$), lactate dehydrogenase ($a_e \sim 41 \text{ \AA}$) and IgG ($a_e \sim 55 \text{ \AA}$)) the kidney plays a minimal role in their clearance. Very high molecular weight proteins, i.e. α_2 -macroglobulin ($a_e \sim 90 \text{ \AA}$), IgM ($a_e \sim 120 \text{ \AA}$)

and LDL (a_e ~140-150 Å), are only found in the urine when the GFB is severely damaged, and then signal a worse prognosis of the underlying renal disease²⁸.

Proteins are normally reabsorbed efficiently in the proximal tubule system by two membrane bound receptors; megalin and cubilin, and the cooperating amnionless, resulting in almost protein-free urine²⁹. Megalin is an endocytotic receptor belonging to the low density lipoprotein (LDL) family and is heavily expressed in the kidney proximal tubule. It binds a number of different proteins, such as albumin, hemoglobin, myoglobin and lipoproteins. Cubilin is a large protein that is identical to the vitamin B₁₂ receptor found in the small intestinal mucosa. Cubilin share some ligands with megalin, such as albumin and immunoglobulins and is also seen to bind, for example, transferrin²⁹. Both the receptors play an essential role in the protein reabsorption in the proximal tubule³⁰. These proteins and the protein reabsorption process in proximal tubules have been described in detail elsewhere²⁹⁻³¹, and knockout mice for the different receptor proteins have been developed³⁰. The θ_{alb} measured in megalin knock-out mice is low (2×10^{-4}) as further discussed below³². In other experimental animal models, the use of lysine, by inhibiting the tubular protein reabsorption, has also made it possible to study the urinary leakage of large proteins in rats³³.

Proteinuria

Proteinuria designates the presence of elevated (nonphysiological) levels of proteins in the urine (>200 mg/24 h). During proteinuria the urine consists mainly of filtered plasma proteins and tubular Tamm-Horsfall proteins. The latter is a normal compound of urine produced mainly locally in the thick ascending limb of loop of Henle. Albumin is the main plasma protein, and an increased concentration of albumin in the urine is usually referred to as albuminuria. Even a small increase in the urinary excretion rate of albumin (UAER), microalbuminuria (30-300 mg/24 h), is an early feature of many renal diseases but is also an established marker of endothelial dysfunction or the general health of the vascular system. Microalbuminuria may also be a normal phenomenon, e.g. in strenuous physical exercise³⁴, or is seen in early diabetes, myocardial infarction, after trauma, and after knee and hip surgery³⁵⁻³⁹. Low molecular weight proteinuria can occur in interstitial renal disease, such as in interstitial nephritis, lithium-nephropathy, or unspecifically, in chronic kidney disease (CKD) (interstitial fibrosis). Some rare renal syndromes can also present with tubular, low molecular weight proteinuria. These syndromes include for example Dent's disease (CLC5-defect), Imerslund-Gräsbeck syndrome (cubilin deficiency), Lowe syndrome and cystinosis, all due to deficient proximal tubular reabsorption (PTR)²⁹.

Glomerular filtration of albumin is followed by tubular reabsorption (up to 98 %) and thus albuminuria reflects the net result of these two processes together. Glomerular proteinuria is caused by a defect in the GFB. Characteristic for this type of proteinuria

is that large plasma proteins that normally not are filtered, or only filtered to a limited extent, appear in the urine. Tubular proteinuria involves an impaired reabsorption of proteins by the tubular system. Smaller proteins that are freely filtered in the glomerulus and normally completely reabsorbed, can reach the urine when there is damage to the tubular system. Even for a normally functioning proximal tubule, tubular proteinuria can occur. Thus, when increasing amounts of proteins are filtered across the glomerular barrier they start to interfere with the normal tubular reabsorption of low molecular weight proteins, competing for the binding sites on the receptors in the tubular system. This is generally called “overload proteinuria”. Overproduction of various proteins, such as light chains in plasma in multiple myeloma, usually also produces a kind of overload proteinuria, “overproduction proteinuria” (cf. Bence Jones proteinuria). Low-molecular weight proteins are then, due to their increased plasma concentrations, filtered in higher amounts and when the tubular maximum is exceeded, they appear in the urine.

Molecular probes

The basic approach of permeability studies is to study how molecular probes, differing in physical and chemical properties, traverse biological membranes. The sieving coefficients (i.e. the steady state filtrate-to-plasma concentration ratios, θ) obtained, tell us about the properties of the membrane. Proteins and polysaccharides have been extensively used as molecular probes to study the permselectivity of the capillary wall and the glomerular filter⁴⁰⁻⁴³. Polysaccharides are polydisperse, inert (uncharged) and insignificantly reabsorbed by the proximal tubules, which makes them suitable for measuring glomerular permeability. Proteins have the main drawback that they are reabsorbed by the proximal tubules and they are usually charged, which makes their study difficult due to the complicated techniques needed to measure their glomerular θ 's.

Ficoll is a neutral and highly branched, crosslinked polymer of epichlorhydrine and sucrose. As a synthetic molecule it is not to a significant extent reabsorbed by the tubular system⁴⁴ except from insignificant fluid phase endocytosis⁴⁴⁻⁴⁵. Ficoll has been postulated to be a spherical molecule, with characteristics similar to those of a globular protein. However, it is neither spherical nor as compact as a globular protein⁴⁴⁻⁴⁶ (see below). Albumin is a compact protein molecule and the main plasma protein, produced by the liver. Native albumin has a net negative charge (-20), the Stoke-Einstein radius of albumin being 36 Å (its “real” shape is that of an ellipsoid of diameter ~40 Å and length ~140 Å) and its MW being 69 kDa.

The ability of a solute to pass the glomerular barrier depends on its size, shape, flexibility and charge. The GFB is size as well as charge selective, but the relative importance of its charge selectivity and its size selectivity is under intense debate⁴⁷. The view on charge selectivity of the glomerular barrier has mainly been based on studies using nega-

tively charged sulphated dextrans⁴⁸⁻⁴⁹ and on neutral *vs.* charged proteins of equivalent size^{47, 50-51}. In the classical studies from Brenner's group, the glomerular permeability of negatively charged dextran was decreased compared to neutral dextran, and the permeability to positively charged dextran was increased compared to that of neutral⁴⁸⁻⁴⁹. A number of studies have challenged these results^{50, 52-53}. It has been shown that negatively charged, sulphated dextran can bind to plasma proteins⁵² and cell membranes, and therefore show low glomerular sieving coefficients, whereas results using positively charged dextran could not be reproduced, or was attributed to conformational changes of the dextran molecules, or permeability changes of the barrier (which can be altered by polycations)^{48, 52, 54}. The glycocalyx with its negative charges is by many authors believed to be the main charge barrier of the glomerular filter^{15, 55}.

Renkin and Gilmore⁴² proposed already 30 years ago that polysaccharides, due to their extended structure, may be hyperpermeable across the glomerular filtration barrier compared to proteins. Asgeirsson *et al.*⁵⁶ confirmed these findings, and explained the hyperpermeability seen for polysaccharides by the fact that they have an extended molecular conformation, i.e. an increased "frictional ratio" and an increased flexibility. It is now generally accepted that neutral dextran (frictional ratio 2.1-2.8), a random coil polysaccharide, is hyperpermeable across the glomerular filter^{40, 57-58}. Bohrer *et al.*⁵⁷ furthermore showed that dextran is hyperpermeable relative to Ficoll. Furthermore the markedly elongated protein, bikunin, of the same SE-radius and negative charge (-20) as albumin but with a "frictional ratio" of 2.0, shows a 1000-fold higher permeability across the GFB than albumin (with a frictional ratio of 1.28)⁵⁹. Since Ficoll is expected to have a spherical shape, Ficoll has been accepted as the ideal probe for measuring glomerular permeability. However it has been shown that Ficoll is neither a completely spherical, nor an undeformable molecule⁴⁴⁻⁴⁶. Ficoll seems to behave as an intermediate between a hard spherical molecule and a flexible random coil polysaccharide. The frictional ratio of Ficoll is 1.7 (to 1.9), which would render it slightly hyperpermeable across the GFB⁵⁶. It is evident, however, that Ficoll is hyperpermeable across the GFB only when the molecule radius exceeds 60 % of the pore radius ($\lambda > 0.6$) or 70 % of the slit width. This indicates that Ficoll can be utilized as a probe (like neutral proteins) across the large pores of the glomerular filter (Ficoll 50-80 Å) but is hyperpermeable across the small pores (Ficoll 20-50 Å), because then $\lambda > 0.6$.

Models of glomerular membrane permselectivity

A number of models are available to describe the solute and solvent transport across biological membranes. From experimental data in the form of fractional clearances (sieving curves) and prevalent hemodynamic conditions, a mathematical model is put forth to describe the membrane properties without being biased by hemodynamic effects. The most common models are the pore model and the fiber matrix model, which

in their simplest forms represent a single population of either pores or fibers that impose restriction to movement of molecules. They are made more complex by making the population of pores and fibers conform to a dual selectivity concept or to some statistical distribution, i.e. heteroporous or distributed (log-normal) pore models or fiber models. Charge can also be introduced into these models¹⁵. The best model will minimize the difference between the experimental data and the theoretical model but still has to be rather simple.

Solute and solvent flux across membranes

Unhindered movement of molecules in solution occurs by diffusion and convection. Stokes law for the frictional coefficient of a spherical particle in solution in combination with the laws of diffusion derived by Fick and Einstein gives the solute diffusion coefficient (D_s):

$$D_s = \frac{R \cdot T}{6\pi \cdot N_A \cdot a_e \cdot \eta} \quad (1)$$

When traversing biological barriers, such as the glomerular filtration barrier, molecule transport is hindered and occurs at a slower rate than in free solution. This is described by the terms A/A_0 for molecules transported by diffusion and by $(1-\sigma)$ for molecules transported with convection⁶⁰⁻⁶¹. In the pore model, the formulas developed by Mason *et al.*^{60, 62} is used, where restriction factors are a function of λ , the ratio of solute SE-radius (a_e) to pore size (r_p) and can have a value between 0 and 1.

$$\frac{A}{A_0} = \frac{(1-\lambda)^{3/2}}{1-0.3956\lambda+1.0616\lambda^2} \quad (2)$$

$$(1-\sigma) = \frac{(1-\lambda)^2[2-(1-\lambda)^2]\left(1-\frac{\lambda}{3}\right)}{1-\frac{\lambda}{3}+\frac{2}{3\lambda^2}} \quad (3)$$

Based on irreversible thermodynamics, equations have been developed to describe solute (J_s) and solvent (J_v) movement across membranes⁶³⁻⁶⁴.

$$J_v = L_p S (\Delta P - \sigma \Delta \pi) \quad (4)$$

$$J_s = J_v (1 - \sigma) \bar{C} + PS \Delta C \quad (5)$$

where $L_p S$ represents the hydraulic conductance, ΔP the transmembrane hydrostatic pressure gradient, σ the reflection coefficient of the membrane to the solute, $\Delta \pi$ the transvascular osmotic pressure gradient, PS the solute permeability surface area product, ΔC the transmembrane solute gradient ($C_p - C_i$) where C_p is the solute concentration in plasma and C_i in the interstitium, \bar{C} is the mean intramembrane solute concentration.

Integration of equation (5) across the membrane, between the boundary conditions C_p and C_i yields equation (6) (Patlak equation or the nonlinear global convection/diffusion equation):

$$J_s = J_v(1 - \sigma) \frac{C_p - C_i \cdot e^{-Pe}}{1 - e^{-Pe}} \quad (6)$$

Where Pe is representing the modified Peclet number. By dividing equation (6) by the plasma concentration of the solute an equation for solute clearance is obtained (7).

$$Cl = J_v(1 - \sigma) \frac{1 - (C_i/C_p) \cdot e^{-Pe}}{1 - e^{-Pe}} \quad (7)$$

Two-pore model of glomerular permselectivity

According to the two-pore theory, the equivalent small pores of the glomerular filter are approximately 37.5 Å in radius and the large equivalent pores are approximately 110 Å in radius, based on tissue uptake experimental data for neutral proteins⁶⁵ and data from experiments in rats with lysine inhibited PTR³³. The presence of negative charge in the small pores seems to almost totally exclude albumin from the small pore pathway. However, in large pores the charge effect is minor. The large pores are represented by only one large pore per 10^7 of the small pores.

Using a two pore model, there is convection dominated flux through the large pores where any diffusive contribution can be calculated to be negligible⁶⁶. The main output from this model are: the small pore radius (r_s), the large pore radius (r_L), the fractional hydraulic conductance accounted for by the large pores (α_L) and the total unrestricted pore area over diffusion path length ($A_0/\Delta X$). These parameters describe the membrane properties without being influenced by hemodynamic factors. The α_L reflects the abundance of large pores in the glomerular filter and is calculated from the fractional GFR diverted through the large pores i.e. J_{vL}/GFR . Both α_L and J_{vL}/GFR can be mathematically obtained by extrapolating the “flat” part of the sieving curve for molecules with a radius larger than 50 Å back to the ordinate. α_L is calculated according to equation 8, where P_{UF} represents the net filtration pressure.

$$\alpha_L = \frac{J_{vL}/GFR}{\frac{\Delta\pi}{P_{UF}}(1 - \sigma_L) + 1} \quad (8)$$

The small pore radius is mainly dependent on sieving data close to the region where there is a “knee” of the large pore and small pore curve, ~40-46 Å. $A_0/\Delta X$ is the diffusive parameter essentially describing the surface area of the small pores.

Some pathophysiological conditions provoking microalbuminuria

Sepsis

Sepsis is a serious medical condition in which the bloodstream is overwhelmed with bacteria and/or bacterial toxins. This medical condition is characterized by a systemic inflammatory response state (SIRS), in the presence of an infection. In sepsis, the blood pressure drops due to vasodilatation and plasma loss from the circulation and major organ body systems, including the kidneys, may stop working properly, ending up in acute kidney injury (AKI) or multi-organ dysfunction (MODS).

The gram-negative bacterium, *E. coli*, is often found in the lower intestine of mammals. Most *E. coli* strains are harmless, but some strains of the bacteria can cause severe illness. The most common bacterial component implicated in initiating the septic syndrome is a cell wall molecule known as lipopolysaccharide (LPS) or endotoxin, which causes severe illness if entering the blood stream. The LPS molecule is composed of two biosynthetic entities, the lipid-A core and the O-polysaccharide⁶⁷. Most of the biological effects are due to lipid-A, which is seen to stimulate the mammalian immune system. LPS thus is a strong activator of various immune responses. It binds to TLR-4 receptors, thereby causing cytokine release (TNF- α , IL-6 etc.) and immune cell activation⁶⁸⁻⁶⁹. TLR-4 receptors are most highly expressed on leukocytes but are also present in the kidney⁶⁹. Injection of LPS into animals can reproduce many of the manifestations of sepsis, including AKI⁶⁹.

Anaphylactic shock

Anaphylaxis is a severe, rapidly-progressing, whole-body, IgE-mediated reaction to a substance that has become an allergen. Mast cells in different parts of the body rapidly release histamine and other substances, such as 5-HT and heparin, in response to the allergen. Some drugs can cause this type of reactions, otherwise insect bites and food allergens are common causative agents. Signs of anaphylactic shock include low blood pressure, urticaria and, in the worst cases, swelling of the glottis, respiratory obstruction and death.

Trauma

Gross medical trauma refers to a serious or critical body injury, wound or shock, involving activation of various cascade systems in the body, including cytokine release, complement activation and activation of the coagulation cascade (eventually leading to disseminated intravascular coagulation, DIC). Body trauma may also involve massive

release of myoglobin, from the muscles, leading to “pigment-nephropathy” and AKI which is usually irreversible. However during the initial phases of gross body trauma, microalbuminuria may occur due to cytokine release (IL-6) and activation of immune cells.

Hyperglycemia

Hyperglycemia (high blood glucose) is the condition when excessive amounts of glucose circulate in the plasma. Normal blood glucose in fasting human is about 4-7 mmol/l. Blood glucose levels can rise up to 10 mmol/l normally without producing adverse permanent effects or symptoms. Diabetes mellitus is by far most common cause of chronic hyperglycemia. Chronic hyperglycemia or recurrent (post-prandial) hyperglycemia, with glucose levels moderately higher than normal, can produce a variety of serious complications, such as macrovascular and microvascular and renal damage. Acute hyperglycemia with blood glucose levels that are high (>20 mmol/l), is not uncommon in persons with uncontrolled type-II diabetes, or, in rare cases, in type I diabetes.

Congestive heart failure

Congestive heart failure is among the most common causes of hospitalization. Heart failure is a state when the heart is unable to pump enough oxygen rich blood to the rest of the body due to decreased cardiac myocyte contractility. Common causes of heart failure are myocardial infarction, ischemic heart disease and cardiomyopathy. Symptoms seen in heart failure are peripheral edema, dyspnea and venous congestion. On the cellular level, decreased contractility can be a result of cardiac hypertrophy reflecting alterations in the (transient) increases of Ca^{2+} and/or expression of the contractile proteins in the myocytes. Atrial natriuretic peptide (ANP) is a peptide released from the cardiac cells (atrial myocytes) when stretched, i.e. in volume-overload, or in ischemia, i.e. during myocardial infarction. ANP is a potent vasodilator causing diuresis, and it thus enhances GFR and the renal excretion of Na^+ (i.e. natriuresis). By increasing capillary permeability ANP acts to lower the effective circulating blood volume and blood pressure.

Material and methods

Animals

The studies were performed in male Wistar rats. All experiments were approved by the Animal Ethics Committee at Lund University, Sweden.

Surgery

Anesthesia was induced by intraperitoneal (ip) injection of pentobarbital sodium (60 mg/kg) and maintained throughout the experiment by intra-arterial injections of the same anesthesia. The animal was placed on a heating pad to keep body temperature at 37°C. A tracheotomy was done to facilitate breathing (PE-240 tube). The tail artery was cannulated (PE-50 cannula) for continuous monitoring of mean arterial blood pressure (MAP) and for registration of heart rate (HR) on a polygraph (model 7B, Grass Instruments, Quincy, MA) and for administration of anesthesia. The left carotid artery was cannulated (PE-50) for blood sampling, and the right (and) left veins for infusion purposes. Access to the left urethra was achieved through a small abdominal incision (6-8 mm). To increase urine production and facilitate the cannulation of the urethra, Furosemide (Furosemid Recip, Årsta, Sweden) was administered in the tail artery. The urethra was dissected free and a PE-10 cannula (connected to a PE-50) was inserted and secured. After the surgery, the animals were allowed to rest for 15-30 min.

Molecular probes

The exact amount of each tracer molecule used in each group of the experiments can be found in the respective paper. To measure the sieving properties of the GFB, the polysaccharide FITC-Ficoll was used. To deliver a broad distribution of molecular sizes, a mixture of Ficoll-70 and Ficoll-400 was used. The relationship between them was

1:24. Inulin was used to measure GFR, during the Ficoll sieving measurements and could be used as an “internal standard” to convert final urine Ficoll concentration into Bowman’s capsule (primary urine) concentration. All polysaccharides used were labeled with FITC by TdB Consultancy (Uppsala, Sweden).

I¹²⁵ Human Serum albumin (RISA) for measurements of albumin clearance was obtained from Isopharma (Kjeller, Norway). ⁵¹Cr-EDTA was used to measure GFR during the whole experiments and was obtained from Amersham Bioscience (Buckinghamshire, UK).

Experimental procedures

The experimental procedures were different between the different studies and are explained in each study.

Paper I

Endotoxemia was induced by an intravenous (i.v.) bolus of lipopolysaccharide (LPS) followed by a constant i.v. infusion. Measurements were continued for 60 and 90 min, and in a separate group of animals, for 120 min. To induce anaphylaxis, rats were given 0.25 ml Dextran-70 i.v. as a bolus (Wistar rats are Dextran hypersensitive). Sieving measurements took place 5 and 40 min after the dextran injection in two separate groups of animals. FITC-Ficoll was infused during 20 min before measurement of Ficoll sieving coefficient and the measurement continued for 5 min. SHAM animals were given 0.9% saline mimicking the volume load in the experimental animal groups and followed for the same time as the experimental groups. Glomerular sieving of albumin was measured in the endotoxemia animals after 90 and 120 min as well as in the anaphylaxis groups and in the SHAM animals.

Paper II

Trauma was primarily induced by performing a laparotomy, ~50 mm long. The laparotomy was performed in the abdominal midline and along the linea alba of the abdominal muscle wall. This was the only trauma induced for two different groups of animals, followed for either 5 or 60 min. In an additional group, the skin was dissected away from *m. rectus abdominis* (following the laparotomy) bilaterally (~25 mm) at each side of the incision. This additional trauma was done in one group of animals followed for 60 min. In yet three additional groups of laparotomized animals (skin dissected away), crush injury was inflicted to the abdominal muscle by topically pinching the *m.*

rectus abdominis bilaterally by using a pair of hemostatic forceps according to Bansch *et al.*⁷⁰. Muscle crush injury was induced either as a small injury (2×2 pinches) or a large injury (2×5 pinches) and followed for 60 min, and the latter one also for 5 min. The trauma was standardized by closing and opening the forceps for 10 s three times at each location. In the SHAM animals no laparotomy was done and these animals were followed for 5 and 60 min. FITC-Ficoll was infused 20 min before the measurement, and the measurement took place during 5 min. Sieving measurements for albumin took place right after the measurement for Ficoll in all of the experimental groups as well as for the SHAM animals. (The initial surgical trauma was followed in some experiments and yielded an initial increase in glomerular permeability which however, reversed in ~20 min.)

Paper III

Hyperglycemia was induced by i.v. administration of hypertonic glucose (40 %) in saline, given as a bolus and followed by i.v. infusion throughout the experiment. Blood glucose was “clamped” between 20-25 mmol/l. Blood glucose levels were measured approximately every 5 min and the glucose infusion adjusted to maintain the desired blood glucose level. Sampling of urine and plasma for Ficoll sieving measurements was performed at 20 min, or sequentially, at 5, 20 and 60 min. Hyperosmolarity was induced by i.v. infusion of either hypertonic NaCl or hypertonic mannitol to raise the plasma osmolarity by 14-15 mmol/l. Both hypertonic NaCl and hypertonic mannitol was given as a bolus followed by a constant infusion and urine and plasma samples for Ficoll measurements were taken 20 min after the start of the hypertonic insult. One separate group of animals was given Rho-kinase inhibition (Y-27632) during hyperglycemia (bolus and constant infusion) starting 5 min prior the hyperglycemia. Glomerular sieving measurements occurred 20 min after the induction of hyperglycemia. SHAM animals were given physiological saline as a bolus and constant infusion in a way mimicking the experimental interventions and were followed for 20 min, at which time the glomerular sieving measurements for Ficoll were performed.

Paper IV

Atrial natriuretic peptide (ANP) was given i.v. as a bolus followed by constant infusion throughout the experiment. Sampling for glomerular Ficoll sieving measurements was performed sequentially at 5, 15, 30, 60 and 120 min after starting the ANP infusion. In SHAM animals 0.9% saline was given, mimicking the volume load seen during the ANP experiments and sampling for Ficoll measurements performed at start 0-5 min and at 60 and 120 min.

High performance size exclusion chromatography (HPSEC). Ficoll_{50-80Å} serve as probes for the large pore equivalent

FITC-Ficoll in all the studies were size separated and their concentrations determined by high performance size exclusion chromatography (HPSEC). The plasma and urine samples were assessed using an Ultrahydrogel 500 column (Waters, Milford, MA) using a phosphate buffer (0.15 M NaCl, pH 7.4) as the mobile phase. The mobile phase was driven by a pump (Waters 1525). Fluorescence was detected at excitation wavelength 492 nm and emission wavelength at 518 nm (Waters 2475). The samples were loaded to the system by an autosampler (Waters 717 plus), and the system was controlled by Breeze software 3.3 (Waters).

The system was calibrated using narrow Ficoll and dextran standards. The polydispersity-corrected SE radii of the Ficoll standards were 70.2, 57.2, 45.1, 36.4 and 28.4 Å and the dextran standards were 164, 125.1, 105.6, 82.8, 63.7, 38.2 and 18.7 Å respectively. The proteins albumin, apoferritin, IgM, alcohol dehydrogenase and vitamin B₁₂ were also used to calibrate the column. These were detected with an absorbance detector (Waters 2487). The void volume (V_0) was measured with blue dextran (2×10^6 Da) and the total volume (V_T) with glycine (75 Da). From the results of the different measurements a distribution coefficient (K_{av}) was calculated according to formula 9:

$$K_{av} = (V_e - V_0) / (V_T - V_0) \quad (9)$$

where V_e is the elution volume for each standard molecule. K_{av} was plotted against the log of the SE radii of the respective standard molecule and fitted to a third polynomial.

The sieving coefficient for Ficoll was calculated by analyzing data from the HPSEC, i.e. the Ficoll concentration *vs.* elution time (translated into relative distribution volumes in the column of the different size Ficoll molecules), from urine and plasma (C_{PF}) samples from each experiment. The urine Ficoll concentration *vs.* the Stoke-Einstein radius curve was divided by the Inulin concentration to obtain the fractional primary urine concentration of Ficoll (C_{UF}). For each Ficoll radius the sieving coefficient was calculated by dividing C_{UF} by C_{PF} .

Basically nearly identical methods are used throughout the four studies (study I-IV). Our HPSEC system enabled us to measure both molecular size as well as concentration of tracer molecules, and from these data to calculate θ for a broad range of molecular sizes. Our permeability model is extremely sensitive and can measure extremely low concentrations of tracer molecules ($\theta \sim 10^{-5}$) in the urine, which requires a very stable baseline of a fine-tuned HPSEC system and at least four hours of buffer washout between each test sample.

By using the polysaccharide Ficoll in the studies, one can ignore the tubular reabsorption and charge effects which must be considered using proteins. The most favorable option would be to use FITC-labeled Ficoll and radiolabeled proteins (albumin)

together. In study I and II we were able to apply this principle, but due to insufficient radiolabeling of albumin, we were unable to use radiolabeled albumin in study III and IV. We have in all other studies showed a near perfect coupling between θ for albumin and that for Ficoll_{50-80Å} under conditions of increased permeability, and therefore find it reliable to use Ficoll_{50-80Å} as an indicator of glomerular permeability^{56, 71-72}. Both albumin and Ficoll_{50-80Å} pass, according to the two-pore model, the same pathway, namely “large pores” in the glomerular filter, and should therefore be interchangeable as probes for the large-pore equivalent. The presence of free label or albumin degradation products in study III and IV (unpublished observations) yielded very high θ values for albumin, particularly during normal conditions. Even in study I and II there may have been some free ¹²⁵I, and, to some extent, degraded albumin, which must have caused overestimation of the θ for albumin under control conditions. This is conceivably the reason why changes in θ are generally lower than the concomitant changes in Ficoll_{50-80Å}. It should be noted that the θ_{alb} values measured during control conditions ($3 \times 10^{-4} - 4.6 \times 10^{-4}$) represent “upper estimates” of the real θ_{alb} . In these respects, θ for Ficoll_{50-80Å} can be considered more reliable than θ_{alb} as probes for the large pore equivalent.

Radioactivity measurements

Radioactivity in urine and blood was measured using a gamma counter (Wizard 1480, LKP Wallac, Turku, Finland), correcting for radioactive decay and radioactive spill-over (¹²⁵I and ⁵¹Cr).

The glomerular filtration rate (GFR) was measured as the clearance (Cl) of inulin or ⁵¹Cr-EDTA according to the formula:

$$\text{Cl} = (\text{U}_{\text{Cr}} \times \text{V}_{\text{u}}) / \text{P}_{\text{Cr}} \quad (10)$$

where U_{Cr} is the concentration of ⁵¹Cr-EDTA in urine, P_{Cr} the concentration of ⁵¹Cr-EDTA in plasma and V_{u} the urine flow.

Tissue-uptake technique

Glomerular sieving coefficient for albumin was measured (paper I and II) using tissue-uptake technique⁷³⁻⁷⁴. Radiolabeled (¹²⁵I) albumin (RISA) was injected i.v., after which the protein was allowed to circulate in plasma for eight minutes, during which time it dissipated within the extracellular space and filtered across the glomerular barrier. Thereafter, a whole body washout was performed via the carotid artery to remove any remaining tracer in the vasculature of the kidney during an additional eight minute period. The washout fluid was a mixture of equal amounts of 0.9% saline and heparinized

horse serum (SVA, Uppsala, Sweden). During the eight minute period, the breakdown of protein in the proximal tubular cells and the subsequent reabsorption of amino acids to the plasma is negligible, whereas a small fraction of the tracer will appear in urine. The filtered albumin will be found in the kidney cortex (medulla dissected away) and in the urine (the trichloroacetic acid precipitated fraction).

To calculate the glomerular protein clearance of albumin (ml/min), the mass transport (CPM/min) was divided by the plasma concentration of the tracer protein (CPM/ml). The glomerular sieving coefficient was then calculated by dividing the clearance by the simultaneously measured ^{51}Cr -EDTA clearance (GFR).

The tissue-uptake technique has received critique in that it may underestimate the protein sieving coefficients. The critical part of this technique is, however, the wash-out-period and the quality of the radiolabeled tracer used. An incomplete washout or a bad quality of the tracer (denaturated protein) and a high fraction of free label (^{125}I) can only lead to overestimation of the sieving coefficients by contamination of tissue sample by free label or degraded proteins. High concentrations of free label thus yielded abnormally high θ values in tissue uptake studies under control (SHAM) conditions in study III-IV (unpublished data).

Another technical aspect is the eight minute time period from the injection of tracer to the start of the body washout, and hence, the cessation of the glomerular filtration of the filtered protein tracer. Because of marked dilution of RISA at eight minutes, it is reasonable to assume that filtration of albumin really stopped. However, at eight minutes, amino acids from the catabolized protein tracer may start to be reabsorbed to the circulation, which may lead to a slight underestimation of PTR.

The validity of the tissue-uptake technique is supported by the fact that the θ for albumin obtained agrees quite well with that obtained by independent techniques such as micropuncture⁷⁵ and lysine inhibition of PTR³³. Furthermore, patients with Dent's disease, who have a congenital defect in PTR, show a similar glomerular θ_{alb} as that determined in rat with the tissue uptake technique⁷⁶.

Transmission electron microscopy (TEM)

In paper III transmission electron microscopy was done to investigate possible morphological changes in the glomerular barrier. Biopsies were taken from rat kidneys using a human (percutaneous) biopsy needle. Biopsies were immediately placed in fixative. After fixation, biopsies were rinsed in buffer and post-fixed before they were dehydrated and embedded. Ultrathin sections were then cut and placed on copper grid and stained with uranyl acetate and lead citrate. Sections were examined using a CM-10 transmission electron microscope (Philips Scientific, Eindhoven, The Netherlands).

Two-pore analysis

A two-pore model^{33, 62, 65} was used to analyze the θ data for Ficoll (mol. radius 15-80 Å). A nonlinear least-squares regression analysis was used to obtain the best curve fit, using scaling multipliers, as described in Lund *et al.*⁶⁵.

Statistics

Values are expressed as mean \pm SE, or as median and ranges. Differences between groups were tested using non-parametric analysis with Kruskal-Wallis test and post-hoc tested using Mann-Whitney U test. Bonferroni corrections for multiple corrections were made as needed. Significance levels were set at * $p < 0.05$, ** $p < 0.01$ and *** $p < 0.001$. All statistical calculations were made using SPSS 17.0 and 18.0 for Windows or Mac (SPSS, Chicago, IL).

Results

Endotoxemia and anaphylaxis alter glomerular permeability (study I)

In study I, increased sieving coefficients for Ficoll_{50-80Å} and albumin after 120 min of endotoxemia were observed (Fig. 4a). This increased permeability to high MW Ficoll was, however, not seen at either 60 min or 90 min after the induction of endotoxemia. Figure 4b shows the time dependence of the changes in glomerular permeability following injection of endotoxin.

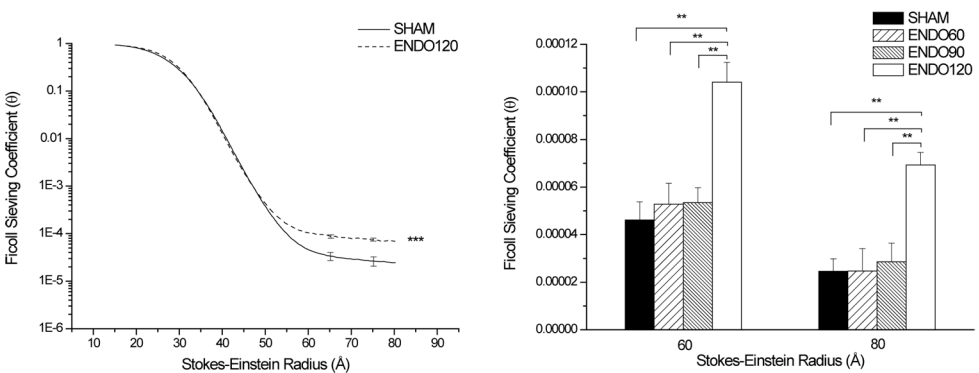


Figure 4a and b. Glomerular sieving coefficients *vs.* Stokes-Einstein radius (a.) for Ficoll (15-80 Å) in the endotoxemia group followed for 120 min (ENDO-120) *vs.* SHAM (a.). Time dependency of Ficoll sieving coefficients for Ficoll 60 and 80 Å (b.). Increases occurred only for endotoxemia 120 min compared to SHAM.

In the acute anaphylaxis group, followed for 5 min, there was significantly higher sieving coefficients for Ficoll_{50-80Å} than in the SHAM-5 group. However, there was no significant difference between the group followed for 40 min and the SHAM group. Acute anaphylaxis thus caused a rapid, transient increase in glomerular permeability, completely reversible within 40 min.

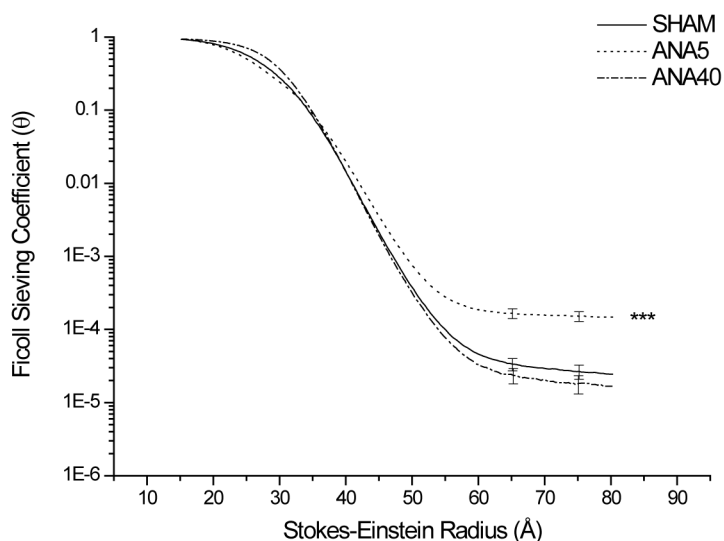


Figure 5. The glomerular sieving coefficient *vs.* molecular radius of SHAM, 5 min of anaphylaxis and 40 min of anaphylaxis.

θ for albumin in the endotoxemia groups were measured at 90 and 120 min (Fig. 6a). After 120 min the θ was significantly increased *vs.* SHAM, but remained unchanged in the 90 min group. In the anaphylaxis groups, an increase in θ for albumin was seen both after 5 and 40 min (Fig. 6b). The increase at 40 min is not in agreement with the results from Ficoll_{50-80Å}, and may be explained by an increased permeability of peritubular capillaries, but not in glomerular capillaries, during later phases of the 40 min of acute anaphylaxis.

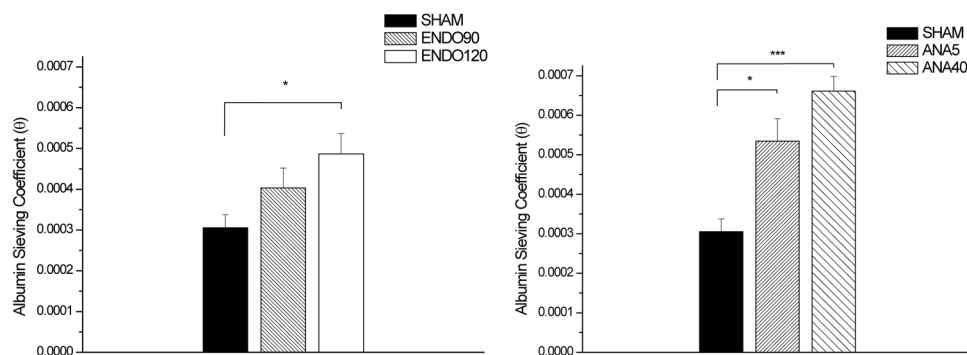


Figure 6a and b. θ for albumin in the endotoxemia groups *vs.* SHAM (a.) and anaphylaxis groups *vs.* SHAM (b.). Significant increases can be seen for endotoxemia at 120 min *vs.* SHAM as well as for both the anaphylaxis groups *vs.* SHAM.

Effects of trauma on glomerular permselectivity (study II)

The study showed that there was an immediate increase in glomerular sieving coefficient for albumin and Ficoll_{50-80Å} after a laparotomy, i.e. already after 5 min, and that this increase was sustained for at least 60 min. Adding skin dissection and/or muscle crush injury to the laparotomy did not further increase the glomerular sieving coefficient for Ficoll molecules of radius 50-80 Å (significantly). Again, there was a rapid and sustained increase in these groups of animals, with no significantly graded response relative to the magnitude of trauma induced. The two SHAM groups (followed for 5 and 60 min, in which no laparotomy was performed) showed almost unchanged and identical glomerular Ficoll sieving coefficients over time.

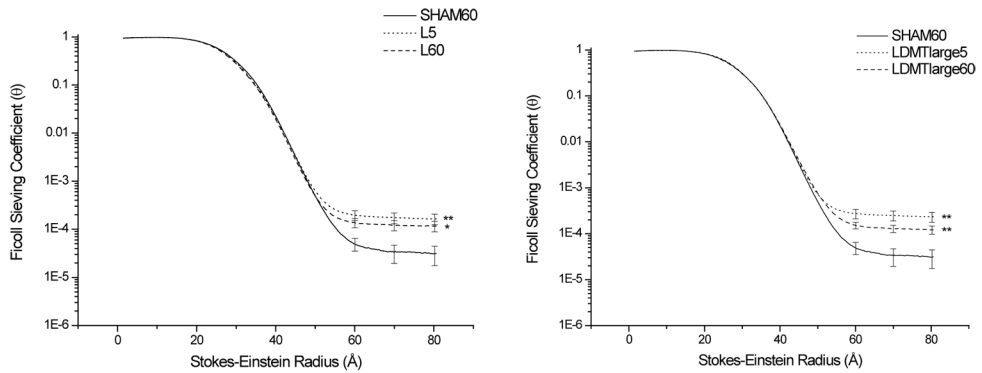


Figure 7a and b. Glomerular Ficoll θ vs. molecular radius for the different experimental groups exposed to laparotomy alone for 5 and 60 min (a.) and animals exposed for laparotomy followed by large muscle trauma for 5 and 60 min (b.).

The θ for albumin showed a significant increase at both 5 and 60 min compared to their respective SHAM groups (Fig. 8 and 9). As for Ficoll_{50-80Å} there was no graded response relative to the trauma inflicted.

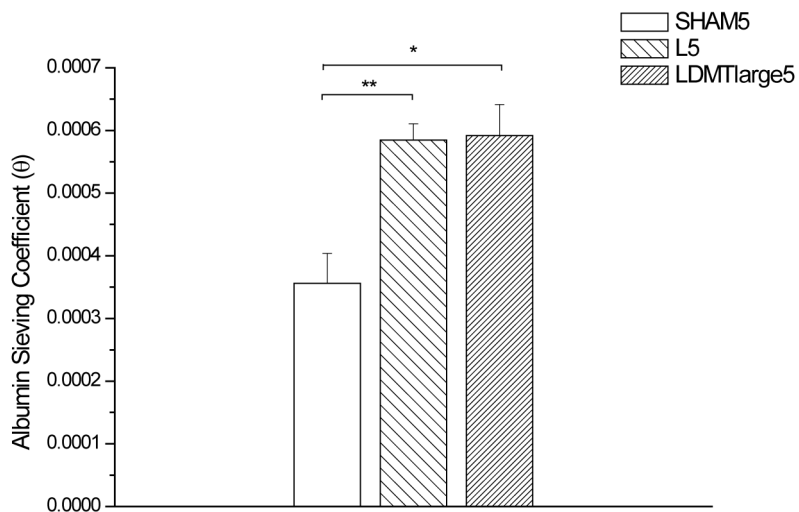


Figure 8. θ_{alb} in groups followed for 5 min, SHAM *vs.* trauma.

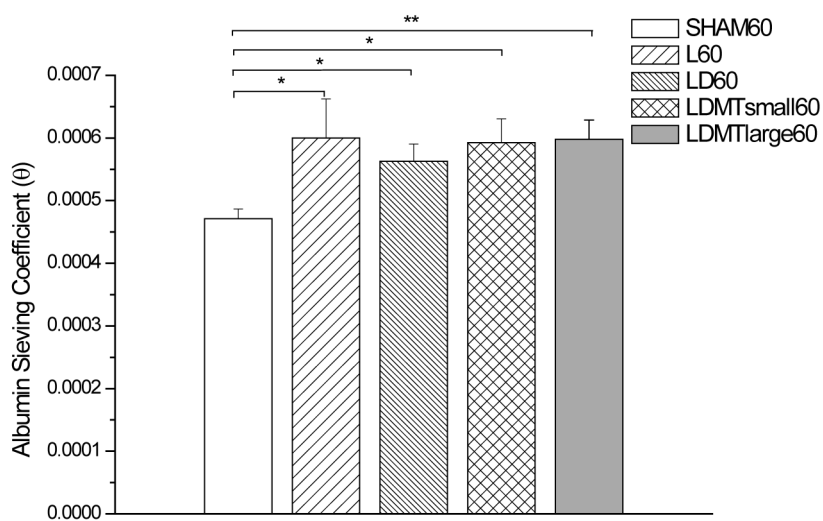


Figure 9. θ_{alb} for groups followed for 60 min. There was a significant increase in θ_{alb} between each of the trauma groups and SHAM.

Rapid, reversible increases in glomerular permeability due to hyperglycemia. Inhibition by a Rho-kinase inhibitor (study III)

Animals exposed to hyperglycemia were followed over time, at 5, 20 and 60 min (Fig. 10). Hyperglycemia caused significant increases in θ for large Ficoll molecules at 20 min, but the changes were completely reversible within 60 min. However, in contrast to the changes seen in anaphylactic shock and after laparotomy there were no changes in glomerular permeability observed already after 5 min.

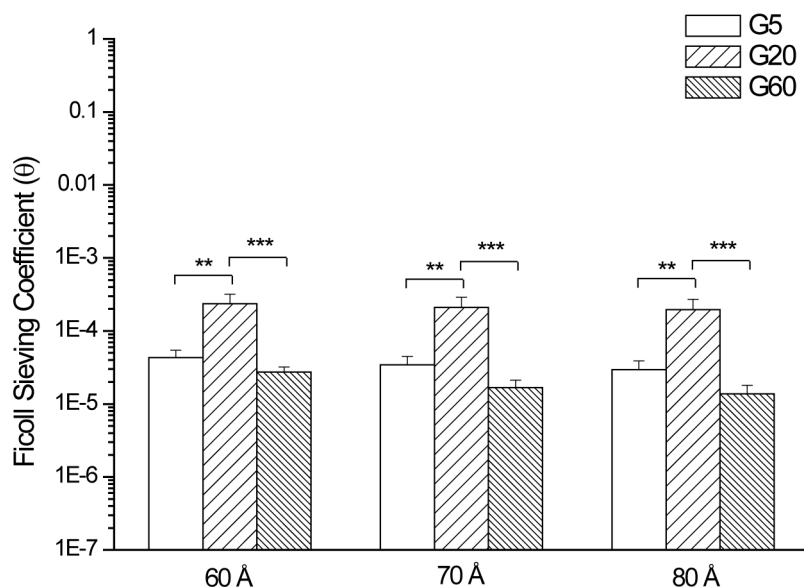


Figure 10. θ of Ficoll 60, 70 and 80 Å as a function of time in animals receiving glucose. There was a complete reversal of the glomerular permeability increase noted at 20 min, at 60 min.

After 20 min, animals exposed to hyperglycemia showed an increase in θ for Ficoll_{50-80Å} compared to SHAM. These results are in line with findings by Hempel *et al.*⁷⁷, using high concentrations of glucose in studies on endothelial monolayers. By contrast, animals receiving hypertonic mannitol or hypertonic NaCl showed no changes in θ for high MW Ficoll, similar to the SHAM group, indicating that the increase in plasma crystalloid osmotic pressure was not responsible for the θ increase. Furthermore mannitol is not known to induce permeability changes⁷⁸, rather the contrary. Thus an increased crystalloid osmotic pressure *per se* is not likely to be responsible for the increased glomerular permeability seen during acute hyperglycemia.

When giving glucose together with a Rho-kinase inhibitor (Y-27632), the glucose induced increase in glomerular permselectivity was totally abrogated, and the perm-

selectivity for this group was comparable to the SHAM animals. These results imply that acute hyperglycemia may involve changes in the F-actin cytoskeleton of either the endothelial cells or the podocytes, since RhoA and Rho-kinase are important players in the signaling of the cytoskeleton.

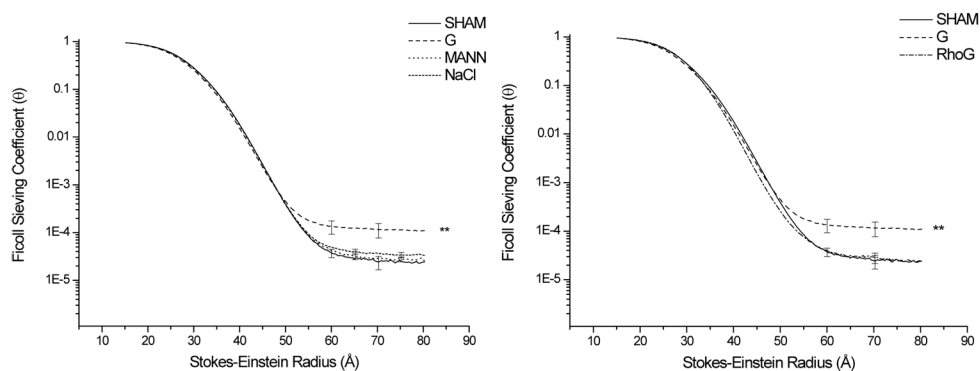


Figure 11a and b. Glomerular sieving coefficients for Ficoll 15-80 Å for animals injected with glucose, mannitol or NaCl *vs.* SHAM (a.) and during Rho-kinase inhibition (b.). During Rho-kinase inhibition, the permeability increase seen during glucose infusion alone, was completely abolished.

Morphological examination of kidney ultrastructure of animals receiving glucose *vs.* SHAM animals showed no significant changes (Fig. 12). All structures of the glomerular filter were investigated at high magnification, and no overt morphological changes with respect to endothelial cells, glomerular basement membrane or podocytes were found.

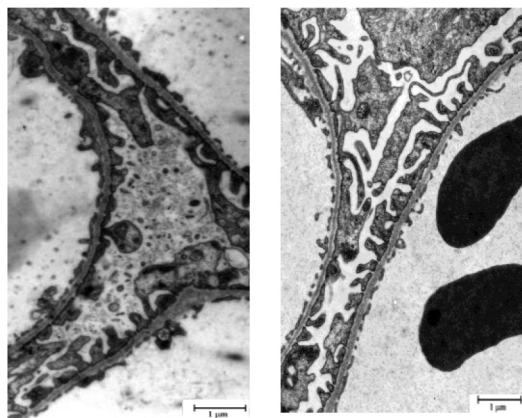


Figure 12. Morphological examination of SHAM animals (left) and animals exposed to hyperglycemia, followed for 20 min (right).

ANP induced rapid, cyclic alterations in glomerular permselectivity (study IV)

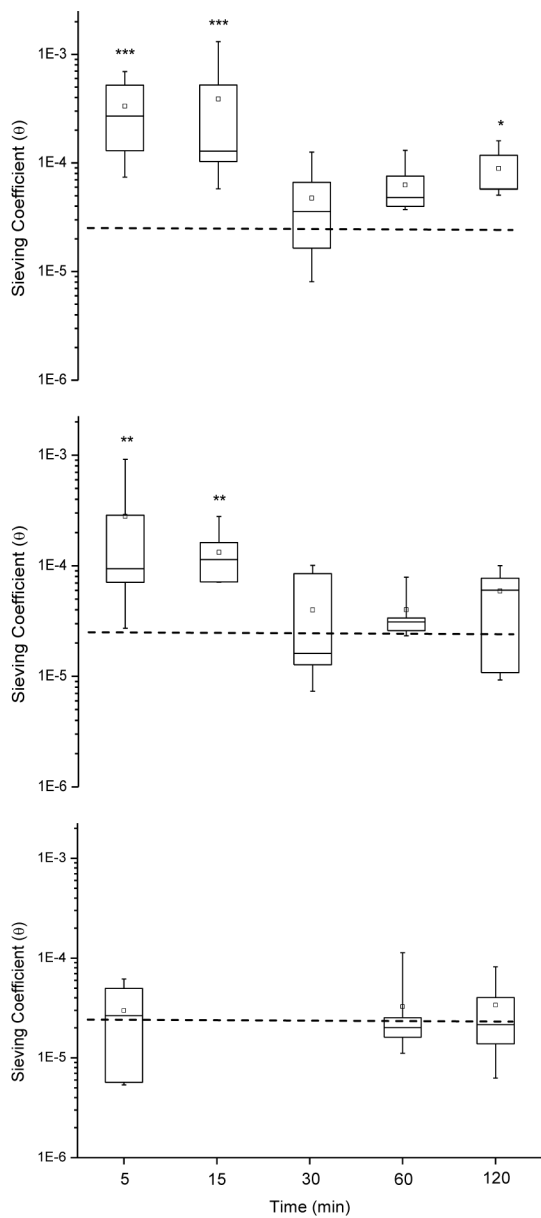


Figure 13. θ for Ficoll 70 Å for high dose ANP (top), low dose ANP (middle) and SHAM (bottom) as a function of time. Values are given as medians and ranges within the boxes. Hatched lines represent SHAM values.

Sequential measurements of animals intravenously infused with ANP demonstrated an immediate increase in θ for Ficoll_{50-80 Å}. Thus, already after 5 min there was a significant increase in glomerular permeability that was still evident after 15 min for both the low (30 ng·kg⁻¹·min⁻¹) and high dose (800 ng·kg⁻¹·min⁻¹) ANP groups (Fig. 13). For both the low and the high dose ANP group this increase was reversed at 30 min to near SHAM values. In the high dose ANP group there was a bimodal glomerular permeability increase. After the initial large peak (at 5 and 15 min) and a dip (at 30 min), there was a moderate increase at 60 and 120 min in θ for Ficoll_{50-80 Å}, which was statistically significant. For the low dose ANP group there was only a tendency of a glomerular permeability increase at 60 and 120 min (which was not statistically significant).

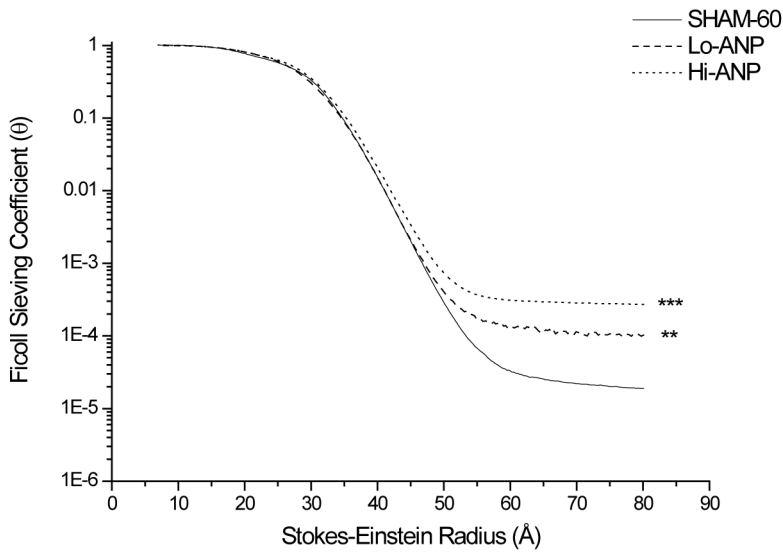


Figure 14. Median curves for Ficoll 15-80 Å *vs.* molecular radius for low and high doses of ANP after 15 min *vs.* SHAM.

Discussion

Glomerular permeability under normal conditions

Though highly variable, normal UAER is about 5 mg to 30 mg daily in man. For 20 mg in UAER per day and 95 % of albumin being subject to proximal tubular reabsorption (PTR), 400 mg of albumin will appear in the primary urine daily. This corresponds to a θ_{alb} of $400 / 180 \times 40\,000 = 6 \times 10^{-5}$. This θ_{alb} is consistent with 8×10^{-5} measured in patients with Dent's disease, lacking PTR⁷⁶, and with 2×10^{-4} measured in megalin knock-out mice, also largely devoid of PTR³². It is also consistent with measurements in rats, in which the PTR was inhibited by lysine³³ and conforms to the value given in the recent review by Haraldsson *et al.*¹⁵.

Contrary to this "glomerulocentric" view of glomerular proteinuria, Comper's group⁷⁹ suggests that the glomerulus produces nephrotic range proteinuria. Recent two-photon detection of fluorescently labeled albumin filtration into the Bowman's space would indicate a θ_{alb} of 0.02, i.e. a value two orders of magnitude higher than the micropuncture assessed values^{43, 80} and results from recent tissue uptake studies⁶⁵. The very high θ of albumin assessed by photometric detection may be due to free label, continuously produced during the measurements, and/or, partially, by quenching of fluorescence in blood by erythrocytes⁸¹.

The GFB as a dynamic barrier

As mentioned above the urinary excretion of albumin and other proteins is highly variable during 24 h and from day to day, both during normal (physiological) and pathophysiological conditions. Reversible increases in UAER, up to the range of micro-albuminuria, can also occur during physical exercise³⁴ and fever etc. The reason for this variability is poorly understood. Hemodynamic factors, i.e. variations in renal blood flow, and, hence in glomerular capillary pressure and GFR, may be partly responsible. Time-dependent variation in the proximal tubular reabsorption of urinary proteins is another tentative explanation. Finally, the phenomenon may be related to direct changes in glomerular permeability, either due to size or charge selective alterations.

From the present thesis, in which it was possible to assess glomerular permeability to macromolecules (Ficoll) in a time-dependent fashion in the absence of proximal tubular reabsorption and charge dependent effects, all during controlled hemodynamic conditions, it is evident that the GFB is not a static barrier. On the contrary, the GFB was found to be highly dynamic and to respond promptly, and mostly reversibly, to a number of different stimuli and challenges. This is a novel concept of the physiology of the GFB²³. The different patterns of acute glomerular permeability changes as a function of time, studied after a number of challenges in this thesis are shown in Figure 15.

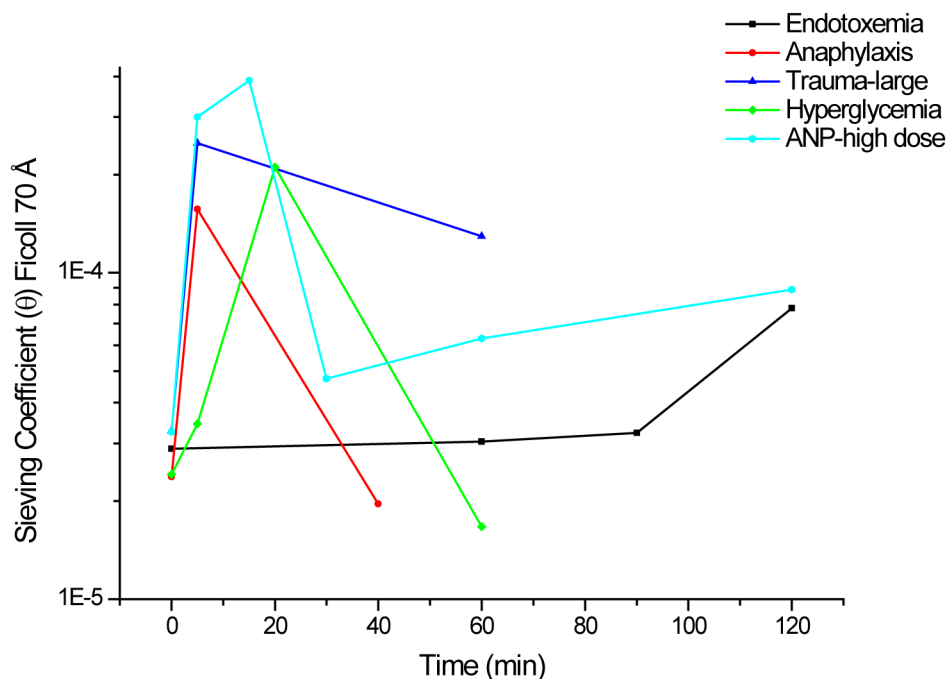


Figure 15. The different patterns of glomerular permeability as a function of time, study I-IV.

All these changes are in the non-nephrotic, microalbuminuria range (20-200 $\mu\text{g}/\text{min}$ in man) and are not *a priori* assumed to be linked to gross morphological changes of the GFB, such as foot process effacement, as seen in the nephrotic syndrome.

The different patterns of glomerular permeability seemed to be individual for each substance or challenge. The slow increase in glomerular permeability seen during endotoxemia, evidently parallels the many events taking place in the induction phase of the systemic inflammation response syndrome (SIRS), involving immune responses and release of cytokines. In the same study (study I), anaphylaxis induced a completely different permeability pattern, with a rapid permeability increase, that was reversed within 40 min. This rapid response reflects the rapid release of mediators, such as histamine, 5-HT and heparin, from mast cells and other immune cells, as a consequence of an acute IgE-mediated type I allergic response.

Body trauma induced a fast increase in glomerular permeability, that was still evident at 60 min after the injury. This rapid increase occurred more or less in all or none fashion, probably as a consequence of release of cytokines⁷⁰ and not to myoglobin (unpublished observations). Laparotomy alone was sufficient to induce marked increase in permeability, but added skin dissection and/or muscle trauma did not increase glomerular permeability further. The response to body trauma may be mediated by activation of immune cells and the release of cytokines, predominantly interleukin (IL)-6 (and IL-10)⁷⁰. Activated leukocytes may also adhere to the endothelium and cause local damage by releasing agents such as reactive oxygen species (ROS).

The transiently increased GFB permeability during acute hyperglycemia had a delayed pattern, similar to what has been observed in hyperglycemia induced permeability changes in endothelial monolayers *in vitro*⁷⁷. Sequential measurements during hyperglycemia demonstrated a peak after 20 min, while the permselectivity was comparable to the SHAM animals both at 5 and 60 min. The mechanisms of an increased glomerular permeability in hyperglycemia will be discussed separately.

High and low doses of ANP showed a rather similar pattern of glomerular permeability. For high dose ANP there was a rapid permeability increase already at 5 (and 15) min. However the ANP induced glomerular leakage seemed to be biphasic, with an initial increase at 5 and 15 min followed by a dip at 30 min, but a moderate subsequent increase at 60 and 120 min. The first permeability peak of ANP was actually quite similar to that seen during anaphylaxis, with a rapid increase, followed by a decline in glomerular permeability within 30-40 min. The direct assessment of glomerular permeability in study IV supports the concept that ANP increased glomerular permeability by direct effects on the glomerular filtration barrier, which did not involve charge dependent changes. ANP (and BNP) acts on the ANP/BNP receptor, guanylyl cyclase-A (GC-A). ANP receptors are seen on podocytes, mostly localized to the foot processes⁸²⁻⁸³. It is evident that ANP might produce podocyte relaxation¹⁹ and it is thus speculated that ANP may alter the shape of the podocyte. These changes apparently involve changes in the F-actin cytoskeleton, and hence the tension the podocytes exert on the GBM, thereby affecting the permeability of the entire GFB.

Microalbuminuria

Microalbuminuria is an established marker of endothelial dysfunction, but can be found normally and in several renal diseases. Microalbuminuria may be an early sign in uncontrolled diabetes mellitus. Microalbuminuria is as common feature following the systemic inflammation response syndrome (SIRS)⁸⁴ and other acute inflammation states, but also after physical exercise³⁴. Microalbuminuria is however not seen during anaphylaxis due to the transient nature of the glomerular permeability changes (study I). Several investigators have shown the presence of microalbuminuria after serious

trauma, thermal injury and after operations, such as after knee and hip surgery^{37-38,85-86}. It has not been established whether the microalbuminuria is due to a glomerular dysfunction, due to either size-selectivity or due to charge selectivity defects, or to a decrease in the tubular reabsorption of albumin. Nergelius *et al.*³⁸ showed a maximal increase in urinary albumin (and IgG) excretion in man one day after surgery, while protein HC showed a maximal increase in the urine two days after surgery, indicating glomerular leakage immediately after surgery and a defect in tubular reabsorption appearing after 24h. During heart failure, often associated with myocardial infarction and ischemic heart disease or cardiomyopathy, the presence of microalbuminuria (and sometimes overt proteinuria) has been shown by different investigators^{36, 71}.

Fundamental behavior of the two-pore model

The two-pore model⁶² has been used throughout the studies (study I-IV) to model the properties of the glomerular filtration barrier and the filtration across the barrier. The radius of the small pore was fairly consistent throughout the studies, and changes in this parameter were uncommon in-between and between the experimental and the SHAM groups. The morphological correlate to the “small pore equivalent” is conceivably the meshes in a rather regular network of molecules (laminin and collagen) in the GBM, and possibly, in the gel-like structure of the endothelial glycocalyx. The large pores may represent very rare ($1/10^7$ of the small pores) irregularities in this meshwork. Whereas an increase in the number of large pores was the regular response when the permeability of the GFB increased, the large pore radius tended to increase in some of the experimental groups, i.e. for low dose ANP, during hyperglycemia and during the rapid increase in glomerular permeability during anaphylaxis. During trauma there was also a tendency of increase in large pore radius. This may reflect an opening of large shunts within the GFB (a third pore), in excess of an increased number of large pores (radius 110-120 Å).

According to the two-pore model albumin is excluded from the small pore pathway by size-selectivity and due to a negatively charged glomerular filter. Due to the negative charges of albumin it thus behaves similar to Ficoll_{50-80Å}⁵⁵ which according to the two-pore theory, solely pass through the large pores. By contrast neutral albumin can, due to its lack of negative charges, pass the small pore pathway, explaining its much higher glomerular permeability than albumin^{65, 71}. Ficoll_{36Å} is hyperpermeable across the GFB compared to native albumin⁴⁷ and will overestimate the radius of the small pores.

For stable GFR, the J_{v_L}/GFR is a more stable and direct parameter than α_L . J_{v_L}/GFR and α_L are mathematically obtained by extra-polating the r_L -curve (for molecules >50 Å in radius) back to the ordinate scale (to 0 Å). This imparts some uncertainty, if r_L is altered. If there is an increment in r_L , α_L and J_{v_L}/GFR tend to be underestimated, and if there is a decrease in r_L , they tend to be overestimated. Both α_L and J_{v_L}/GFR are in

study I-IV seen to increase, when permeability is affected, correlating with the increase in θ for Ficoll_{50-80Å} and θ_{alb} , indicating the presence of an increase in the number of large pores in the GFB.

Possible mechanisms of increased glomerular permeability

The rapid response of the GFB to permeability enhancing stimuli and the (near) complete reversibility of this response within 30–40 min is reminiscent of the cyclic changes that occur in endothelial permeability in response to e.g. histamine, bradykinin or substance P. These alterations are dependent upon the contractile machinery of the endothelium, i.e. F-actin and non-muscle myosin, and are thus known to be Ca^{2+} dependent and rapidly reversible (max 10–15 min), i.e. cyclic, and also subject to tachyphylaxis⁸⁷⁻⁸⁸. After the first bout of permeability increase, the endothelium in rat hindquarter muscle capillaries was found to be refractory for another hour, but still responded to markedly higher doses within that time frame⁸⁷.

Similar to the endothelial cells, podocytes are not static, but contain a contractile system. The contractile system contains actin, myosin and α -actinin-4, among other molecules. Via α -actinin-4 and CD2AP the contractile system is linked to the podocyte slit diaphragm (PSD) and via a $\alpha 3\beta 1$ -integrin and a dystroglycan complex it is linked to the GBM⁸⁹. Although PSD is not believed to be the critical size-selectivity barrier^{65, 90}, the contractile system seems to be of importance to maintain the GFB intact, when e.g. challenged by increased transmural pressure. Alterations in the podocytes may therefore be responsible for secondary changes in the size-selectivity of the GBM and the endothelium.

Hyperglycemia

Acute hyperglycemia in cultured aortic porcine endothelial cell monolayers, induced a rapid increase in monolayer permeability⁷⁷. The effects began within 20 minutes, reached a maximum after 30 minutes and returned to control values within 100 minutes. Administration of a protein kinase C (PKC) inhibitor counteracted the acutely increased endothelial monolayer permeability mediated by hyperglycemia⁷⁷. Several investigators support the notion that PKC is an important mediator of hyperglycemia-induced permeability *in vitro*, suggesting that PKC may be a mediator of hyperglycemia induced hyperpermeability of the GFB. PKC inhibitors are, however, in general too unspecific *in vivo*. Another investigation has shown that hyperglycemia may prime monolayers of cultured bovine glomerular endothelial cells to produce endothelial cell-to-cell disruptions and endothelial cell contraction, and thereby, paracellular holes when co-exposed to e.g. a thromboxane A₂ (TXA₂)-analogue⁹¹. The Rho-kinase inhibi-

tor Y-27632 abrogated the increased permeability induced by the TXA₂ analogue during hyperglycemia in a manner similar to what has been shown in study III. In spite of the increased glomerular permeability following 20 minutes of hyperglycemia, there were no morphological changes observed in the glomerular filtration barrier investigated using TEM.

Podocytes have a highly evolved GLUT glucose transport system⁹² and are one of the cell-types, beside muscle cells and adipocytes, which have been shown to be insulin-sensitive⁹³. After i.v. insulin infusion (unpublished observations), we found no effect of insulin on the rat glomerular permeability. The glucose-lowering effect of the human and porcine insulin used (canine insulin was no longer available), was, however low under the conditions of marked hyperglycemia, which raises some questions of the reliability of these experiments. Furthermore there is no obvious support in the literature that insulin should increase the permeability of the GFB.

A few days of sustained hyperglycemia (20 mM) exposure of cultured endothelial cells has been shown to permanently alter cell structure, with centralization of actin filaments in the endothelial cells⁹⁴. Hyperglycemia for 72 hours has been shown to induce apoptosis and foot process effacement of cultured podocytes, and ROS generation has been shown in podocytes after six hours of hyperglycemic exposure⁹⁵. Furthermore glomerular permeability was found to be unaltered in rats exposed to hyperglycemia for three weeks, but not for nine weeks⁷². This is in contrast to the rapid, reversible alterations found in study III.

Rho-kinase and glomerular hyperpermeability during hyperglycemia

The RhoA/Rho-kinase pathway plays an important role in the structure and function of various kidney cells including tubular epithelial cells, mesangial cells and podocytes⁹⁶. Although the many aspects of signaling upstream and downstream of RhoA/Rho-kinase is not understood, it has become evident that RhoA/Rho-kinase pathway is involved in a variety of diseases⁹⁷.

Dynamic rearrangements of the cytoskeleton and cell adhesion are required for various cellular processes such as shape changes and migration. Rho-kinase can exert its actions by the signal molecule RhoA, activating the Rho-kinase by phosphorylating, and thereby, inactivating myosin phosphatase. It is assumed that Rho-mediated inactivation of myosin phosphatase favors myosin light-chain (MLC) phosphorylation in the presence of MLC kinase activity. Conversely, when Rho is inhibited, MLC phosphatase activity increases and MLC phosphorylation is favored. Rho-kinase is an important mediator not only of vascular contraction but also of actin cytoskeleton reorganization, cellular morphology, motility, adhesion and proliferation⁹⁶. With respect to podocyte morphology, some data support that RhoA has a “stabilizing” effect on the F-actin cytoskeleton⁹⁸ while in endothelium RhoA seems to increase F-actin contractility. Our data and the data from Nobe *et al.*⁹¹ do not support the notion that RhoA/Rho-kinase system acts as a “stabilizing podocyte factor”. On the contrary, this system seems to be

involved in the active rearrangements of the F-actin system conceivably occurring in hyperglycemia.

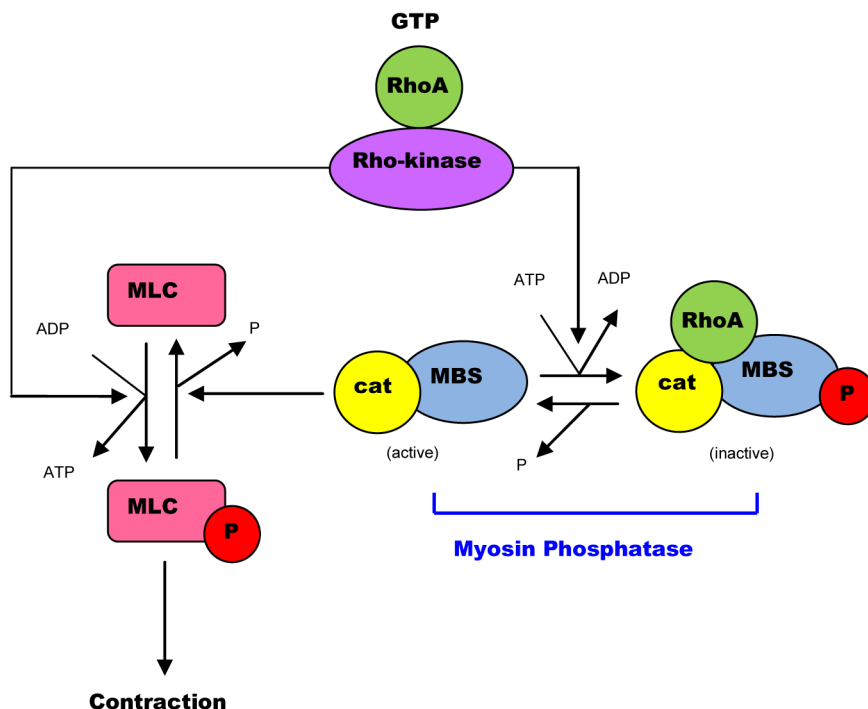


Figure 16. Signalling pathway of RhoA/Rho-kinase. MBS – myosin binding subunit of myosin phosphatase, cat – catalytic subunit of myosin phosphatase and MLC – myosin light chain

Hemodynamic parameters

It has been demonstrated that the sieving coefficients for Ficoll_{13-43A} are reduced when GFR is raised from initially low values to higher (normal range) values in hydropenic rats⁹⁰. This finding contradicts the notion that the PSD would be the critical sieving barrier in the GFB, in which case the opposite would have occurred. The same study also showed a tendency toward a reduction in θ for large Ficoll molecules ($>60\text{-}70\text{\AA}$) with increased GFR. This study supports two previous studies investigating θ *vs.* GFR^{65, 99}, indicating that there is a decrease in θ , for small endogenous proteins and albumin, following increases in GFR. This behavior reflects the increased importance of filtration, as compared to diffusion, (i.e. an increased Peclet number) when GFR is increased.

A parallel increase in $A_0/\Delta X$ together with an increase in GFR will leave the sieving curve unchanged, since both the parameters are changed in the same direction (Peclet number unchanged). The same is true, if both parameters decrease. If a decrease is seen in GFR or an increase occurs for $A_0/\Delta X$, the sieving curve would however, become steeper (a sharper cut-off), while the opposite occurs (i.e. the sieving curve would flatten) when GFR is increased or $A_0/\Delta X$ reduced. It is then important that the Peclet number (essentially GFR over $A_0/\Delta X$) is preserved for all challenges delivered.

Mean arterial pressure (MAP), heart rate and glomerular filtration rate was measured continuously during the experiments in all studies. A summary of average MAP and GFR, respectively, for the four different studies is shown in Figure 17 and 18 respectively.

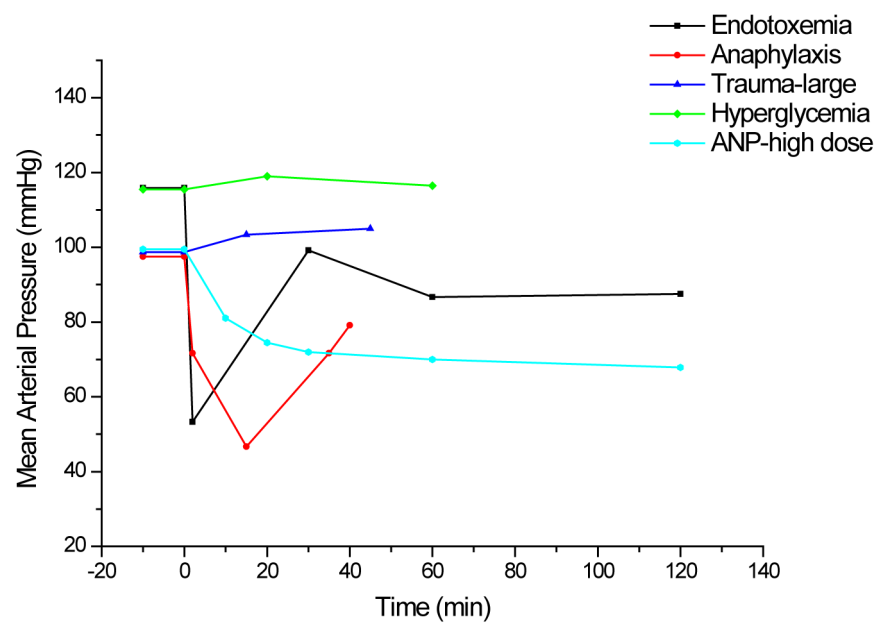


Figure 17. MAP of the four different studies (Study I-IV).

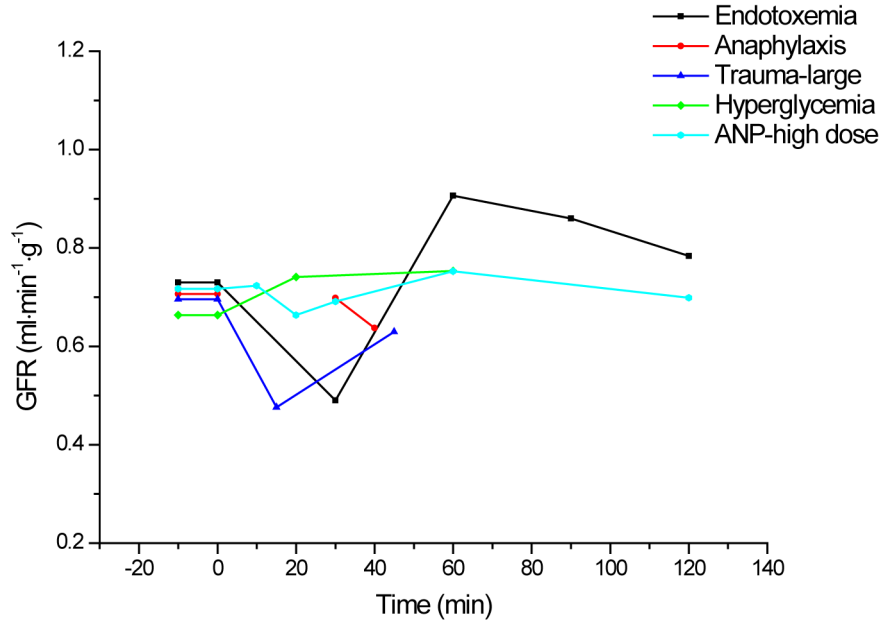


Figure 18. GFR of the four different studies (Study I-IV).

Even though great variability was seen for MAP and/or GFR during the experiments, i.e. in LPS induced sepsis, in anaphylactic shock, in large body trauma and in high dose ANP, measurements of θ_{Ficoll} and θ_{alb} were done during rather stable hemodynamic conditions. The significant decrease in MAP during high dose of ANP was not seen during infusion of low dose ANP. Furthermore, whereas there was a decrease in MAP for the high dose of ANP, the GFR was still rather stable (conceivably due to precapillary vasodilatation and postcapillary vasoconstriction). Even though the MAP and GFR varied in some of the other experiments, the θ measurements were done when MAP and GFR showed stable values, i.e. close to the initial values.

Conclusions

- The normal permeability of the rat GFB is very low. The ratio of the albumin concentration in the glomerular ultrafiltrate over that in plasma (θ_{alb}) was only 3×10^{-4} during control conditions and θ for Ficoll_{50-80A} was even lower.
- The GFB is highly dynamic and can respond rapidly, and mostly reversibly, to different stimuli and challenges, such as sepsis, anaphylactic shock, trauma, acute hyperglycemia and ANP infusion (cf. congestive heart failure) to cause microalbuminuria.
- Changes in glomerular permeability can occur without visible changes in the structure of the glomerular barrier. These changes are thus different from those occurring in nephrotic range albuminuria, in which foot process effacement is a regular phenomenon.
- The glomerular permeability changes studied seem to reflect a real decrease in size-selectivity, due to increases in the number of large pores in the GFB, and are not linked to changes in charge or to changes in proximal tubular protein reabsorption.
- Hyperglycemia induced glomerular hyperpermeability was transient and could be abrogated by Rho-kinase inhibition, suggesting involvement of the cellular F-actin cytoskeleton in this response.

Populärvetenskaplig sammanfattning (Swedish summary)

Njuren är kroppens reningsfilter, vars främsta uppgift är att befria blodet från avfallsprodukter men också att upprätthålla kroppens vätskebalans. Små molekyler och vätska passerar fritt genom njurens filter medan stora molekyler som proteiner (äggvita) nästan helt förhindras att passera. Den mycket lilla mängd protein som passerar filtret tas normalt tillbaka i njurens tidiga kanalsystem (tubuli). Vid flertalet njursjukdomar fungerar inte njurens filter och proteiner läcker ut i urinen (proteinuri). Vid proteinuri har således njurfiltrets genomsläpplighet förändrats. Små mängder av äggvita (albumin) i urinen (mikroalbuminuri) är utmärkande för många sjukdomstillstånd och ses vid diabetes, hjärtinfarkt, feber samt efter trauma, såsom knä- och höftledsoperation. Det är viktigt att studera njurens grundläggande egenskaper för att öka insikten i hur äggvita i urinen uppstår. En ökad förståelse för detta kan leda till bättre diagnostik av njursjukdomar och till att njursvikt, med dialys och njurtransplantation som följd, kan bromsas eller eventuellt förhindras.

Den minsta funktionella enheten i njuren kalas nefron (Fig. 1) och består i dess första del av ett kärlnystan (glomerulus) med en omgivande kapsel, Bowmans kapsel. Glomerulus utgörs av små blodkärl, så kallade kapillärer. Kapillärers unika egenskaper gör det möjligt för blodplasma att filtreras över kapillärväggen, ungefär som passagen av vatten och kaffepartiklar i kaffebryggarens kaffefilter. Den filtrerade plasma som passerat kapillärväggen (äggvitefritt plasmavatten) bildar primärurin. Njurens filter utgörs av tre lager: endotelcellerna, det glomerulära basalmembranet (GBM) och podocyterna (Fig. 2). Endotelceller finns närmast blodet och har ett slemartat ytskikt som kallas glykokalyx (med negativa laddningar). Basalmembranet är uppbyggt av ett nätverk av trådliknande molekyler, såsom laminin och kollagen. Podocyterna omsluter kapillärerna och bildar så kallade filtrationsspalter mellan sina fotutskott. Sannolikt spelar alla tre lager roll för att hålla filtret tätt och för att njuren ska fungera korrekt. En störning i något av dessa lager, oavsett i vilket, leder till att protein filtreras ut i urinen. Med hjälp av porer i njurfiltret, små och stora, separeras stora molekyler från vatten och salter från plasma och blir till primärurin.

Det finns en svårighet med att studera proteinuri, vilken består i att de proteiner som filtreras över kapillärväggen i njurens filter nästan fullständigt återupptas tidigt i nefronet (proximala tubuli). Därför använder vi oss av en icke kroppsegen substans när vi studerar njurens filter; icke kroppssega substanser återupptas nämligen nästan inte alls. Vi använder oss av en polysackarid (sockerart) som kallas Ficoll för att mäta njurens genomsläpplighetsegenskaper. Det finns skillnader mellan att använda polysackarider och proteiner. Proteiner är "hårda", kompakta, och i många fall runda, medan polysackarider har en lägre täthet och är mer flexibla.

Experimenten i denna avhandling är gjorda på råtta. Efter sövning opererades katetrar in i svansartär, halsartär samt i de båda halsvenerna. I svansens artär mättes blodtryck och hjärtfrekvens, medan de andra katetrarna användes för tillförsel av olika substanser. En tub lades in i luftstrupen för att underlätta andningen, och i den vänstra uretären sattes en kateter för urinsamling. Ficoll (märkt med fluorescerande markörer) gavs intravenöst (i.v.), det vill säga via en ven. Urin för att mäta koncentrationen av Ficoll samlades under fem minuter, samtidigt som ett blodprov togs i mitten av denna period. De blod- och urinprover som togs för mätning av koncentrationen av Ficoll analyserades sedan genom att använda en så kallad gelfiltrationskolonn, HPSEC, som kan separera polysackariderna efter storlek. Från de koncentrationer som mättes upp för Ficoll i urin och plasma beräknades filtrat-till-plasmakoncentrationskvoten (sieving koefficienter, θ) för respektive molekyelstorlek ($\sim 15\text{--}80$ Ångström, Å) och från denna analys erhöles "glomerulära sievingkurvor" för Ficoll. De användes sedan för att bestämma storleken på små och stora porer i njurfiltret med hjälp av en pormodell. Radioaktivt albumin användes för mätning av dess filtration (och återupptag) i njuren med en så kallad vävnadsupptagsteknik.

I den första studien (study I) undersöktes hur njurfiltrets genomsläpplighet i råtta förändras vid blodförgiftning orsakat av ett gift från coli-bakterier (lipopolysackarid, LPS), samt vid allergisk chock (anafylaktisk chock). Studien visade att blodförgiftning under 120 min orsakar en ökning i sievingkoefficient för Ficollmolekyler i storlek 50-80 Å. Hos djur som erhöles LPS och följdes under bara 60 och 90 min sågs ingen ökning av genomsläppligheten för Ficoll. Radioaktivt albumin visade överensstämmande resultat med Ficoll. Anafylaktisk chock orsakades genom att ge djuren polysackariden dextran, vilken i rättor framkallar ett chocktillstånd. Efter 5 min påvisades en förhöjd genomsläpplighet för Ficoll_{50-80Å}, som tecken på öppning av "stora porer" i njurfiltret, som helt gick tillbaka efter 40 min. Mätningar med radioaktivt albumin påvisade dock ett ökat njurbarksupptag av albumin vid båda tidpunkterna. Ett ökat upptag av albumin till njurbarken vid 40 min kan bäst förklaras med att andra kapillärer än glomeruluskapillärer i njuren har fått en ökad genomsläpplighet för albumin vid den framkallade chocken även efter det att glomeruluskapillärer "stängts".

Studie nummer två (study II) fokuserade på den glomerulära genomsläppligheten efter kroppsskada (trauma) med eller utan krosskada. För att framkalla ett trauma gjordes ett medellinjessnitt i buken på djuret (laparotomi). Utöver detta trauma gjordes sedan på vissa djur en krosskada genom att krossa främre bukmuskeln på höger och vänster sida med en grov peang. Resultaten visade att en öppning av buken var tillräcklig för

att ge en kraftig ökning av genomsläppligheten för Ficoll_{50-80Å}. Tillägg av krosskada ökade inte ytterligare genomsläppligheten för Ficoll_{50-80Å}. Dessa resultat gällde vid såväl 5 som 60 min efter orsakat trauma. Studier med radioaktivt albumin påvisade en ökad sievingkoefficient vid laparotomi samt laparotomi med extra krosskada vid båda tidpunkterna. Poranalysen påvisade ett ökat antal stora porer i njurens filter efter trauma, såväl som en ökning i dess storlek.

I studie nummer tre (study III) studerades njurens genomsläpplighet för Ficoll vid högt blodsocker. Högt blodsocker orsakades i djuren genom att ge dessa en stark druvsocker (glukos) – blandning. Tjugo minuter efter blodsockerhöjning (>20 mmol/l) sågs genomsläppligheten för Ficoll_{50-80Å} öka i njurens filter. Men redan efter 5 min och efter 60 min sågs ingen ökning. Stark mannitollosning (en annan sockerart som liknar glukos) eller en stark saltblandning innehållande natriumklorid (NaCl) gavs till två grupper av djur. Resultaten visade att genomsläppligheten inte ökade för Ficoll_{50-80Å} under dessa förhållanden. Vi undersökte också om en specifik signalmolekyl-hämmare (Rho-kinashämmare) kunde motverka den ökade genomsläppligheten vid ett blodsocker över 20 mmol/l. Om vi gav djuren denna substans samtidigt som vi orsakade högt blodsocker sågs ingen ökning i genomsläpplighet för Ficoll_{50-80Å}, vilket visar att vår utvalda signalmolekyl spelar en viktig roll för en ökad genomsläpplighet över njurens filter vid högt blodsocker. Eftersom Rho-kinas kan påverka cellers förmåga att ändra form, tycks den ändrade permeabiliteten bero på cellförändring. Poranalysen visade ett ökat antal stora porer i njurens filter 20 min efter givande av högt blodsocker samt en ökning av de stora porernas storlek.

Mikroalbuminuri är en vanlig företeelse vid hjärtsvikt. I studie nummer fyra (study IV) studerades hur ANP (atrial natriuretic peptide), som frisätts hos patienter med hjärtinfarkt eller hjärtsvikt påverkar njurens filter. ANP gavs till djuren och den glomerulära genomsläppligheten för Ficoll studerades under 120 min med sekventiella mätningar vid 5, 15, 30, 60 och 120 min. ANP gavs i antingen en låg eller en hög dos. Resultaten visade att ANP, både i låg och hög dos, orsakar en ökning av genomsläppligheten för Ficoll_{50-80Å} med start vid 5 min och maximal effekt efter 15 min. Vid 30 min återgick genomsläppligheten till det normala, för att sedan återigen sakta öka vid 60 och 120 min. Dessa resultat talar för att ANP kan vara ansvarigt för den mikroalbuminuri som ses hos patienter med hjärtsvikt eller hjärtinfarkt.

Det primära syftet med avhandlingen är att försöka förstå bakgrunden till äggvita (albumin) i urinen vid en rad olika sjukdomstillstånd som blodförgiftning, hjärtsvikt, anafylaktisk chock och efter trauma.

Grants

This work was supported by the Swedish Medical Research Council, grant #08285 (Vetenskapsrådet); ALF grant from the Medical Faculty, Lund University; Swedish Heart and Lung Foundation (Hjärt-Lungfonden); Kungliga Fysiografiska Sällskapet, Lund; Vascular Wall Programme, Lund University and The Lundberg Foundation. All support is gratefully acknowledged!

Acknowledgements

Jag vill tacka alla som på ett eller annat sätt har bidragit till förverkligandet av denna avhandling och som dessutom under årens lopp har förgyllt min tillvaro som doktorand. Jag vill särskilt framföra ett stort tack till följande personer:

Min handledare **Bengt Rippe**, för att du gav mig chansen att vara en del av din forskningsgrupp och för allt du har lärt mig om forskning och vetenskap. Tack för din entusiasm, support och ditt engagemang. För att du alltid tar dig tid att diskutera problem och för att du alltid har svar på mina frågor. Jag kan inte tänka mig en bättre handledare!

Anna Rippe, laboratorieassistent och min kompanjon på labbet. Tack för ett suveränt samarbete under dessa år och för att du alltid har tid och alltid vill hjälpa mig med allt. Tack för skratt, vänskap, intressanta diskussioner och för din enorma generositet och värme!

Kerstin Wihlborg, Avd. för Njurmedicin. Tack för att du alltid hjälper mig med alla möjliga små och stora uppgifter/problem och för att du är den glada, omtänksamma och positiva människa som du är.

Catarina Rippe, min handledare under examensarbetet och som sedan har fortsatt att vara till stor hjälp under min doktorandtid. Tack för att du alltid har tid att svara på mina frågor och hjälpa mig med små och stora problem!

Alla nuvarande och tidigare kollegor i forskningsgruppen; **Daniel, Daniele, Sudi, Berra, Irma, Pelle** och **Kristinn**. Tack för alla intressanta diskussioner, luncher och fikastrunder under dessa år.

Per-Olof Grändes forskningsgrupp på BMC F11. Tack för alla skratt, vetenskapliga och icke vetenskapliga diskussioner på luncher och fikastrunder. Ett extra stort tack till **Helén Axelberg** för mycket trevligt sällskap på eftermiddagar och kvällar. Det har blivit en hel del trevliga pratstrunder under dessa år.

Martin Nyström för all hjälp med mina datorer.

Lina Gefors och **Eric Carlemalm** på Elektronmikroskopienheten, Medicinska fakulteten, Lunds Universitet, för utmärkt introduktion och hjälp med TEM och TEM förberedelser.

Markus, för att du orkar med mig alla dagar, alla år. ☺ För all support du har gett mig under dessa år, för all tid, alla tankar och för att du är den fina människa du är! Tack för att du finns!

Min fina syster **Fredrika**, för att du får mig att tänka på annat och tar med mig på en promenad eller en shoppingrunda. Tack för alla fikastunder och middagar! Tack också till **Jalle** och älskade **Algot** för att ni alltid får mig att skratta och le.

Min **mormor**, för all kärlek och stöd under dessa år. För ditt intresse för det jag gör och för att din stora envishet har gjort mig till en lagom envis människa.

Alla mina vänner, för att ni är fantastiska, omtänksamma och inspirerande människor som stöttar en i vått och torrt! Det finns några av er som jag vill rikta ett extra stort tack till: **Sandy**, min underbara vän, för att du alltid får mig att skratta och le. You are my sunshine! För att du alltid har en stund över till mig och för att du intresserar dig för det jag gör! **Sofia** för att du är en fantastisk och positiv vän. För alla timmar vi har spenderat tillsammans på Gerdahallen, på luncher och inte minst på danskan ☺. För att du alltid har tid att lyssna och för att du alltid ger mig värdefull vetenskaplig input. **Therese** för att du är en fantastisk och underbar vän. Vi har delat skratt och tårar och shoppat alldeles för mycket. För att du alltid finns där, för en lång eller kort pratstund! **Linda och Josefine**, mina vänner sedan långt tillbaka. Tack för alla AWs, fester och fikastunder. Ni gör mig alltid glad!

Mitt fotbollslag under större delen av doktorandtiden, **Sjöbo IF dam**. Tack till alla medspelare, tränare och ledare genom åren!

Slutligen, **mamma och pappa**. För att ni alltid finns där för mig. För all kärlek och omtanke. För allt ert engagemang i allt jag gör. Ni är fantastiska! Jag älskar er!

References

1. Beltina. Encyclopedia of health. In: <http://www.beltina.org/health-dictionary/nephron-function-kidney-definition.html>; 2011.
2. Deen W. M., Lazzara M. J., Myers B. D. Structural determinants of glomerular permeability. *Am J Physiol Renal Physiol* 2001;281:F579-96.
3. Rostgaard J., Qvortrup K. Electron microscopic demonstrations of filamentous molecular sieve plugs in capillary fenestrae. *Microvasc Res* 1997;53:1-13.
4. Jeansson M., Haraldsson B. Morphological and functional evidence for an important role of the endothelial cell glycocalyx in the glomerular barrier. *Am J Physiol Renal Physiol* 2006;290:F111-6.
5. Pries A. R., Secomb T. W., Gaetgens P. The endothelial surface layer. *Pflügers Arch* 2000;440:653-66.
6. Hudson B. G., Tryggvason K., Sundaramoorthy M., Neilson E. G. Alport's syndrome, Goodpasture's syndrome, and type IV collagen. *N Engl J Med* 2003;348:2543-56.
7. Miner J. H. Renal basement membrane components. *Kidney Int* 1999;56:2016-24.
8. Pavenstadt H., Kriz W., Kretzler M. Cell biology of the glomerular podocyte. *Physiol Rev* 2003;83:253-307.
9. Rodewald R., Karnovsky M. J. Porous substructure of the glomerular slit diaphragm in the rat and mouse. *J Cell Biol* 1974;60:423-33.
10. Sellin L., Huber T. B., Gerke P., Quack I., Pavenstadt H., Walz G. NEPH1 defines a novel family of podocin interacting proteins. *FASEB J* 2003;17:115-7.
11. Tryggvason K., Patrakka J., Wartiovaara J. Hereditary proteinuria syndromes and mechanisms of proteinuria. *N Engl J Med* 2006;354:1387-401.
12. Ruotsalainen V., Ljungberg P., Wartiovaara J., Lenkkeri U., Kestila M., Jalanko H., Holmberg C., Tryggvason K. Nephin is specifically located at the slit diaphragm of glomerular podocytes. *Proc Natl Acad Sci U S A* 1999;96:7962-7.
13. Tryggvason K. Unraveling the mechanisms of glomerular ultrafiltration: nephrin, a key component of the slit diaphragm. *J Am Soc Nephrol* 1999;10:2440-5.
14. Cheng H., Harris R. C. The glomerulus--a view from the outside--the podocyte. *Int J Biochem Cell Biol* 2010;42:1380-7.
15. Haraldsson B., Nystrom J., Deen W. M. Properties of the glomerular barrier and mechanisms of proteinuria. *Physiol Rev* 2008;88:451-87.
16. Churg J Bernstein J, Glassock RJ. *Renal Disease. Classification and Atlas of Glomerular Diseases*. In: Atlas of Diseases of the Kidney. New York: SpringerImages; 2011.

17. Kestila M., Lenkkeri U., Mannikko M., Lamerdin J., McCready P., Putaala H., Ruotsalainen V., Morita T., Nissinen M., Herva R., Kashtan C. E., Peltonen L., Holmberg C., Olsen A., Tryggvason K. Positionally cloned gene for a novel glomerular protein--nephricin--is mutated in congenital nephrotic syndrome. *Mol Cell* 1998;1:575-82.
18. Hsu H. H., Hoffmann S., Endlich N., Velic A., Schwab A., Weide T., Schlatter E., Pavenstadt H. Mechanisms of angiotensin II signaling on cytoskeleton of podocytes. *J Mol Med* 2008;86:1379-94.
19. Sharma R., Lovell H. B., Wiegmann T. B., Savin V. J. Vasoactive substances induce cytoskeletal changes in cultured rat glomerular epithelial cells. *J Am Soc Nephrol* 1992;3:1131-8.
20. Weins A., Kenlan P., Herbert S., Le T. C., Villegas I., Kaplan B. S., Appel G. B., Pollak M. R. Mutational and Biological Analysis of alpha-actinin-4 in focal segmental glomerulosclerosis. *J Am Soc Nephrol* 2005;16:3694-701.
21. Jarad G., Cunningham J., Shaw A. S., Miner J. H. Proteinuria precedes podocyte abnormalities in *Lamb2*^{-/-} mice, implicating the glomerular basement membrane as an albumin barrier. *J Clin Invest* 2006;116:2272-9.
22. Karumanchi S. A., Maynard S. E., Stillman I. E., Epstein F. H., Sukhatme V. P. Preeclampsia: a renal perspective. *Kidney Int* 2005;67:2101-13.
23. Jarad G., Miner J. H. Update on the glomerular filtration barrier. *Curr Opin Nephrol Hypertens* 2009;18:226-32.
24. Kalluri R. Proteinuria with and without renal glomerular podocyte effacement. *J Am Soc Nephrol* 2006;17:2383-9.
25. Mathieson P. W. The cellular basis of albuminuria. *Clin Sci (Lond)* 2004;107:533-8.
26. Jeansson M., Haraldsson B. Glomerular size and charge selectivity in the mouse after exposure to glucosaminoglycan-degrading enzymes. *J Am Soc Nephrol* 2003;14:1756-65.
27. Bolton G. R., Deen W. M., Daniels B. S. Assessment of the charge selectivity of glomerular basement membrane using Ficoll sulfate. *Am J Physiol* 1998;274:F889-96.
28. Bakoush O., Torffvit O., Rippe B., Tencer J. Renal function in proteinuric glomerular diseases correlates to the changes in urine IgM excretion but not to the changes in the degree of albuminuria. *Clin Nephrol* 2003;59:345-52.
29. Nielsen R., Christensen E. I. Proteinuria and events beyond the slit. *Pediatr Nephrol* 2010;25:813-22.
30. Amsellem S., Gburek J., Hamard G., Nielsen R., Willnow T. E., Devuyst O., Nexø E., Verroust P. J., Christensen E. I., Kozyraki R. Cubilin is essential for albumin reabsorption in the renal proximal tubule. *J Am Soc Nephrol* 2010;21:1859-67.
31. Birn H., Christensen E. I. Renal albumin absorption in physiology and pathology. *Kidney Int* 2006;69:440-9.
32. Christensen E. I., Birn H., Rippe B., Maunsbach A. B. Controversies in nephrology: renal albumin handling, facts, and artifacts! *Kidney Int* 2007;72:1192-4.
33. Tencer J., Frick I. M., Oquist B. W., Alm P., Rippe B. Size-selectivity of the glomerular barrier to high molecular weight proteins: upper size limitations of shunt pathways. *Kidney Int* 1998;53:709-15.
34. Bellinghieri G., Savica V., Santoro D. Renal alterations during exercise. *J Ren Nutr* 2008;18:158-64.
35. Dronavalli S., Duka I., Bakris G. L. The pathogenesis of diabetic nephropathy. *Nat Clin Pract Endocrinol Metab* 2008;4:444-52.

36. Gosling P, Hughes E. A., Reynolds T. M., Fox J. P. Microalbuminuria is an early response following acute myocardial infarction. *Eur Heart J* 1991;12:508-13.
37. Gosling P, Sanghera K., Dickson G. Generalized vascular permeability and pulmonary function in patients following serious trauma. *J Trauma* 1994;36:477-81.
38. Nergelius G., Vinge E., Grubb A., Lidgren L. Renal impairment after hip or knee arthroplasty. Urinary excretion of protein markers studied in 59 patients. *Acta Orthop Scand* 1997;68:34-40.
39. Nielsen S. H., Petersen J. S., Magid E. Albuminuria in ischemic heart disease. *Scand J Clin Lab Invest Suppl* 1999;230:143-52.
40. Maddox D., Deen WM., Brenner BM. Glomerular Filtration. In: *Handbook of Physiology-Renal Physiology*: Bethesda, MD: American Physiological Society; 1992:545-638.
41. Michel CC. Fluid movements through capillary walls. In: *Handbook of physiology - Renal physiology*: American Physiological Society; 1984:375-409.
42. Renkin EM., Gilmore, JP. Glomerular filtration. In: *Handbook of physiology - Renal physiology*: Washington DC: American Physiological Society; 1973:185-248.
43. Maack T., Park Hyung C., Camargo F José M. Renal Filtration, Transport and Metabolism of Proteins. In: *The Kidney: Physiology and Pathophysiology*. New York: Raven Press; 1985.
44. Fissell W. H., Manley S., Dubnisheva A., Glass J., Magistrelli J., Eldridge A. N., Fleischman A. J., Zydny A. L., Roy S. Ficoll is not a rigid sphere. *Am J Physiol Renal Physiol* 2007;293:F1209-13.
45. Lavrenko P. N., Mikriukova O. I., Okatova O. V. On the separation ability of various Ficoll gradient solutions in zonal centrifugation. *Anal Biochem* 1987;166:287-97.
46. Fissell W. H., Hofmann C. L., Smith R., Chen M. H. Size and conformation of Ficoll as determined by size-exclusion chromatography followed by multiangle light scattering. *Am J Physiol Renal Physiol* 2010;298:F205-8.
47. Venturoli D., Rippe B. Ficoll and dextran vs. globular proteins as probes for testing glomerular permselectivity: effects of molecular size, shape, charge, and deformability. *Am J Physiol Renal Physiol* 2005;288:F605-13.
48. Bohrer M. P., Baylis C., Humes H. D., Glasscock R. J., Robertson C. R., Brenner B. M. Permselectivity of the glomerular capillary wall. Facilitated filtration of circulating polycations. *J Clin Invest* 1978;61:72-8.
49. Chang R. L., Deen W. M., Robertson C. R., Brenner B. M. Permselectivity of the glomerular capillary wall: III. Restricted transport of polyanions. *Kidney Int* 1975;8:212-8.
50. Comper W. D., Glasgow E. F. Charge selectivity in kidney ultrafiltration. *Kidney Int* 1995;47:1242-51.
51. Lindstrom K. E., Johnsson E., Haraldsson B. Glomerular charge selectivity for proteins larger than serum albumin as revealed by lactate dehydrogenase isoforms. *Acta Physiol Scand* 1998;162:481-8.
52. Guasch A., Deen W. M., Myers B. D. Charge selectivity of the glomerular filtration barrier in healthy and nephrotic humans. *J Clin Invest* 1993;92:2274-82.
53. Vyas S. V., Comper W. D. Dextran sulfate binding to isolated rat glomeruli and glomerular basement membrane. *Biochim Biophys Acta* 1994;1201:367-72.
54. Adal Y., Pratt L., Comper W. D. Transglomerular transport of DEAE dextran in the isolated perfused kidney. *Microcirculation* 1994;1:169-74.

55. Ohlson M., Sorensson J., Lindstrom K., Blom A. M., Fries E., Haraldsson B. Effects of filtration rate on the glomerular barrier and clearance of four differently shaped molecules. *Am J Physiol Renal Physiol* 2001;281:F103-13.
56. Asgeirsson D., Venturoli D., Fries E., Rippe B., Rippe C. Glomerular sieving of three neutral polysaccharides, polyethylene oxide and bikunin in rat. Effects of molecular size and conformation. *Acta Physiol (Oxf)* 2007;191:237-46.
57. Bohrer M. P., Deen W. M., Robertson C. R., Troy J. L., Brenner B. M. Influence of molecular configuration on the passage of macromolecules across the glomerular capillary wall. *J Gen Physiol* 1979;74:583-93.
58. Rennke H. G., Venkatachalam M. A. Glomerular permeability of macromolecules. Effect of molecular configuration on the fractional clearance of uncharged dextran and neutral horseradish peroxidase in the rat. *J Clin Invest* 1979;63:713-7.
59. Lindstrom K. E., Blom A., Johnsson E., Haraldsson B., Fries E. High glomerular permeability of bikunin despite similarity in charge and hydrodynamic size to serum albumin. *Kidney Int* 1997;51:1053-8.
60. Mason EA Wendt RP and Bresler EH. Similarity relations (dimensional analysis) for membrane transport. *Journal of Membrane science* 1980;6.
61. Renkin E. M. Filtration, diffusion, and molecular sieving through porous cellulose membranes. *J Gen Physiol* 1954;38:225-43.
62. Rippe B., Haraldsson B. Transport of macromolecules across microvascular walls: the two-pore theory. *Physiol Rev* 1994;74:163-219.
63. Kedem O., Katchalsky A. Thermodynamic analysis of the permeability of biological membranes to non-electrolytes. *Biochim Biophys Acta* 1958;27:229-46.
64. Kedem O., Katchalsky A. A physical interpretation of the phenomenological coefficients of membrane permeability. *J Gen Physiol* 1961;45:143-79.
65. Lund U., Rippe A., Venturoli D., Tenstad O., Grubb A., Rippe B. Glomerular filtration rate dependence of sieving of albumin and some neutral proteins in rat kidneys. *Am J Physiol Renal Physiol* 2003;284:F1226-34.
66. Rippe B., Haraldsson B. Fluid and protein fluxes across small and large pores in the microvasculature. Application of two-pore equations. *Acta Physiol Scand* 1987;131:411-28.
67. Rietschel E. T., Kirikae T., Schade F. U., Mamat U., Schmidt G., Loppnow H., Ulmer A. J., Zahring U., Seydel U., Di Padova F., et al. Bacterial endotoxin: molecular relationships of structure to activity and function. *FASEB J* 1994;8:217-25.
68. Bosshart H., Heinzelmann M. Targeting bacterial endotoxin: two sides of a coin. *Ann N Y Acad Sci* 2007;1096:1-17.
69. Cunningham P. N., Wang Y., Guo R., He G., Quigg R. J. Role of Toll-like receptor 4 in endotoxin-induced acute renal failure. *J Immunol* 2004;172:2629-35.
70. Bansch P., Lundblad C., Grande P. O., Bentzer P. A model for evaluating the effects of blunt skeletal muscle trauma on microvascular permeability and plasma volume in the rat. *Shock* 2010;33:399-404.
71. Rippe C., Rippe A., Larsson A., Asgeirsson D., Rippe B. Nature of glomerular capillary permeability changes following acute renal ischemia-reperfusion injury in rats. *Am J Physiol Renal Physiol* 2006;291:F1362-8.
72. Rippe C., Rippe A., Torffvit O., Rippe B. Size and charge selectivity of the glomerular filter in early experimental diabetes in rats. *Am J Physiol Renal Physiol* 2007;293:F1533-8.

73. Tenstad O., Roald A. B., Grubb A., Aukland K. Renal handling of radiolabelled human cystatin C in the rat. *Scand J Clin Lab Invest* 1996;56:409-14.
74. Tenstad O., Williamson H. E., Clausen G., Oien A. H., Aukland K. Glomerular filtration and tubular absorption of the basic polypeptide aprotinin. *Acta Physiol Scand* 1994;152:33-50.
75. Tojo A., Endou H. Intrarenal handling of proteins in rats using fractional micropuncture technique. *Am J Physiol* 1992;263:F601-6.
76. Norden A. G., Lapsley M., Lee P. J., Pusey C. D., Scheinman S. J., Tam F. W., Thakker R. V., Unwin R. J., Wrong O. Glomerular protein sieving and implications for renal failure in Fanconi syndrome. *Kidney Int* 2001;60:1885-92.
77. Hempel A., Maasch C., Heintze U., Lindschau C., Dietz R., Luft F. C., Haller H. High glucose concentrations increase endothelial cell permeability via activation of protein kinase C alpha. *Circ Res* 1997;81:363-71.
78. Lindstrom K. E., Ronnstedt L., Jaremko G., Haraldsson B. Physiological and morphological effects of perfusing isolated rat kidneys with hyperosmolal mannitol solutions. *Acta Physiol Scand* 1999;166:231-8.
79. Russo L. M., Sandoval R. M., McKee M., Osicka T. M., Collins A. B., Brown D., Molitoris B. A., Comper W. D. The normal kidney filters nephrotic levels of albumin retrieved by proximal tubule cells: retrieval is disrupted in nephrotic states. *Kidney Int* 2007;71:504-13.
80. Landwehr D. M., Carvalho J. S., Oken D. E. Micropuncture studies of the filtration and absorption of albumin by nephrotic rats. *Kidney Int* 1977;11:9-17.
81. Peti-Peterdi J. Independent two-photon measurements of albumin GSC give low values. *Am J Physiol Renal Physiol* 2009;296:F1255-7.
82. Shimonaka M., Saheki T., Hagiwara H., Hagiwara Y., Sono H., Hirose S. Visualization of ANP receptor on glomeruli of bovine kidney by use of a specific antiserum. *Am J Physiol* 1987;253:F1058-62.
83. Lewko B., Stepinski J. Cyclic GMP signaling in podocytes. *Microsc Res Tech* 2002;57:232-5.
84. Davies M. G., Hagen P. O. Systemic inflammatory response syndrome. *Br J Surg* 1997;84:920-35.
85. Gosling P., Shearman C. P., Gwynn B. R., Simms M. H., Bainbridge E. T. Microproteinuria: response to operation. *Br Med J (Clin Res Ed)* 1988;296:338-9.
86. Vlachou E., Gosling P., Moiem N. S. Microalbuminuria: a marker of endothelial dysfunction in thermal injury. *Burns* 2006;32:1009-16.
87. Haraldsson B., Zackrisson U., Rippe B. Calcium dependence of histamine-induced increases in capillary permeability in isolated perfused rat hindquarters. *Acta Physiol Scand* 1986;128:247-58.
88. McDonald D. M., Thurston G., Baluk P. Endothelial gaps as sites for plasma leakage in inflammation. *Microcirculation* 1999;6:7-22.
89. Mundel P., Shankland S. J. Podocyte biology and response to injury. *J Am Soc Nephrol* 2002;13:3005-15.
90. Rippe C., Asgeirsson D., Venturoli D., Rippe A., Rippe B. Effects of glomerular filtration rate on Ficoll sieving coefficients (theta) in rats. *Kidney Int* 2006;69:1326-32.
91. Nobe K., Miyatake M., Sone T., Honda K. High-glucose-altered endothelial cell function involves both disruption of cell-to-cell connection and enhancement of force development. *J Pharmacol Exp Ther* 2006;318:530-9.

92. Lewko B., Stepinski J. Hyperglycemia and mechanical stress: targeting the renal podocyte. *J Cell Physiol* 2009;221:288-95.
93. Coward R. J., Welsh G. I., Yang J., Tasman C., Lennon R., Koziell A., Satchell S., Holman G. D., Kerjaschki D., Tavare J. M., Mathieson P. W., Saleem M. A. The human glomerular podocyte is a novel target for insulin action. *Diabetes* 2005;54:3095-102.
94. Salameh A., Zinn M., Dhein S. High D-glucose induces alterations of endothelial cell structure in a cell-culture model. *J Cardiovasc Pharmacol* 1997;30:182-90.
95. Eid A. A., Gorin Y., Fagg B. M., Maalouf R., Barnes J. L., Block K., Abboud H. E. Mechanisms of podocyte injury in diabetes: role of cytochrome P450 and NADPH oxidases. *Diabetes* 2009;58:1201-11.
96. Wakino S., Kanda T., Hayashi K. Rho/Rho kinase as a potential target for the treatment of renal disease. *Drug News Perspect* 2005;18:639-43.
97. Wettschureck N., Offermanns S. Rho/Rho-kinase mediated signaling in physiology and pathophysiology. *J Mol Med* 2002;80:629-38.
98. Mundel P., Reiser J. Proteinuria: an enzymatic disease of the podocyte? *Kidney Int* 2010;77:571-80.
99. Chang R. L., Ueki I. F., Troy J. L., Deen W. M., Robertson C. R., Brenner B. M. Permeability of the glomerular capillary wall to macromolecules. II. Experimental studies in rats using neutral dextran. *Biophys J* 1975;15:887-906.

Appendix – Study I-IV

”The beginning of knowledge is the discovery of something we do not understand”

Frank Herbert

Paper I

TRANSLATIONAL PHYSIOLOGY

Effects of early endotoxemia and dextran-induced anaphylaxis on the size selectivity of the glomerular filtration barrier in rats

Josefin Axelsson, Anna Rippe, Daniele Venturoli, Per Swärd, and Bengt Rippe

Department of Nephrology, University Hospital of Lund, Lund, Sweden

Submitted 21 April 2008; accepted in final form 10 November 2008

Axelsson J, Rippe A, Venturoli D, Swärd P, Rippe B. Effects of early endotoxemia and dextran-induced anaphylaxis on the size selectivity of the glomerular filtration barrier in rats. *Am J Physiol Renal Physiol* 296: F242–F248, 2009. First published November 12, 2008; doi:10.1152/ajprenal.90263.2008.—This study was performed to investigate the glomerular permeability alterations responsible for the microalbuminuria occurring in endotoxemia and during anaphylactic shock. In anesthetized Wistar rats, the left ureter was catheterized for urine collection while, simultaneously, blood access was achieved. Endotoxemia was induced by lipopolysaccharide (LPS) from *Escherichia coli*, and glomerular permeability was assessed at 60 and 90 ($n = 7$) and 120 ($n = 7$) min. Anaphylaxis was induced by a bolus dose of Dextran-70, and glomerular permeability assessed at 5 min ($n = 8$) and 40 min ($n = 9$). Sham animals were followed for either 5 or 120 min. The glomerular sieving coefficients (θ) to fluorescein isothiocyanate-Ficoll (70/400) were determined from plasma and urine samples and assessed using size-exclusion chromatography (HPLC). After start of the LPS infusion (2 h), but not at 60 or 90 min, θ for Ficoll_{70A} had increased markedly [from $2.91 \times 10^{-5} \pm 6.33 \times 10^{-6}$ to $7.78 \times 10^{-5} \pm 6.21 \times 10^{-6}$ ($P < 0.001$)]. In anaphylaxis, there was a large increase in θ for Ficolls >60 Å in molecular radius already at 5 min, but the glomerular permeability was completely restored at 40 min. In conclusion, there was a transient, immediate increment of glomerular permeability in dextran-induced anaphylaxis, which was completely reversible within 40 min. By contrast, endotoxemia caused an increase in glomerular permeability that was manifest first after 2 h. In both cases, θ to large Ficoll molecules were markedly increased, reflecting an increase in the number of large pores in the glomerular filter.

endotoxin; systemic inflammatory response syndrome

MICROALBUMINURIA, I.E., JUST moderately increased urinary albumin excretion rates (20–200 $\mu\text{g}/\text{min}$ in humans), is an early predictor of many glomerular diseases, such as various glomerulonephritides and diabetic nephropathy and is an established marker of endothelial dysfunction. It is also a feature of acute systemic inflammation or stress, such as following trauma (18), operations (6, 16), thermal injury (30), or in the systemic inflammatory response syndrome (SIRS) (4). The pathophysiological alterations resulting in microalbuminuria have only rarely been investigated. For example, it is not precisely known whether (proximal) tubular dysfunction is the major cause of microalbuminuria or whether charge- or size-selective alterations of the glomerular filtration barrier, or both, are affected. In a recent study, we found that early diabetic

microalbuminuria in rats was mainly related to size-selective changes in the glomerular barrier (25) and that charge alterations were just secondary. Also, the glomerular alterations following pronounced ischemia-reperfusion (I/R) injury could be mainly ascribed to size-selective changes, although after less severe I/R challenge, charge-selective alterations were also implicated (24).

The purpose of the present study was to investigate how systemic inflammation induced by bacterial lipopolysaccharide (LPS) affects the glomerular filtration barrier and to compare these changes with those occurring in acute anaphylaxis. It should be noted that not only cells of the innate immune system, but also podocytes (5), have LPS receptors, such as toll-like receptor-4 (TLR-4) and CD14 (2). Exposure of mammals to relatively small quantities of LPS leads to an acute inflammatory response, mediated in part by the release of proinflammatory cytokines, such as interleukin (IL)-1, IL-6, and tumor necrosis factor (TNF)- α . SIRS, such as induced by LPS, involves vasodilatation and increases in vascular permeability, leading to an increased vascular leakage of macromolecules in many organs. The renal responses to early septicemia with respect to tubular function, changes in glomerular filtration rate (GFR), and in renal blood flow, particularly that in the renal medulla, have been thoroughly investigated earlier (17). However, the effects of systemic inflammation on glomerular permselectivity *in vivo* have not been assessed in depth. Even though SIRS, or postoperative or posttraumatic conditions (16, 18), often leads to microalbuminuria, it is actually not known to what extent the increased urinary albumin excretion rate may just be due to a tubular defect, or really reflects an increased glomerular permeability.

Dextran causes anaphylaxis in rats by inducing degranulation of mast cells, with massive release of serotonin (5-HT) and histamine, a marked fall in mean arterial blood pressure (MAP), and peripheral edema (19, 31). Both 5-HT and histamine cause vascular protein leakage via gaps that form between endothelial cells, mostly in postcapillary venules (11, 15). These changes are transient and occur within 10–15 min. In this study, we wanted to study whether such rapid alterations also occur within the glomerular filtration barrier and to compare such glomerular permeability changes with those occurring in endotoxemia-induced systemic inflammation.

To study the functional glomerular alterations occurring in early septicemia and in anaphylactic shock in rats, we inves-

Address for reprint requests and other correspondence: B. Rippe, Dept. of Nephrology, Lund Univ., Univ. Hospital of Lund, S-211 85 Lund, Sweden (e-mail: Bengt.Rippe@med.lu.se).

The costs of publication of this article were defrayed in part by the payment of page charges. The article must therefore be hereby marked "advertisement" in accordance with 18 U.S.C. Section 1734 solely to indicate this fact.

tigated the urine excretion of infused fluorescein isothiocyanate (FITC)-Ficoll (70/400), a neutral, polydisperse polysaccharide that is not reabsorbed by the proximal tubules, allowing the assessment of glomerular permeability by the simultaneous measurement of fractional glomerular clearances (θ ; sieving coefficients) of a broad spectrum of molecular sizes. The experiments were specially designed so as to detect changes in the sieving pattern of Ficolls of high molecular weight (MW $\sim 400,000$). Furthermore, using a tissue uptake technique, we also assessed the θ for native (negatively charged) ^{125}I -labeled human serum albumin (RISA). Although we noted rapid, transient, and reversible changes in glomerular permeability to Ficoll after dextran-induced anaphylaxis, increases in glomerular permeability during endotoxemia-induced inflammation occurred first after 2 h of LPS exposure.

MATERIALS AND METHODS

Animals. Experiments were performed in 46 male Wistar rats (Møllegaard, Lille Stensved, Denmark) with an average body weight of 279.5 ± 6.3 g. The rats were kept on standard chow and had free access to water until the day of the experiment. The animal Ethics Committee at Lund University approved the animal experiments.

Surgery. The rats were anesthetized with an intraperitoneal injection of pentobarbital sodium, 60 mg/kg, and animals were placed on a thermostatically controlled heating pad to keep body temperature at 37°C . A tracheotomy was performed to facilitate breathing. The tail artery was cannulated (PE-50 cannula) for blood pressure monitoring and registration of heart rate (HR) on a polygraph (model 7B; Grass Instruments, Quincy, MA) and for repeated injections of maintenance anesthesia (pentobarbital sodium). The left carotid artery and the left and right external jugular veins were cannulated (PE-50 cannulas) for blood sampling and infusion purposes, respectively. After a small flank incision, the left ureter was cannulated (PE-10 cannula) for urine sampling, and the incision was sealed with Histoacryl (Melsungen, Germany).

Experimental procedures. Depending on exposure schedule and time to glomerular sieving measurements, rats were divided into four experimental groups and two sham groups described below. Drug (or saline) infusion started after an initial resting period (20 min), during which a control GFR measurement was performed.

Endotoxemia. Endotoxemia was induced by an intravenous bolus dose of 3 mg/kg of LPS (*Escherichia coli* 0111:B4; Sigma, St. Louis, MO), followed by a constant intravenous infusion of 6 mg/kg LPS for 30 min. To find out the response time to LPS, measurements were continued for an additional 60 min in one group of rats, in which Ficoll sieving measurements were performed at 60 and 90 min [ENDO-(60)/90; $n = 7$] after start of the infusion, or for 120 min in another group (ENDO-120; $n = 7$). For the last 33 min in the ENDO-120 group and the last 63 min in the ENDO-(60)/90 group, FITC-Ficoll (70/400) was infused intravenously, of which the first 20 min (in the ENDO-60 and ENDO-120 groups) or 50 min (in the ENDO-90 group) served as a "Ficoll saturation period" and the following 5 min as a period of glomerular Ficoll sieving assessment. RISA was given intravenously for the last 8 min of the experiment, as described below.

Anaphylaxis. Rats immediately develop anaphylaxis in response to dextran (31). Thus, to induce anaphylaxis, Dextran-70, 250 μl Macrodex (60 mg/kg; Meda, Solna, Sweden), was given intravenously as a bolus. It was possible to obtain urine and to measure Ficoll sieving and GFR during the first 5 min following dextran administration (ANA-5; $n = 8$), but after 10 min urinary flow was markedly reduced. In this group, FITC-Ficoll (70/400) was infused (for equilibration) for 25 min before the dextran challenge, with a Ficoll measurement period starting at 2 min after the dextran bolus and ending at 7–8 min after the bolus. In a second group of rats followed for 40 min after the

dextran injection, we noted a large fall in urine flow and MAP after ~ 10 min following the dextran challenge, and, because of that, 200 μl of horse serum (SVA, Uppsala, Sweden) were given one time or several times to try to normalize urine flow and MAP to preanaphylactic levels. The rationale for performing this "volume resuscitation," except for keeping the animals alive during the anaphylactic shock, was to obtain urine for measurement of GFR or θ in the time period following the hyperacute reaction to anaphylaxis. Thanks to the volume replenishment, measurements could be performed at 40 min (ANA-40; $n = 9$), but, because of subsequent reductions in urine flow and GFR, we were unable to follow the animals adequately for time periods essentially longer than 40 min during anaphylaxis.

Sham animals. The θ to high-MW Ficolls (mol. radius $>50 \text{ \AA}$) in sham animals in vivo in this experimental setting are extremely low and comparable to the fractional clearance of proteins of equivalent size (24, 25). Sham animals for the ENDO groups (SHAM-120; $n = 7$) received 120 min of constant NaCl infusion, $10 \text{ ml} \cdot \text{kg}^{-1} \cdot \text{h}^{-1}$, and, matching (in time) the infusion of LPS in the ENDO groups, a sham infusion of an extra 200 μl NaCl during 30 min. Sham animals for the ANA-5 group (SHAM-5; $n = 8$) obtained a bolus of NaCl (250 μl) 5 min before the Ficoll sieving assessment. Because there were no indications of changes in glomerular permeability between 5 and 120 min in the sham animals in the present experiments, nor in control rats in previous studies (24, 25), we employed the glomerular sieving curves for the SHAM-120 animals as control curves for the ENDO-(60)/90 groups and those for SHAM-5 as controls for the ANA-40 group. In all sham groups, FITC-Ficoll (70/400) was infused intravenously using a protocol identical to those in the experimental groups.

Sieving of FITC-Ficoll. A mixture of FITC-labeled Ficoll-400 (10 mg/ml) (TdB Consultancy, Uppsala, Sweden) and FITC-Ficoll-70 (10 mg/ml) (TdB Consultancy) in a 24:1 relationship, was administered as a bolus together with FITC-inulin (TdB Consultancy). The bolus dose (FITC-Ficoll-70, 40 μg ; FITC-Ficoll-400, 960 μg and FITC-Inulin, 500 μg) was followed by a constant infusion of $10 \text{ ml} \cdot \text{kg}^{-1} \cdot \text{h}^{-1}$ (FITC-Ficoll-70, 20 $\mu\text{g}/\text{ml}$; FITC-Ficoll-400, 0.48 mg/ml; FITC-inulin, 0.5 mg/ml; Cr-EDTA, 0.3 MBq/ml) for 20 min, after which urine was collected for a 5-min period, with a midpoint (2.5 min) plasma sample (80 μl) also collected. For animals treated with dextran, the intravenous infusion rate was increased to $15 \text{ ml} \cdot \text{kg}^{-1} \cdot \text{h}^{-1}$ throughout the experiments to avoid dehydration and to try to preserve MAP in the animals. A high-performance size exclusion chromatography (HPLC) system (Waters, Milford, MA) was used to determine size and concentration of the Ficoll samples. Size exclusion was achieved using an Ultrahydrogel-500 column (Waters). The mobile phase was driven by a pump (Waters 1525), and fluorescence was detected with a fluorescence detector (Waters 2475) with an excitation wavelength at 492 nm and an emission wavelength at 518 nm. The system was controlled by Breeze Software 3.3 (Waters). The column was calibrated with Ficoll standards and protein standards described at some length in a previous paper (1). The θ of FITC-Ficoll 70/400 was determined as the fractional clearance from:

$$\theta = (C_{\text{FU}} \times C_{\text{IP}}) / (C_{\text{FP}} \times C_{\text{IU}}) \quad (1)$$

where C_{FU} represents the Ficoll urine concentration, C_{IP} represents the inulin concentration in plasma, C_{FP} the Ficoll concentration in plasma, and C_{IU} the inulin concentration in urine.

GFR. GFR was determined by measuring renal clearance of ^{51}Cr -EDTA (Amersham Bioscience, Buckinghamshire, UK) and FITC-inulin. ^{51}Cr -EDTA was given as a bolus dose at the start of the experiments (0.3 MBq in 0.2 ml iv) followed by a constant infusion of $10 \text{ ml} \cdot \text{kg}^{-1} \cdot \text{h}^{-1}$ (0.3 MBq/ml) (together with NaCl) throughout the experiments. For repeated measurements of the plasma to urine ^{51}Cr -EDTA clearance during the study, blood sampling was performed approximately every 20 min using microcapillaries (10 μl). Urine was sampled every 10–30 min of the experiment. Radioactivity in blood samples and urine samples was measured in a gamma counter (Wizard 1480; LKP Wallace, Turku, Finland). Hematocrit (50 μl) was

assessed two or three times throughout the experiment, to be able to convert blood radioactivity into plasma radioactivity.

The urinary excretion of ^{51}Cr -EDTA (and FITC-inulin) per minute ($U_i \times V_u$) divided by the concentration of tracer in plasma (P_i) was used to calculate GFR according to:

$$\text{GFR} = (U_i \times V_u) / P_i \quad (2)$$

where U_i represents the tracer concentration in urine, and V_u the flow of urine per minute.

Tissue uptake technique for assessing θ for ^{125}I -HSA. After collection of urine and plasma for Ficoll determinations, ^{125}I -HSA (0.2 MBq; Institute for Energy Technique, Kjeller, Norway) was administered via the tail artery as a bolus. During an 8-min period, six blood samples (25 μl) and one urine sample were collected for estimation of the sieving coefficient of ^{125}I -HSA (RISA). Thereafter, a whole body washout was performed via the left external jugular vein (25 ml/min) for 8 min. The washout fluid mixture contained equal amounts of 0.9% saline and heparinized horse serum (SVA). After a laparotomy, the inferior vena cava was freed (within 1 min after start of the washout) and cut open for collection of the rinse fluid. Following complete washout, the kidneys were removed, and the cortex was dissected out and assessed with respect to radioactivity. To reduce the influence of free ^{125}I , urine samples were precipitated with 10% trichloroacetic acid (TCA) and spun down, and the supernatant (free ^{125}I) was discarded. All samples were measured for radioactivity in the gamma counter mentioned above.

The sieving coefficients for RISA were calculated from the amount of tracer radioactivity accumulated in the left kidney cortex plus the TCA-precipitable urine tracer activity (collected during the tracer infusion period and amounting to a maximum of 5–10% of total cortical radioactivity) divided by the average plasma tracer concentration, by the tracer circulation time, and by GFR.

Pore analysis. The two-pore model (10, 22, 29) was used to analyze the θ data for Ficoll (mol. radius 15–80 \AA). A nonlinear least-squares regression analysis was used to obtain the best curve fit, using scaling multipliers as described at some length previously (10).

Statistics. Values are expressed as means \pm SE. Differences between groups were tested using nonparametric analysis of variance with the Kruskal-Wallis test and post hoc tested using the Mann Whitney *U*-test. Significance levels were set at $*P < 0.05$, $**P < 0.01$, and $***P < 0.001$. All statistical calculations were made using SPSS 11.0.3 for Macintosh OSX (SPSS, Chicago, IL).

RESULTS

MAP and HR. The SHAM group showed a stable, or only moderately reduced, MAP during the course of the experiment (Fig. 1), and also a moderate increase in HR. By contrast, endotoxin caused a rapid (within 5 min) fall in MAP, from 130 ± 2.4 to 54.3 ± 4.6 mmHg ($P < 0.01$) in the ENDO-(60)/90 group and from 116 ± 3.9 to 53.3 ± 4.8 mmHg ($P < 0.01$) in the ENDO-120 group. After a spontaneous recovery of the MAP, which usually occurred within the next 20–30 min, there was again a slow reduction of MAP with time. Thus there appeared to be a bimodal MAP response to endotoxin. Furthermore, endotoxemia caused an increased HR, from 383 ± 13.8 beats/min at the start to 447 ± 17.1 beats/min ($P < 0.05$) after 120 min, which was not seen in the 120 sham group. Similar to the LPS group, the anaphylactic group (Fig. 2) showed an initial, but less rapid, decrease in MAP. Thus, during the first 5 min after the dextran infusion, MAP was rather stable, starting at 116 ± 5.7 and being reduced to 104 ± 6.0 mmHg [not significant (NS); ANA-5 group]. In the ANA-40 group, MAP fell from 99.2 ± 3 to 47.1 ± 1.5 mmHg ($P < 0.01$) 15 min after the dextran administration. The

ANA-40 group nearly recovered their MAP toward the end of the experiment, conceivably mainly because of the volume resuscitation performed (Fig. 2). There was also a slight tendency of increase in HR from 320 ± 18.1 to 332 ± 8.9 (NS).

GFR. In the SHAM group, GFR showed a slightly higher value at the end of the experiments than at the start (Fig. 3), whereas, in the ENDO groups, there was a decrease in GFR, ~ 20 min after start of the LPS infusion, from 0.70 ± 0.05 to 0.35 ± 0.04 $\text{ml} \cdot \text{min}^{-1} \cdot \text{g}^{-1}$ ($P < 0.01$) in the ENDO-(60)/90 group and from 0.73 ± 0.05 $\text{ml} \cdot \text{min}^{-1} \cdot \text{g}^{-1}$ to 0.49 ± 0.09 $\text{ml} \cdot \text{min}^{-1} \cdot \text{g}^{-1}$ ($P < 0.05$) in the ENDO-120 group. In the following period (at ~ 50 min), GFR had recovered, but then again tended to fall as part of the septic condition. In the anaphylaxis groups, GFR could not be measured during the period from 10 to 20 min after the dextran bolus because of the marked reduction in urine flow. However, early in the experiment (0–10 min), urine flow and GFR were remarkably well preserved (Fig. 4) in the ANA-5 and ANA-40 group. By the end of the experiment (at 40 min), conceivably thanks to the volume resuscitation, GFR seemed to have partly recovered vs. preanaphylactic value(s) in the ANA-40 group (0.65 ± 0.06 vs. 0.72 ± 0.04 $\text{ml} \cdot \text{min}^{-1} \cdot \text{g}^{-1}$; NS).

θ for FITC-Ficoll. Figure 5 demonstrates the sieving coefficient (θ) vs. Stokes-Einstein radius (a_e) curves for Ficoll molecules ranging in radius from 15 to 80 \AA for the ENDO-120 group vs. the SHAM-120 group. In the a_e range between 55 and 80 \AA , the ENDO-120 group showed a clearly increased θ compared with SHAM ($P < 0.001$). This increased permeability to high-mol. Ficolls was, however, not seen for either the ENDO-60 or the ENDO-90 measurements, as shown in Fig. 6, demonstrating a time dependency of the changes in glomerular permeability following endotoxin.

In the acute anaphylaxis (ANA-5) group, there were significantly higher sieving coefficients for Ficoll 55–80 \AA ($P < 0.001$) than in the SHAM-5 group (Fig. 7). By contrast, there was no significant difference between the ANA-40 group and either of the SHAM groups.

Two-pore modeling. The best curve fits of θ vs. a_e for Ficoll according to the two-pore model were obtained using the parameters listed in Table 1 (ENDO groups) and Table 2 (ANA

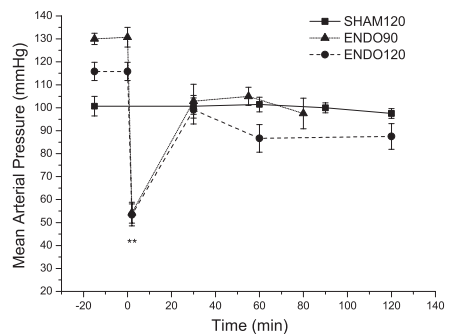


Fig. 1. Mean arterial pressure (MAP) vs. time in the endotoxin (ENDO) groups vs. SHAM. \blacktriangle , Ficoll sieving measurements performed at 60 and 90 min after start of the lipopolysaccharide (LPS) infusion [ENDO-(60)/90]; \bullet , Ficoll sieving measurements performed 120 min after start of LPS infusion (ENDO-120); \blacksquare , SHAM group. Note the marked, immediate fall in MAP by endotoxin.

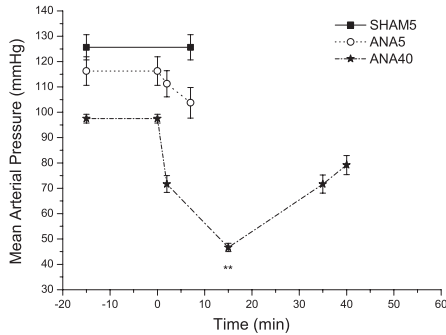


Fig. 2. MAP vs. time in the two anaphylactic groups investigated. \circ , 5-min anaphylactic group (ANA-5); \star , 40-min anaphylactic group (ANA-40). Symbols for the SHAM-5 group are the same as for the SHAM-120 group.

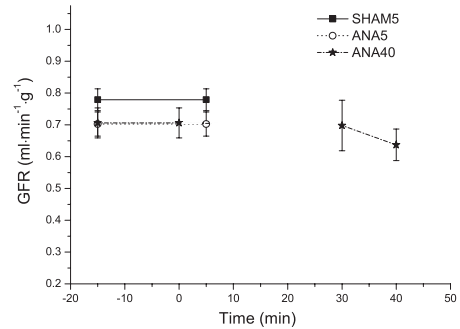


Fig. 4. GFR per gram kidney, measured as a function of time in anaphylaxis. Symbols as in Fig. 2. Note the absence of measurements in the ANA-40 group in the time period between 5 and 30 min because of oliguria.

groups). The fractional ultrafiltration coefficient accounted for by large pores, mainly reflecting the number of large pores, and the fractional fluid flow through large pores were more than doubled in the ENDO-120 group and the acute anaphylactic (ANA-5) group, but remained unchanged vs. control in ENDO-(60)/90 groups and in the ANA-40 group. In acute anaphylaxis, not only the large pore number, but also the large pore radius, was acutely increased (188 ± 10.1 vs. 115 ± 3.0 ; $P < 0.01$). The effective area over unit diffusion path length seems to have been reduced in the ANA-5 group.

θ for albumin. Figure 8 shows θ for albumin in the ENDO groups. Because tissue uptake experiments could only be performed at the termination of the experiments, data could only be obtained at 90 min for the ENDO-(60)/90 group. θ for albumin was significantly increased in the ENDO-120 group vs. the SHAM-120 group [$4.86 \times 10^{-4} \pm 5.1 \times 10^{-5}$ vs. $3.06 \times 10^{-4} \pm 3.22 \times 10^{-5}$ ($P < 0.05$)] but not in the ENDO-90 group ($4.0 \times 10^{-4} \pm 4.89 \times 10^{-5}$ vs. $3.06 \times 10^{-4} \pm 3.22 \times 10^{-5}$; NS). Figure 9 demonstrates the increase in the albumin sieving coefficient in the ANA-5 and ANA-40 groups. In the ANA-40 group, contrary to the unchanging θ for large Ficolls, θ for albumin was significantly increased vs. the

SHAM-5 group, i.e., $6.68 \times 10^{-4} \pm 3.34 \times 10^{-5}$ vs. $3.56 \times 10^{-4} \pm 4.75 \times 10^{-5}$ ($P < 0.01$). The fractional clearance of RISA reaching the final urine (and not being reabsorbed) did not differ significantly between groups and was on average $\sim 3\%$ ($2.83 \pm 0.55\%$) of filtered load, except in the ANA-40 group, where it was only $0.54 \pm 0.20\%$ ($P < 0.05$ vs. SHAM-5) of filtered load.

DISCUSSION

This is, to our knowledge, the first detailed in vivo study of the alterations in the glomerular permeability that occur during systemic inflammation induced by endotoxemia and in anaphylactic shock. The major result of the study is that early endotoxemia-induced systemic inflammation and anaphylactic shock both reduce the size-selectivity of the glomerular filtration barrier by increasing the number of large pores in the glomerular filter, rather than affecting the glomerular charge-selectivity. Acute anaphylaxis caused a rapid, transient change in glomerular permeability, completely reversible within 40

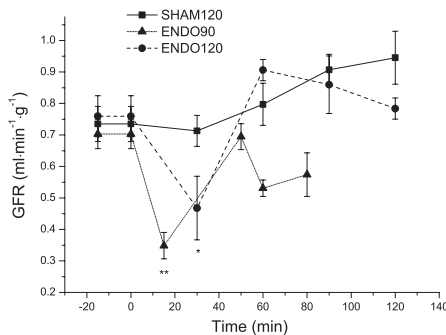


Fig. 3. Glomerular filtration rate (GFR) per gram kidney, measured as a function of time for the two endotoxin groups and for the SHAM group. Note the fall in GFR during the first 10–30 min of the dwell in the ENDO group.

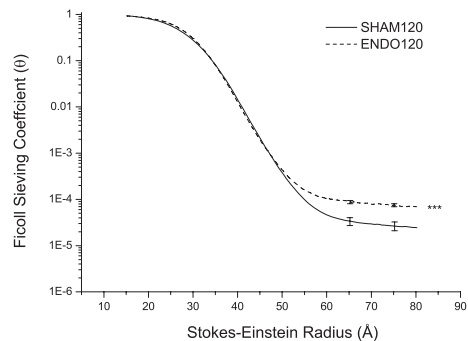


Fig. 5. Sieving coefficients (θ) vs. Stokes-Einstein radius (a_e) for Ficoll in the left kidney for the ENDO-120 group (dashed line) vs. the SHAM group (solid line). 400 data points are sampled between 15 and 80 Å. The sieving coefficients for large Ficoll molecules (mol. radius 50–80 Å) were significantly increased in the ENDO-120 group compared with SHAM or the ENDO-60/90 measurements ($P < 0.001$).

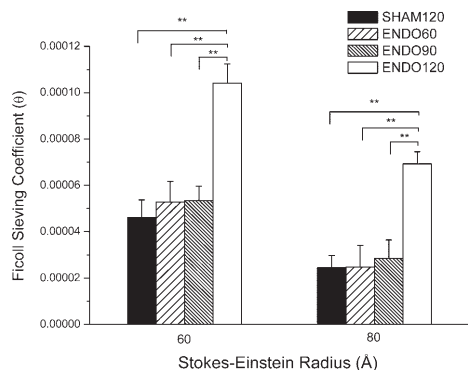


Fig. 6. Time dependency of Fick sieving coefficients for Fick molecules of radius 60 and 80 Å. Significant increases in θ for large Ficks occurred only for the 120-min ENDO group compared with either SHAM or the ENDO-60 and ENDO-90 measurements.

min, whereas LPS induced an increase in the θ to large Fick molecules, which was manifest only after 2 h. These two completely different response patterns apparently reflect two different mechanisms of action of the mediators involved in endotoxin-induced shock and in anaphylactic shock.

It is well accepted that LPS administration leads to activation of TLR4 on cells in the innate immune system (2). TLR4 is present on monocytes and other cell types, including podocytes, and mediates a series of inflammatory events. Exposure to endotoxin thus initiates a complex cascade, involving various proinflammatory and anti-inflammatory cytokines, such as IL-6, TNF- α , IL-10, and IL-18, activating white cells and other inflammatory response mediators, including adhesion molecules, complement factors, oxygen-derived free radicals, and procoagulant factors. Especially, TNF- α is considered a crucial mediator of both acute and chronic inflammatory responses, including microalbuminuria (9). The slow and gradual change in glomerular permeability in response to endotoxin thus seems

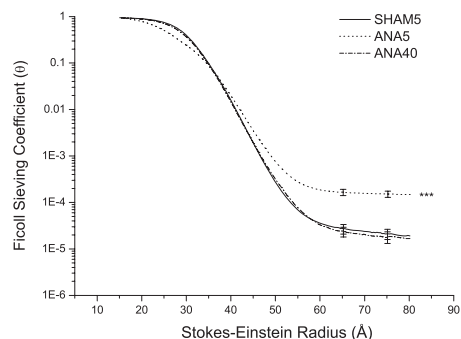


Fig. 7. The θ vs. a_c for Fick in the left kidney for the ANA-5 group (dotted line) and the ANA-40 group (dashed/dotted line) vs. the acute SHAM group (SHAM-5; solid line). Note the marked increase in the sieving coefficient to large Fick molecules ($a_c > 50$ Å; $P < 0.001$) in the ANA-5 group! There was also a moderate increase in large pore radius.

Table 1. Two-pore parameters in the ENDO assessment groups vs. SHAM

Two-Pore Parameters	SHAM-120	ENDO-60	ENDO-90	ENDO-120
<i>n</i>	7	7	7	7
r_s , Å	45.7 \pm 0.20	46.3 \pm 0.26	46.4 \pm 0.09	45.4 \pm 0.20
r_L , Å	138.1 \pm 3.76	132.4 \pm 9.32	146.7 \pm 20.97	143.2 \pm 5.96
$\alpha_L \times 10^5$	4.08 \pm 0.76	3.44 \pm 0.79	3.25 \pm 0.31	10.20 \pm 1.43†
$J_L/GFR \times 10^5$	12.32 \pm 2.56	9.97 \pm 2.40	9.06 \pm 0.78	21.60 \pm 2.82*
$A_o/\Delta X$, $cm \cdot g^{-1} \times 10^{-5}$	3.76 \pm 0.59	1.47 \pm 0.13	1.31 \pm 0.12*	4.56 \pm 0.81

Values are given as means \pm SE; *n*, no. of rats. SHAM-120, 120-min sham group; ENDO-60, ENDO-90, and ENDO-120, Fick sieving measurements performed at 60, 90, and 120 min, respectively, after start of endotoxin (ENDO) infusion; r_s , small pore radius; r_L , large pore radius; α_L , fractional UF coefficient accounted for by large pores; J_L , fractional fluid flow through large pores; GFR, glomerular filtration rate; $A_o/\Delta X$, effective area over unit diffusion path length. Statistical difference between SHAM and endotoxin groups are as follows: * $P < 0.05$ and † $P < 0.01$.

to reflect the gradual activation of multiple and integrated inflammatory response systems over time.

Perhaps the most startling finding of the present study was the immediate and prominent increase in glomerular permeability in anaphylaxis, a response completely reversible within 40 min. In rats, dextran induces anaphylaxis by causing degranulation of mast cells, with massive release of 5-HT and histamine. In turn, these biogenic amines cause precapillary vasodilation (histamine) and/or postcapillary vasoconstriction (5-HT), raising capillary pressure, and an increased microvascular leakage of proteins (12, 22). This leakage occurs via gaps that transiently form between endothelial cells, mostly in postcapillary venules (11, 19). Despite the fall in MAP, there was thus a marked, transient increase in glomerular permeability occurring in parallel with an increased transvascular leakage of RISA in skin, lung, and muscle (presented in a subsequent study) in anaphylaxis.

Overall, it should be noted, however, that the glomerular barrier apparently is rather unresponsive to 5-HT and histamine following the immediate insult, because glomerular permeability was completely restored within 40 min. This is actually in line with previous studies using dextran molecules (18–44 Å in radius) as markers of glomerular permselectivity (8) or using a technique for assessing vascular labeling of endothelial gaps with carbon (27). The mentioned studies thus failed to demonstrate any renal permeability effects of histamine or 5-HT, except for showing some occasional leaky sites in peritubular

Table 2. Two-pore parameters in ANA-5 and ANA-40 groups vs. SHAM

Two-Pore Parameters	SHAM-5	ANA-5	ANA-40
<i>n</i>	8	8	9
r_s , Å	46.0 \pm 0.05	46.9 \pm 0.16	45.8 \pm 0.10
r_L , Å	114.6 \pm 2.95	188.3 \pm 10.13*	140.3 \pm 10.20
$\alpha_L \times 10^5$	3.90 \pm 0.83	8.15 \pm 1.21*	2.94 \pm 0.50
$J_L/GFR \times 10^5$	10.1 \pm 2.21	27.30 \pm 4.07†	6.58 \pm 1.35
$A_o/\Delta X$, $cm \cdot g^{-1} \times 10^{-5}$	6.82 \pm 0.75	1.10 \pm 0.08*	4.41 \pm 0.75

Values are given as means \pm SE; *n*, no. of rats. SHAM-5, 5-min sham group; ANA-5 and ANA-40, respective 5 and 40 min anaphylactic groups. † $P < 0.01$ and * $P < 0.05$, statistical difference between SHAM and anaphylaxis groups.

capillaries (27). Another factor behind the reversibility of the glomerular filter to histamine may be the acute catecholamine release that is usually associated with anaphylaxis, which can abrogate the actions of histamine on vascular permeability (12, 21). Anyway, the present study strongly indicates that, except for the immediate, very marked changes in glomerular permeability, the kidneys are largely protected against the actions of biogenic amines, such as histamine and 5-HT, under conditions of anaphylaxis. In other words, microalbuminuria should just be a very transient and initial event in this condition.

Also, a number of previous *in vitro* studies on isolated glomeruli indicate that glomerular permeability can indeed increase very rapidly and transiently (within 5–15 min) in response to various challenges, such as puromycin aminonucleoside (PAN), TNF- α , vascular endothelial growth factor, or transforming growth factor (3, 13, 14, 26, 28). In isolated glomeruli *in vitro*, the acute permeability effects of TNF- α and PAN were found to be mediated in part by reactive oxygen species, since inhibition of these, or their generation, apparently reduced the changes in glomerular permeability (13). The exact mechanisms of the described rapid, dynamic changes of the glomerular permeability are at present unknown, leaving room for speculation. Previous results from our group strongly indicate that the major barrier to protein permeability of the glomerular filter is not at the podocyte slit diaphragm (10, 23). Thus it seems that all three sequential barriers, i.e., the glomerular basement membrane (GBM) and the two cellular layers, need to interact to create the nearly perfect glomerular permeability barrier normally present (7). Especially, the way that the podocytes interact with the GBM may be crucial. Biogenic amines may interact with the podocytes to produce changes in their actin cytoskeleton that may alter the shape of the podocyte and the tension that they exert on the GBM. Also, endothelial cells may be involved, in a way similar to how they react to biogenic amines in nonfenestrated endothelium. In addition, the molecular complexes in the slit diaphragm and/or the intergrins linking the podocyte foot process to the GBM may be acutely involved in these changes (3).

The Ficoll molecules investigated in this study are largely uncharged, whereas albumin is negatively charged at physiologic pH. Despite the unchanging θ for large Ficoll molecules in the ANA-40 group, there was an increase in θ for albumin in this group. One way of explaining this discrepancy is to

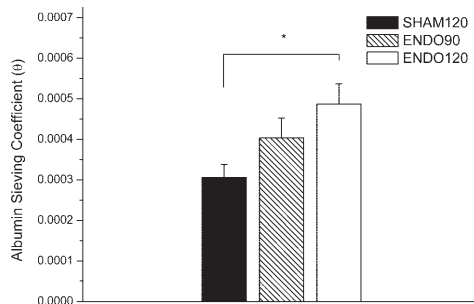


Fig. 8. Albumin sieving coefficient as a function of time in the ENDO groups (ENDO-90: hatched bar; ENDO-120: open bar) vs. SHAM-120 (filled bar). Only the increase in θ for albumin after 2 h was statistically significant.

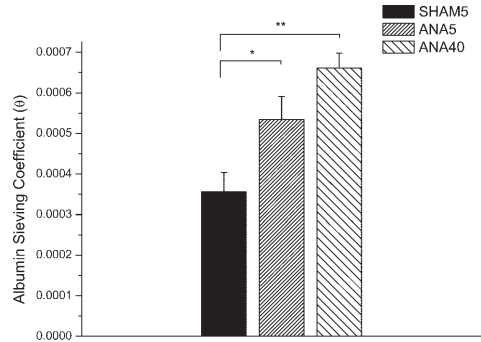


Fig. 9. Sieving coefficient for albumin in the acute anaphylactic (ANA-5) group (densely hatched bar) and the ANA-40 group (loosely hatched bar) vs. SHAM (filled bar). Similar to the large increase in θ for high-molecular-weight Ficoll, there was an increase in the albumin sieving coefficient in the ANA-5 group. However, in stark contrast to the unchanging sieving coefficient to high-molecular-weight Ficoll, θ for albumin was increased also in the ANA-40 group.

imply that a reduction in the negative charge selectivity of the glomerular barrier had occurred by dextran. Indeed, high concentrations of dextran have been shown increase the permeability to albumin in muscle capillaries without markedly affecting the capillary filtration coefficient (20). However, given the low circulating dextran concentrations in the present study, this effect is not the most likely. An alternative explanation may instead be that the increased θ for albumin may have resulted from an early, transient period of leakage of macromolecules from the peritubular capillaries in the cortical interstitium, causing interstitial edema and more space for subsequent (tracer) albumin accumulation. This may have resulted in a “falsely” high accumulation of RISA, assessed by the tissue uptake procedure at 40 min, in excess of that occurring by the albumin reabsorption by the proximal tubular cells. Thus the biogenic amines released in anaphylaxis, through their immediate effects, actually may affect the permeation of proteins across the peritubular capillaries (27) while largely leaving the glomerular permeability unaffected in the long term.

In conclusion, the present study, specially designed to assess glomerular sieving coefficients for high-molecular-weight Ficoll molecules, demonstrated an early, transient increase in glomerular permeability to Ficoll in anaphylactic shock, completely reversible within 40 min. By contrast, endotoxemia increased glomerular permeability first after 2 h. In both endotoxemic and anaphylactic shock, the increased glomerular barrier permeability appeared to occur by an increase in the number of large pores in the glomerular filter, rather than affecting the glomerular charge selectivity.

ACKNOWLEDGMENTS

Kerstin Wihlborg is gratefully acknowledged for skilful typing of the manuscript.

GRANTS

This study was supported by the Swedish Medical Research Council (Grant no. 08285), the Lundberg Medical Foundation, the Heart-Lung Foundation, and the European Union Contract FMRX-CT98-0219.

REFERENCES

1. Asgeirsson D, Venturoli D, Rippe B, Rippe C. Increased glomerular permeability to negatively charged Ficoll relative to neutral Ficoll in rats. *Am J Physiol Renal Physiol* 291: F1083–F1089, 2006.
2. Cunningham PN, Wang Y, Guo R, He G, Quigg RJ. Role of Toll-like receptor 4 in endotoxin-induced acute renal failure. *J Immunol* 172: 2629–2635, 2004.
3. Dahly-Vernon AJ, Sharma M, McCarthy ET, Savin VJ, Ledbetter SR, Roman RJ. Transforming growth factor-beta, 20-HETE interaction, and glomerular injury in Dahl salt-sensitive rats. *Hypertension* 45: 643–648, 2005.
4. Davies MG, Hagen PO. Systemic inflammatory response syndrome. *Br J Surg* 84: 920–935, 1997.
5. Fouqueray B, Philippe C, Herbelin A, Perez J, Ardaillou R, Baud L. Cytokine formation within rat glomeruli during experimental endotoxemia. *J Am Soc Nephrol* 3: 1783–1791, 1993.
6. Gosling P, Shearman CP, Gwynn BR, Simms MH, Bainbridge ET. Microproteinuria: response to operation. *Br Med J (Clin Res Ed)* 296: 338–339, 1988.
7. Haraldsson B, Nystrom J, Deen WM. Properties of the glomerular barrier and mechanisms of proteinuria. *Physiol Rev* 88: 451–487, 2008.
8. Ichikawa I, Brenner BM. Mechanisms of action of histamine and histamine antagonists on the glomerular microcirculation in the rat. *Circ Res* 45: 737–745, 1979.
9. Kalantarina K, Awad AS, Siragy HM. Urinary and renal interstitial concentrations of TNF-alpha increase prior to the rise in albuminuria in diabetic rats. *Kidney Int* 64: 1208–1213, 2003.
10. Lund U, Rippe A, Venturoli D, Tenstad O, Grubb A, Rippe B. Glomerular filtration rate dependence of sieving of albumin and some neutral proteins in rat kidneys. *Am J Physiol Renal Physiol* 284: F1226–F1234, 2003.
11. Majno G, Palade GE. Studies on inflammation. 1. The effect of histamine and serotonin on vascular permeability: an electron microscopic study. *J Biophys Biochem Cytol* 11: 571–605, 1961.
12. Marciniak DL, Dobbins DE, Maciejko JJ, Scott JB, Haddy FJ, Grega GJ. Effects of systemically infused histamine on transvascular fluid and protein transfer. *Am J Physiol Heart Circ Physiol* 233: H148–H153, 1977.
13. McCarthy ET, Sharma R, Sharma M, Li JZ, Ge XL, Dileepan KN, Savin VJ. TNF-alpha increases albumin permeability of isolated rat glomeruli through the generation of superoxide. *J Am Soc Nephrol* 9: 433–438, 1998.
14. McCarthy ET, Sharma R, Sharma M. Protective effect of 20-hydroxy-eicosatetraenoic acid (20-HETE) on glomerular protein permeability barrier. *Kidney Int* 67: 152–156, 2005.
15. McDonald DM, Thurston G, Baluk P. Endothelial gaps as sites for plasma leakage in inflammation. *Microcirculation* 6: 7–22, 1999.
16. Nergelius G, Vinge E, Grubb A, Lidgren L. Renal impairment after hip or knee arthroplasty. Urinary excretion of protein markers studied in 59 patients. *Acta Orthop Scand* 68: 34–40, 1997.
17. Niteanu N, Grimberg E, Ricksten SE, Marcussen N, Nordlinder H, Guron G. Effects of thrombin inhibition with melagatran on renal hemodynamics and function and liver integrity during early endotoxemia. *Am J Physiol Regul Integr Comp Physiol* 292: R1117–R1124, 2007.
18. Pallister I, Dent C, Wise CC, Alpar EK, Gosling P. Early post-traumatic acute respiratory distress syndrome and albumin excretion rate: a prospective evaluation of a “point-of care” predictive test. *Injury* 32: 177–183, 2001.
19. Parratt JR, West GB. 5-Hydroxytryptamine and the anaphylactoid reaction in the rat. *J Physiol* 139: 27–41, 1957.
20. Rippe B, Folkow B. Capillary permeability to albumin in normotensive and spontaneously hypertensive rats. *Acta Physiol Scand* 101: 72–83, 1977.
21. Rippe B, Grega GJ. Effects of isoprenaline and cooling on histamine induced changes of capillary permeability in the rat hindquarter vascular bed. *Acta Physiol Scand* 103: 252–262, 1978.
22. Rippe B, Haraldsson B. Transport of macromolecules across microvascular walls. The two-pore theory. *Physiol Rev* 74: 163–219, 1994.
23. Rippe C, Asgeirsson D, Venturoli D, Rippe A, Rippe B. Effects of glomerular filtration rate on Ficoll sieving coefficients (theta) in rats. *Kidney Int* 69: 1326–1332, 2006.
24. Rippe C, Rippe A, Larsson A, Asgeirsson D, Rippe B. Nature of glomerular capillary permeability changes following acute renal ischemia-reperfusion injury in rats. *Am J Physiol Renal Physiol* 291: F1362–F1368, 2006.
25. Rippe C, Rippe A, Torffvit O, Rippe B. Size and charge selectivity of the glomerular filter in early experimental diabetes in rats. *Am J Physiol Renal Physiol* 293: F1533–F1538, 2007.
26. Salmon AH, Neal CR, Bates DO, Harper SJ. Vascular endothelial growth factor increases the ultrafiltration coefficient in isolated intact Wistar rat glomeruli. *J Physiol* 570: 141–156, 2006.
27. Schwartz MM, Cotran RS. Vascular leakage in the kidney and lower urinary tract: effects of histamine, serotonin and bradykinin. *Proc Soc Exp Biol Med* 140: 535–539, 1972.
28. Sharma R, Khanna A, Sharma M, Savin VJ. Transforming growth factor-beta1 increases albumin permeability of isolated rat glomeruli via hydroxyl radicals. *Kidney Int* 58: 131–136, 2000.
29. Tencer J, Frick IM, Öqvist BW, Alm P, Rippe B. Size-selectivity of the glomerular barrier to high molecular weight proteins: upper size limitations of shunt pathways. *Kidney Int* 53: 709–715, 1998.
30. Vlachou E, Gosling P, Moiemens NS. Microalbuminuria: a marker of endothelial dysfunction in thermal injury. *Burns* 32: 1009–1016, 2006.
31. Voorhees AB, Baker HJ, Pulaski EJ. Reactions of albino rats to injections of dextran. *Proc Soc Exp Biol Med* 76: 254–256, 1951.

Paper II

TRANSLATIONAL PHYSIOLOGY

Loss of size selectivity of the glomerular filtration barrier in rats following laparotomy and muscle trauma

Josefin Axelsson, Irma Mahmutovic, Anna Rippe, and Bengt Rippe

Department of Nephrology, University Hospital of Lund, Lund, Sweden

Submitted 5 May 2009; accepted in final form 1 July 2009

Axelsson J, Mahmutovic I, Rippe A, Rippe B. Loss of size selectivity of the glomerular filtration barrier in rats following laparotomy and muscle trauma. *Am J Physiol Renal Physiol* 297: F577–F582, 2009. First published July 8, 2009; doi:10.1152/ajprenal.00246.2009.—Posttraumatic microalbuminuria may be caused by either charge- or size-selective alterations in the glomerular filtration barrier, or both, and/or to a reduction in proximal tubular protein reabsorption. This study was performed to elucidate the pathophysiology of the increases in glomerular permeability occurring in rats exposed to a laparotomy or to a laparotomy and muscle trauma. In anesthetized Wistar rats (250–280 g), the left ureter was cannulated for urine collection, while simultaneously blood access was achieved. Rats were exposed to trauma by a laparotomy (L; $n = 8$), or by a combination of L and muscle trauma (MT; L+MT) induced by topical blunt injury of the abdominal muscles bilaterally. After L, muscles were crushed using hemostatic forceps at either 2×2 sites (“small” MT; $n = 9$), or at 2×5 sites (“large” MT; $n = 9$). Sham groups ($n = 16$), not exposed to a laparotomy, were used as controls. The glomerular sieving coefficients (θ) to polydisperse FITC-Ficoll-70/400 (molecular radius 13–80 Å) were determined at 5 or 60 min after L and L+MT, respectively, from plasma and urine samples, and analyzed by high-performance size-exclusion chromatography. A tissue-uptake technique was used to assess θ for ^{125}I -labeled serum albumin. L, with or without MT, increased θ for Ficoll_{55–80Å} and albumin rapidly and markedly. θ -Ficoll_{70Å} thus increased approximately threefold, and θ for albumin significantly, for all trauma groups. According to the “two-pore model” of glomerular permeability, these changes mainly reflect an increase in the number of large pores in the glomerular filter without any primary changes in the charge-selective properties of the filter.

microalbuminuria; glomerular sieving coefficients; albumin; Ficoll; capillary permeability

MICROALBUMINURIA, i.e., just moderately elevated rates of albumin excretion in the urine (20–200 μg albumin/min), is an established marker of endothelial dysfunction and occurs in vascular disease (9) and diabetic nephropathy, but also after surgery (6, 13), body trauma (15), and in fever, sepsis (3), etc. The exact pathophysiology of microalbuminuria is not known. Is it primarily due to tubular dysfunction, resulting in a reduced proximal tubular reabsorption (PTR) of albumin, or is it due to alterations of the charge- or size-selective properties of the glomerular filtration barrier, or both? Earlier studies on glomerular Ficoll sieving in intact rats indicate that ischemia-reperfusion (I/R) injury (18), early diabetic nephropathy (19),

or sepsis (LPS infusion) (3) produces increases in glomerular permeability based on reductions in the size selectivity, of the barrier with only secondary changes in charge selectivity.

Various kinds of significant trauma or inflammation may elicit a systemic inflammatory response syndrome (SIRS) (5). Such an inflammatory response involves the activation of multiple pathways, including the coagulation and complement cascades, as well as activation of monocytes, lymphocytes, and other inflammatory cells to release chemokines, cytokines, and reactive oxygen species (ROS) and other proinflammatory (and anti-inflammatory) agents. Interactions of such agents and/or activated cells with the glomerular filtration barrier are thought to result in microalbuminuria. Moderate trauma, such as after hip and knee surgery, thus results in low-grade microalbuminuria, being most prominent during the first day after surgery (13). Since both the urinary albumin/creatinine and IgG/creatinine ratios increased in parallel, and since tubular markers were not seen to peak in the urine until the second day after an operation, it was concluded that posttraumatic proteinuria may be due to a size-selective defect in the filter, and not primarily due to reductions in PTR. In fact, also after burns, there was a biphasic proteinuria response, with an initial microproteinuria resolving within 24 h, reflecting a size-selectivity defect, and with a second protein excretion phase, peaking 3–5 days postinjury, with a pattern signaling tubular proteinuria (22).

In a recent study (3), we found that acute dextran-induced anaphylaxis in rats caused a rapid, transient increase in glomerular permeability, completely reversible within 40 min, whereas after infusion of lipopolysaccharide (LPS), producing sepsis, a more gradual permeability response, evident first after 120 min, was seen. These two different response patterns apparently reflect two different patterns of action of the mediators involved in SIRS. In acute anaphylaxis, the immediate release of histamine (from mast cells) and other proinflammatory agents seemed to have caused an initial glomerular permeability increase, whereas the permeability alterations occurring during endotoxemia appeared to follow upon a more gradual activation of proinflammatory mechanisms.

That the glomerular barrier can reversibly increase its permeability within minutes may seem remarkable. In the present study, we address the question of whether glomerular selectivity can be promptly reduced also upon surgery and/or muscle trauma. Hence, we investigated the functional behavior of the glomerular filtration barrier in response to a laparotomy, with and without skin dissection, and with and without graded muscle trauma in rats. Glomerular size and charge selectivity were assessed in vivo using two different techniques. First, we

Address for reprint requests and other correspondence: B. Rippe, Dept. of Nephrology, Lund Univ., Univ. Hospital of Lund, S-211 85 Lund, Sweden (e-mail: Bengt.Rippe@med.lu.se).

used FITC-Ficoll-70/400, a neutral polysaccharide which is not reabsorbed by the proximal tubules, to assess the glomerular permeability (θ ; sieving coefficients) for a broad spectrum of molecular sizes, emphasizing the glomerular sieving pattern of Ficoll molecules of high molecular weight (MW \sim 400,000). Second, by using a tissue-uptake technique, we were also able to assess the θ for ^{125}I -labeled native (negatively charged) human serum albumin (HSA).

MATERIALS AND METHODS

Animals and general surgery. Experiments were performed in 67 male Wistar rats (Møllegaard, Lille Stensved, Denmark) with an average body weight of 273 ± 4.1 g. The rats had free access to standard food and water until the day of the experiment. The animal Ethics Committee at Lund University approved the animal experiments. Anesthesia was induced by an intraperitoneal injection of pentobarbital sodium (60 mg/kg body wt) and maintained through repeated intra-arterial injections of the same drug. The rats were placed on a heating pad to maintain body temperature at 37°C . The tail artery was cannulated (PE-50 cannula) for continuous monitoring of blood pressure and heart rate registration on a polygraph (model 7B, Grass Instruments, Quincy, MA), and for administration of anesthesia. A tracheotomy was performed to facilitate breathing. The left carotid artery and left jugular vein were cannulated (PE-50) for blood sampling and infusions, respectively. Following an intravenous bolus dose of furosemide (1.5 mg/kg body wt, Furosemid, Recip AB, Årsta, Sweden) to induce diuresis, and after a small abdominal incision (\sim 10 mm), the left ureter was exposed and cannulated (PE-10 connected to a PE-50 cannula) for urine sampling. The dead space of the cannula was 7–8 μl , and the diuresis after furosemide (20–40 $\mu\text{l}/\text{min}$), although somewhat declining over time, essentially remained elevated throughout the experiment (1.5 h).

Experimental protocol. After an initial resting period of 10–15 min following the cannulation of the left ureter, trauma of different types was induced. The primary trauma induced, after the small abdominal incision needed for the ureter cannulation, was a \sim 50-mm-long laparotomy (L) along the abdominal midline and along the linea alba of the abdominal muscle wall. This was the only trauma induced in two groups, followed for either 5 or 60 min, denoted L_5 ($n = 9$) and L_{60} ($n = 8$), respectively. In one additional L group, the skin was dissected (D) away from musculus rectus abdominis following the L, bilaterally (\sim 25 mm), at each side of the incision, and investigated at 60 min, and denoted the LD_{60} group ($n = 8$). In three additional groups, crush injury was inflicted upon the abdominal muscles after L and D, by topically “pinching” (crushing) the m. rectus abdominis bilaterally using a pair of hemostatic forceps according to Bansch et al. (4) following additional intravenous analgesia in the form of phentanyll (0.04 mg/kg body wt, Pharmalink). Muscle crush trauma (MT) was induced by either 2×2 or 2×5 pinches, the former group denoted $LD\text{-}MT_{\text{small}}$ and followed for 60 min (i.e., $LD\text{-}MT_{\text{small}}\text{-}60$; $n = 8$), and the latter denoted $LD\text{-}MT_{\text{large}}$, and followed for either 5 ($LD\text{-}MT_{\text{large}}\text{-}5$; $n = 9$) or 60 min ($LD\text{-}MT_{\text{large}}\text{-}60$; $n = 9$). The trauma force was standardized by closing the forceps for about 10 s three times at every location. Each “pinch” caused a muscle crush injury at a right angle from the free edge of the muscle incision of the L, either at two or at five locations on each side of the L, and each being \sim 3 mm \times 35 mm in size. The L incision was then closed by small clips. θ for Ficoll was thus measured at 60 min after the trauma induction, except in two “acute” groups, L_5 and $LD\text{-}MT_{\text{large}}\text{-}5$, where θ was measured already 5 min posttrauma. For sham animals, no L was done, and θ for Ficoll was measured at 5 or 60 min after the initial control period (SHAM $_5$; $n = 8$ and SHAM $_{60}$; $n = 8$, respectively).

Sieving of FITC-Ficoll. Ficoll 70 (10 mg/ml) and Ficoll 400 (10 mg/ml) labeled with FITC were obtained from TdB Consultancy (Uppsala, Sweden). A mixture containing FITC-Ficoll 400 (0.96 mg),

FITC-Ficoll 70 (40 μg), FITC-labeled inulin (0.5 mg, TdB Consultancy) was given as a priming bolus dose followed by a constant infusion ($12 \text{ ml} \cdot \text{kg}^{-1} \cdot \text{h}^{-1}$) of FITC-Ficoll 400 (0.36 mg/ml), FITC-Ficoll 70 (15 $\mu\text{g}/\text{ml}$), FITC-inulin (0.375 mg/ml), and $^{51}\text{Cr}\text{-EDTA}$ (0.225 MBq/ml) for a minimum of 20 min, after which urine was collected for a 5-min period, with a midpoint (2.5 min) plasma sample collected.

An HPLC system (Waters, Milford, MA) was used to determine size and concentration of the Ficoll samples. Size exclusion was achieved using an Ultrahydrogel-500 column (Waters). The mobile phase was driven by a pump (Waters 1525) and fluorescence was detected with a fluorescence detector (Waters 2475) with an excitation wavelength at 492 nm and an emission wavelength at 518 nm. The samples were loaded to the system with an autosampler (Waters 717 plus), and the system was controlled by Breeze Software 3.3 (Waters). The column was calibrated with Ficoll and protein standards described in a previous paper (1).

θ of FITC-Ficoll 70/400 were determined as the fractional clearance from $\theta = (C_{\text{FU}} \cdot C_{\text{IP}}) / (C_{\text{FP}} \cdot C_{\text{IU}})$, where C_{FU} represents the Ficoll urine concentration, C_{IP} represents the inulin concentration in plasma, C_{FP} the Ficoll concentration in plasma, and C_{IU} the inulin concentration in urine.

Glomerular filtration rate. The glomerular filtration rate (GFR) was assessed as the renal clearance of $^{51}\text{Cr}\text{-EDTA}$ (Amersham, Bioscience, Buckinghamshire, UK) and was measured repeatedly throughout the experiment. During the FITC-Ficoll sieving period, GFR was also assessed from the urine clearance of FITC-inulin. $^{51}\text{Cr}\text{-EDTA}$ was given as a bolus dose at the start of the experiments (0.3 MBq in 0.2 ml intravenously) followed by a constant infusion $12 \text{ ml} \cdot \text{kg}^{-1} \cdot \text{h}^{-1}$ (0.225 MBq/ml; together with NaCl) throughout the experiment. For the animals followed for 60 min, GFR was measured during a period of 5–10 min before the trauma induction and then at 30 and 60 min posttrauma and also during the FITC-Ficoll-sampling period (5 min). Blood sampling, using microcapillaries (10 μl), was performed every 10 min of the experiment, and urine was thus sampled every 30 min of the experiment except in the animals that were followed for only 5 min. Radioactivity in blood and urine samples was measured using a gamma counter (Wizard 1480, LKP Wallac, Turku, Finland). Hematocrit was assessed throughout the experiments so as to convert blood radioactivity into plasma radioactivity. The urinary excretion of $^{51}\text{Cr}\text{-EDTA}$ (and FITC-inulin) per minute ($U_i \cdot V_u$) divided by the concentration of tracer in plasma (P_i) was used to calculate GFR, where U_i represents the tracer concentration in urine and V_u the flow of urine per minute.

Tissue-uptake technique for assessing θ for $^{125}\text{I}\text{-HSA}$. At the end of each experiment, albumin θ was measured using a tissue-uptake technique. $^{125}\text{I}\text{-HSA}$ (0.2 MBq; Institute for Energy Technique, Kjeller, Norway) was administered via the tail artery as a bolus, after Ficoll urine sampling was completed. Six blood samples (25 μl) and one urine sample were collected during 8 min for estimation of the θ for $^{125}\text{I}\text{-HSA}$. Thereafter, a whole body washout was performed via the left external jugular vein (25 ml/min) for 8 min. The washout fluid mixture contained equal amounts of 0.9% saline and heparinized horse serum (SVA, Uppsala, Sweden). The inferior vena cava was freed and cut open for collection of rinse fluid. The kidneys were then removed, and the cortex was dissected and assessed with respect to radioactivity in a gamma counter. To reduce the influence of free ^{125}I , urine samples were precipitated with 10% TCA, centrifuged, and the supernatant (free ^{125}I) was discarded. For the tissue-uptake technique, renal tracer protein $^{125}\text{I}\text{-HSA}$ clearance was calculated from the amount of tracer radioactivity accumulated in the left kidney cortex plus the TCA-precipitable urine tracer activity divided by the average plasma tracer concentration, by the tracer circulation time, and by GFR.

Pore analysis. The two-pore model (10, 16, 20) was used to analyze the θ data for Ficoll (molecular radius 13–80 Å). A nonlinear

least squares regression analysis was used to obtain the best curve fit, using scaling multipliers as described at some length previously (10).

Statistical analysis. Values are presented as means \pm SE. Differences among groups were tested using nonparametric analysis of variance with the Kruskal-Wallis test and post hoc testing using the Mann-Whitney *U*-test. Bonferroni corrections for multiple comparisons were made. Significance levels were set at $P < 0.05$, $P < 0.01$, and $P < 0.001$. All statistical calculations were made using SPSS 11.0.3 for Macintosh OSX (SPSS, Chicago, IL).

RESULTS

Mean arterial pressure and heart rate. The sham groups (SHAM₅ and SHAM₆₀) and the two short experimental groups, L₅ and LD-MT_{large-5}, showed a stable mean arterial pressure (MAP) and heart rate (HR) during the course of the experiment. The L₆₀, LD₆₀, and LD-MT_{small-60} groups showed a minor increment in MAP and HR, peaking at 15 min after the trauma induction. In the LD-MT_{small-60} group, MAP thus increased from 90.6 ± 4.4 to 109.4 ± 4.4 mmHg ($P < 0.05$), and HR increased from 359 ± 13 to 399 ± 6 beats/min ($P < 0.05$) at 15 min after the trauma. The LD-MT_{large-60}, however, showed a more stable MAP and HR following the trauma. All changes tended to be reversed to near starting values by the end of the experiment.

GFR. GFR remained more or less stable in all sham and experimental groups, with the exception of the LD-MT_{large-60} group and the LD₆₀ group, where it decreased from 0.70 ± 0.05 to 0.48 ± 0.04 ml·min⁻¹·g⁻¹ ($P < 0.01$) and from 0.67 ± 0.05 to 0.52 ± 0.06 ml·min⁻¹·g⁻¹ ($P < 0.05$), respectively, at 15 min, and in the L₆₀ group, where GFR increased from 0.61 ± 0.08 to 0.75 ± 0.03 ml·min⁻¹·g⁻¹ ($P < 0.05$) at 15 min after the trauma induction (Fig. 1, A and B). Again, at the end of the experiments, the observed changes were more or less reversed.

Glomerular θ for FITC-Ficoll vs. Stokes-Einstein radius. Figure 2A shows the glomerular Ficoll θ vs. molecular radius [Stokes-Einstein radius (a_e)] for the experimental groups exposed to L alone, i.e., in L₅ and L₆₀, respectively. There was a significant increase in the θ for Ficoll_{55-80Å} compared with sham groups already at 5 min, the increase being largely sustained at 60 min. For Ficoll_{70Å}, θ increased from $2.37 \times 10^{-5} \pm 5.80 \times 10^{-6}$ (in SHAM₅) to $1.71 \times 10^{-4} \pm 4.39 \times 10^{-5}$ in L₅ and from $3.32 \times 10^{-5} \pm 1.38 \times 10^{-5}$ (in SHAM₆₀) to $1.22 \times 10^{-4} \pm 2.88 \times 10^{-5}$ in L₆₀, respectively. Adding skin dissection (D) and/or moderate-to-large muscle crush trauma (MT) to the L did not further increase the θ in the a_e range of 55–80 Å (Fig. 2B). For Ficoll_{70Å}, this increase in θ was from $2.37 \times 10^{-5} \pm 5.80 \times 10^{-6}$ (in SHAM₅) to $2.5 \times 10^{-4} \pm 6.1 \times 10^{-5}$ in LD-MT_{large-5} and from $3.32 \times 10^{-5} \pm 1.38 \times 10^{-5}$ (in SHAM₆₀) to $1.3 \times 10^{-4} \pm 2.34 \times 10^{-5}$ in LD-MT_{large-60}, respectively. Again, there was a rapid and sustained increase in θ for high-molecular-weight Ficolls, with no graded response relative to the magnitude of the trauma induced. Data derived from Ficoll sieving curves for the experimental groups not shown in Fig. 2, A and B, are shown in Tables 1 and 2. The two sham groups showed (near) identical glomerular Ficoll sieving curves.

Two-pore modeling. The parameters generated from the best fit of the measured Ficoll sieving curves to the two-pore model are shown in Tables 1 and 2. Data demonstrate that the fractional hydraulic conductance accounted for by the large

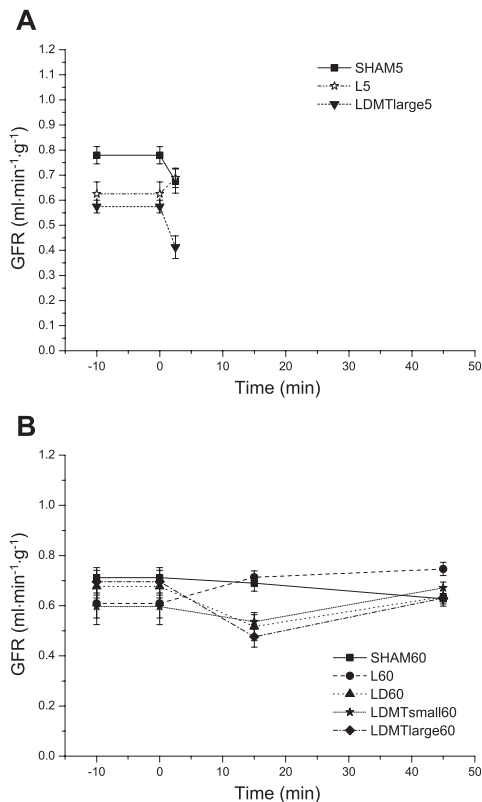


Fig. 1. A: glomerular filtration rate (GFR) per gram kidney as a function of time in control animals (SHAM₅), laparotomized animals (L₅), and animals exposed to laparotomy, skin dissection, and "large" muscle trauma (LD-MT_{large-5}), all observed for 5 min after trauma induction. B: GFR following laparotomy alone (L₆₀), laparotomy, skin dissection, and "small" muscle trauma (LD-MT_{small-60}) and large muscle trauma (LD-MT_{large-60}), all followed for 60 min after trauma. Only LD₆₀ and LD-MT_{large-60} showed a dip in GFR at 15 min. L₆₀ showed a trend toward an increase in GFR over time ($P < 0.05$).

pores (α_L) had increased at least twofold in all of the experimental groups compared with the sham groups, indicating the formation of an increased fraction of large pores in the glomerular filter induced by the laparotomy and/or muscle trauma. The fractional fluid flow through large pores/GFR ratio was more than doubled in all of the groups compared with sham rats. In L₅ and LD-MT_{large-5}, not only the large pore number but also the large pore radius acutely increased compared with SHAM₅. Furthermore, the effective diffusion area over diffusion path length ($A_0/\Delta X$) was reduced in both of these groups.

Glomerular θ for albumin. Figure 3A demonstrates an acutely significant increase in θ for albumin in L₅ and LD-MT_{large-5} vs. SHAM₅ ($5.85 \times 10^{-4} \pm 2.56 \times 10^{-5}$ and $5.92 \times 10^{-4} \pm 4.97 \times 10^{-5}$ vs. $3.56 \times 10^{-4} \pm 4.75 \times 10^{-5}$). Figure 3B shows θ for albumin in experiments continued for 60

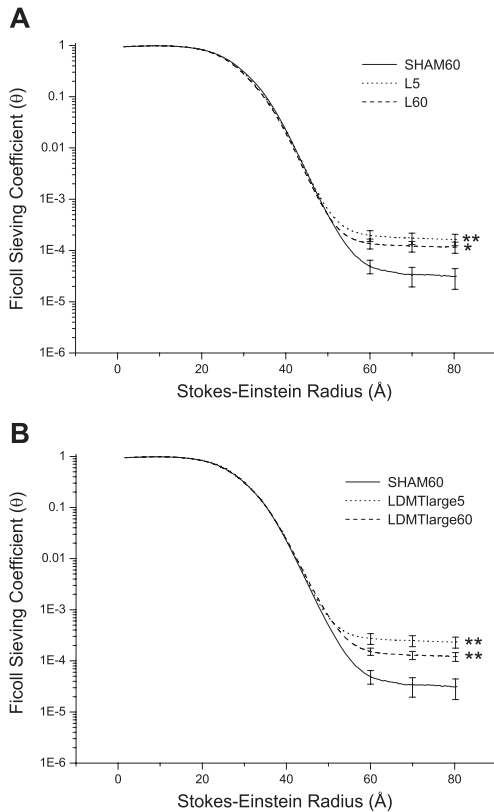


Fig. 2. A: glomerular sieving coefficients (θ) vs. Stokes-Einstein radius (a_s) for Ficoll in the left kidney for groups subjected to laparotomy alone and observed for either 5 min (L_5) or 60 min (L_{60}). There was a rapid increment in θ for Ficoll_{55–80Å}, which was more or less sustained over 60 min. B: glomerular θ vs. a_s for Ficoll in the left kidney for animals exposed to laparotomy, skin dissection, and large muscle trauma observed for either 5 min ($LD-MT_{large-5}$) or 60 min ($LD-MT_{large-60}$). There was a rapid and large increase in θ for Ficoll_{55–80Å} already at 5 min, being sustained at 60 min. Similar results were obtained for rats exposed to skin dissection (LD_{60}) and moderate muscle trauma ($LD-MT_{small-60}$) (not shown).

min. The θ for albumin showed a significant increase in all groups compared with SHAM₆₀.

DISCUSSION

Laparotomy, with or without skin dissection, and with or without ensuing muscle trauma, caused a rapid and sustained increase in θ for large Ficoll molecules and for albumin. According to the two-pore model of glomerular permeability, these changes reflect an increase in the number, and, to some extent, the radius, of large pores in the glomerular filter with only secondary changes in its charge-selective properties. Hence, L alone was sufficient to produce prompt and marked alterations of the glomerular filtration barrier, while adding further trauma by skin dissection and blunt muscle injury

caused no further significant increases in glomerular permeability.

Major body trauma or systemic inflammation may result in excessive inflammatory response patterns, leading to an increased microvascular permeability in the form of increases in the transcapillary escape rate of albumin and microalbuminuria, and in severe cases, acute respiratory distress syndrome (7, 15). This response is mediated in part by activation of monocytes and other inflammatory cells and by the release of proinflammatory cytokines, such as interleukin (IL)-1 and IL-6. Activated leukocytes adhere to the endothelium and may cause additional local, reversible increases in capillary permeability, or endothelial damage, by releasing permeability-increasing agents and/or reactive oxygen species. Furthermore, hemodynamic alterations occur, in this study being most evident directly after the trauma induction (see below). The present study emphasizes the rapidity by which glomerular permeability can increase after trauma. Indeed, we found large increases in glomerular permeability already ~5 min after the trauma induction. Although the response showed a tendency to “fade” over time, it was still largely sustained at 60 min, conceivably reflecting a continual release of proinflammatory mediators initiated by the trauma induction. This is in stark contrast to the glomerular permeability response in anaphylactic shock (3), which was also very pronounced after 5 min, but which was completely reversible within 40 min. These different response patterns conceivably reflect two different types of inflammatory stimulation. In anaphylaxis, there is a rapid degranulation of mast cells with release of histamine and other mediators to the circulation, which results in very prompt and dramatic initial vascular permeability changes. In posttraumatic conditions (and in sepsis), there is obviously a more continual activation of proinflammatory mechanisms, causing more sustained responses, even though in LPS-induced septicemia, the onset of these changes was relatively slow (3).

Immediately posttrauma (in the L_5 and $LD-MT_{large-5}$ groups), there was a reduction in $A_0/\Delta X$, indicating an altered glomerular hemodynamic situation. Conceivably, following trauma, similar to the situation in acute anaphylaxis, there is an acute renal vasoconstriction, mainly affecting the efferent arteriole, preventing large reductions in GFR, but reducing renal blood flow, and hence, $A_0/\Delta X$. Theoretically, if $A_0/\Delta X$ is reduced considerably more than GFR, then there will be a reduction in θ s for Ficoll_{20–40Å} and a tendency of an increase in θ s for Ficoll_{55–80Å} (17). Although slight, a depression of the

Table 1. Two-pore parameters measured 5 min after trauma in L_5 and $LD-MT_{large-5}$ groups vs. SHAM₅ group

Two-Pore Parameters	SHAM ₅ (n = 8)	L_5 (n = 9)	$LD-MT_{large-5}$ (n = 8)
Small-pore radius (r_s), Å	46.0 ± 0.05	47.0 ± 0.16†	47.2 ± 0.16†
Large-pore radius (r_L), Å	114.6 ± 2.95	172.6 ± 6.60†	164.1 ± 11.9†
$\alpha_L \times 10^5$	3.90 ± 0.83	8.67 ± 1.82	10.24 ± 2.19*
$J_{V1}/GFR \times 10^5$	10.1 ± 2.21	29.3 ± 6.34*	41.2 ± 8.03*
$A_0/\Delta X$, cm/g $\times 10^{-5}$	6.82 ± 0.75	1.77 ± 0.11†	1.24 ± 0.20†

Values are given \pm SE; n = no. of rats. See text for definitions of groups. α_L , Fractional ultrafiltration coefficient accounted for by large pores; J_{V1}/GFR , fractional fluid flow through large pores; GFR, glomerular filtration rate; $A_0/\Delta X$, effective area of unit diffusion path length. Statistical difference between SHAM and experimental groups (L_5 and $LD-MT_{large-5}$): * $P < 0.05$, † $P < 0.01$.

Table 2. Two-pore parameters in L_{60} , LD_{60} , $LD-MT_{small}-60$, and the $LD-MT_{large}-60$ groups vs. $SHAM_{60}$ group

Two-Pore Parameters	$SHAM_{60}$ (n = 8)	L_{60} (n = 8)	LD_{60} (n = 9)	$LD-MT_{small}-60$ (n = 8)	$LD-MT_{large}-60$ (n = 9)
Small-pore radius (r_s), Å	47.3±0.08	46.7±0.14	47.1±0.17	47.3±0.10	47.4±0.22
Large-pore radius (r_L), Å	136.5±9.95	172.4±9.88*	163.11±9.74	157.5±3.35	167.6±4.72*
$\alpha_L \times 10^5$	2.98±0.77	6.09±1.11	6.16±1.8	6.83±1.32*	7.05±0.91*
$J_{V1}/GFR \times 10^5$	9.09±2.6	20.0±3.9	20.1±6.29	21.7±4.38*	23.4±3.30*
$A_0/\Delta X \text{ cm/g} \times 10^{-5}$	1.84±0.14	1.29±0.21	2.09±0.20	1.26±0.09	1.45±0.26

Values are given \pm SE; n = number of rats. See text for definitions of groups. * $P < 0.05$.

sieving curve for Ficoll_{20–40Å} can be seen in Fig. 2A. Due to the increase in glomerular permeability, θ s for Ficoll_{55–80Å} increased acutely. A further increment in θ s for high-molecular-weight Ficolls can be expected to occur for hemodynamic reasons (reduction in GFR). Since, however, θ s for Ficoll_{55–80Å} 5 min after the trauma were actually not significantly different from those measured at 60 min posttrauma, when MAP and GFR had been more or less normalized, we consider the hemodynamic effects on the Ficoll sieving curves to be rather moderate.

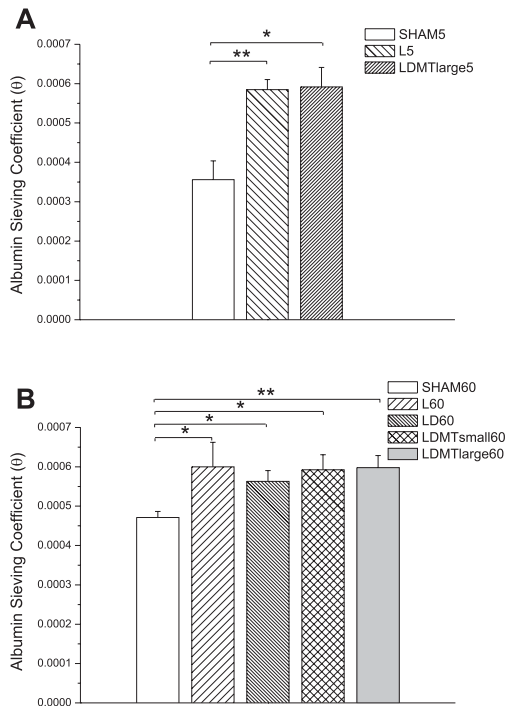


Fig. 3. A: glomerular θ for albumin immediately after laparotomy alone (L_5) or laparotomy and large muscle trauma ($LD-MT_{large-5}$). Laparotomy with and without muscle trauma caused significant increases in θ for albumin. B: glomerular albumin θ in animals exposed to laparotomy (L_{60}), laparotomy and skin dissection (LD_{60}), laparotomy and small muscle trauma ($LD-MT_{small-60}$), and laparotomy and large muscle trauma ($LD-MT_{large-60}$), all followed for 60 min. All changes in θ were significant ($P < 0.05$).

Much to our surprise, the glomerular permeability increases in this study occurred more or less in an "all-or-none" fashion. Thus L alone caused very marked and rapid increases in glomerular permeability. No significant further increments in glomerular permeability occurred for additional trauma, in the form of skin dissection or graded muscle injury, despite the fact that very large increases in glomerular permeability have been noted in this model in puromycin aminonucleoside-induced glomerulopathy (2). Evidently, L alone seems to lead to an acute, nearly full-fledged, inflammatory response, at least with respect to the alterations causing an increased glomerular permeability. Indeed, when glomerular Ficoll sieving curves in sham (control) animals in the present study were compared together with those in a previous study (3), in which L was not done to access the left ureter, with experiments in which L had been performed (1, 17, 18), there is a much higher glomerular permeability to Ficoll_{55–80Å} in the latter experiments. Thus, already from these data, it seems evident that L represents a major trauma, inducing sustained increases in glomerular permeability. Indeed, animals not exposed to L show very low θ for Ficoll_{55–80Å}, being of the same order of magnitude as θ for proteins of equivalent chromatographic radii in patients lacking PTR (Dent's disease) (14). It has thus previously been shown that the "hyperpermeability" of Ficoll_{25–50Å} (relative to proteins having equivalent chromatographic radii) manifested across the small pores of the glomerular filter is not manifested for Ficoll_{55–80Å} in large pores of the filter (21). This is conceivably owing to the lower ratio of a_e to pore radius (<0.7) in the large pores than in small pores, so that Ficoll hyperpermeability is not manifested, (17, 18, 21).

While the Ficoll molecules in this study are largely uncharged, albumin is negatively charged at a physiological pH. According to the two-pore model of glomerular transport, negatively charged albumin ($a_e = 36$ Å), unlike Ficoll_{36Å}, is more or less totally confined to the large pores for its transport across the negatively charged glomerular filtration barrier, similar to Ficoll_{55–80Å}. Thus, according to the Debye-Hückel theory of ion-ion interactions (16), negative albumin dissolved in physiological saline (or plasma) and interacting with negatively charged surfaces (e.g., pore walls), would behave similarly to a neutral molecule of radius $(36+8) = 44$ Å, where 8 Å is the so-called Debye length, whereas a negatively charged cylindrical small pore, having a radius of 47 Å, as in this study, interacting with a negatively charged molecule would have an effective pore radius of $(47-8) = 39$ Å. Thus, because negative albumin (effective radius 44 Å) is excluded from the negatively charged small pores (effective radius 39 Å), but is permeable across large pores (radius >110 Å), one would expect θ s for Ficoll_{55–80Å} and that for albumin to change more or less in parallel for purely size-selective changes in the glomerular

filter affecting the large pores (18). By contrast, for exclusive changes in charge selectivity, θ for albumin would change in excess of those for Ficoll_{55–80Å}, because albumin will now, unlike Ficoll_{55–80Å}, be able to permeate also the small pores. In the present study, θ s for albumin seemed to change less than θ s for Ficoll_{55–80Å}. It thus seems clear that charge selectivity may not be primarily responsible for posttraumatic microalbuminuria. However, it should also, in this context, be noted that with the tissue-uptake technique there is a tendency of overestimating θ to albumin under normal (sham) conditions. The reason for this may be incomplete renal vascular tracer washout at the end of the experiment, and the presence of some free (unbound) iodine in the radiolabeled albumin preparations used. Since the albumin θ is somewhat overestimated in the control situation, the relative changes after surgery and trauma seemed to have been underestimated. At any rate, assuming an albumin θ of the normal glomerular filter to be on the order of $1\text{--}2 \times 10^{-4}$, the changes posttrauma do still not exceed those measured for Ficoll_{55–80Å}.

Previous studies from our groups strongly indicate that the major barrier to protein permeability of the glomerular filter is not at the level of the podocyte slit diaphragm (10, 17). Thus apparently all the three sequential barriers, i.e., the glomerular basement membrane (GBM) and the two cellular layers, need to interact to form the nearly perfect glomerular permeability barrier normally present (8). However, the way that podocytes interact with the GBM may be crucial. Release of acute proinflammatory mediators and activation of white blood cells by the trauma may interact with the podocytes to produce the changes in their actin cytoskeleton that may alter the shape of the podocyte and the tension that the podocytes exert on the GBM. Also, the integrins linking the podocyte foot processes to the GBM may be acutely involved in the rapid increases in glomerular permeability. Furthermore, it can be speculated that also the endothelial layer may be affected by permeability substances in a way similar to what occurs in peripheral capillaries after release of e.g., histamine, substance P, or cytokines (11, 12, 16).

In conclusion, a laparotomy with or without ensuing muscle trauma caused a rapid and sustained increase in the glomerular permeability to large Ficoll molecules and albumin in a way that seems to reflect a reduced size selectivity of the glomerular filtration barrier, without any primary changes in charge selectivity. According to the two-pore model of glomerular permeability, these changes reflect an increase in the number, and, to some extent, in the radius, of the large pores in the glomerular filter. The rapidity by which these changes occur emphasizes the fact that the permeability of the glomerular filtration barrier is variable over time and can promptly increase in response to inflammation and trauma.

ACKNOWLEDGMENTS

The skillful typing of the manuscript by Kerstin Wihlborg is gratefully acknowledged.

GRANTS

This study was supported by Swedish Medical Research Council Grant 08285, the Heart and Lung Foundation, and the Medical Faculty at Lund University (ALF grant).

REFERENCES

1. Asgerisson D, Venturoli D, Rippe B, Rippe C. Increased glomerular permeability to negatively charged Ficoll relative to neutral Ficoll in rats. *Am J Physiol Renal Physiol* 291: F1083–F1089, 2006.
2. Asgerisson D, Rippe C, Rippe A, Rippe B. Glomerular sieving of Ficoll compared with that of proteins in paraaminonucleoside (PAN) induced nephrosis in rats (Abstract). *J Am Soc Nephrol* 17: 717A, 2006.
3. Axelsson J, Rippe A, Venturoli D, Swärd P, Rippe B. Effects of early endotoxemia and dextran-induced anaphylaxis on the size selectivity of the glomerular filtration barrier in rats. *Am J Physiol Renal Physiol* 296: F242–F248, 2009.
4. Bansch P, Lundblad C, Grände PO, Bentzer P. A trauma model for evaluation of the effects of blunt skeletal muscle trauma on microvascular permeability, plasma volume and cytokine release in the rat. *Shock*. In press.
5. Davies MG, Hagen PO. Systemic inflammatory response syndrome. *Br J Surg* 84: 920–935, 1997.
6. Gosling P, Shearman CP, Gwynn BR, Simms MH, Bainbridge ET. Microproteinuria: response to operation. *Br Med J (Clin Res Ed)* 296: 338–339, 1988.
7. Gosling P, Sanghera K, Dickson G. Generalized vascular permeability and pulmonary function in patients following serious trauma. *J Trauma* 36: 477–481, 1994.
8. Haraldsson B, Nystrom J, Deen WM. Properties of the glomerular barrier and mechanisms of proteinuria. *Physiol Rev* 88: 451–487, 2008.
9. Jensen JS, Borch-Johnsen K, Jensen G, Feldt-Rasmussen B. Microalbuminuria reflects a generalized transvascular albumin leakiness in clinically healthy subjects. *Clin Sci* 88: 629–633, 1995.
10. Lund U, Rippe A, Venturoli D, Tenstad O, Grubb A, Rippe B. Glomerular filtration rate dependence of sieving of albumin and some neutral proteins in rat kidneys. *Am J Physiol Renal Physiol* 284: F1226–F1234, 2003.
11. Majno G, Palade GE. Studies on inflammation. I. The effect of histamine and serotonin on vascular permeability: an electron microscopic study. *J Biophys Biochem Cytol* 11: 571–605, 1961.
12. McDonald DM, Thurston G, Baluk P. Endothelial gaps as sites for plasma leakage in inflammation. *Microcirculation* 6: 7–22, 1999.
13. Nergelius G, Vinge E, Grubb A, Lidgren L. Renal impairment after hip or knee arthroplasty. Urinary excretion of protein markers studied in 59 patients. *Acta Orthop Scand* 68: 34–40, 1997.
14. Norden AG, Lapsley M, Lee PJ, Pusey CD, Scheinman SJ, Tam FW, Thakker RV, Unwin RJ, Wrong O. Glomerular protein sieving and implications for renal failure in Fanconi syndrome. *Kidney Int* 60: 1885–1892, 2001.
15. Pallister I, Dent C, Wise CC, Alpar EK, Gosling P. Early post-traumatic acute respiratory distress syndrome and albumin excretion rate: a prospective evaluation of a 'point-of care' predictive test. *Injury* 32: 177–181, 2001.
16. Rippe B, Haraldsson B. Transport of macromolecules across microvascular walls. The two-pore theory. *Physiol Rev* 74: 163–219, 1994.
17. Rippe C, Asgerisson D, Venturoli D, Rippe A, Rippe B. Effects of glomerular filtration rate on Ficoll sieving coefficients (θ) in rats. *Kidney Int* 69: 1326–1332, 2006.
18. Rippe C, Rippe A, Larsson A, Asgerisson D, Rippe B. Nature of glomerular capillary permeability changes following acute renal ischemia-reperfusion injury in rats. *Am J Physiol Renal Physiol* 291: F1362–F1368, 2006.
19. Rippe C, Rippe A, Torffvit O, Rippe B. Size and charge selectivity of the glomerular filter in early experimental diabetes in rats. *Am J Physiol Renal Physiol* 293: F1533–F1538, 2007.
20. Tencer J, Frick IM, Öqvist BW, Alm P, Rippe B. Size-selectivity of the glomerular barrier to high molecular weight proteins: upper size limitations of shunt pathways. *Kidney Int* 53: 709–715, 1998.
21. Venturoli D, Rippe B. Ficoll and dextran vs. globular proteins as probes for testing glomerular permselectivity: effects of molecular size, shape, charge, and deformability. *Am J Physiol Renal Physiol* 288: F605–F613, 2005.
22. Vlachou E, Gosling P, Moiemmen NS. Microalbuminuria: a marker of endothelial dysfunction in thermal injury. *Burns* 32: 1009–1016, 2006.

Paper III

Acute hyperglycemia induces rapid, reversible increases in glomerular permeability in nondiabetic rats

Josefin Axelsson, Anna Rippe, and Bengt Rippe

Department of Nephrology, Lund University, Lund, Sweden

Submitted 11 December 2009; accepted in final form 12 March 2010

Axelsson J, Rippe A, Rippe B. Acute hyperglycemia induces rapid, reversible increases in glomerular permeability in nondiabetic rats. *Am J Physiol Renal Physiol* 298: F1306–F1312, 2010. First published March 17, 2010; doi:10.1152/ajprenal.00710.2009.—This study was performed to investigate the impact of acute hyperglycemia (HG) on the permeability of the normal glomerular filtration barrier in vivo. In anesthetized Wistar rats (250–280 g), the left ureter was catheterized for urine collection, while simultaneously blood access was achieved. Rats received an intravenous (iv) infusion of either 1) hypertonic glucose to maintain blood glucose at 20–25 mM (G ; $n = 8$); 2) hypertonic glucose as in 1) and a RhoA-kinase inhibitor (Y-27632; Rho-G; $n = 8$); 3) 20% mannitol (MANN; $n = 7$) or 4) hypertonic (12%) NaCl to maintain plasma crystalloid osmotic pressure (π_{cr}) at ~ 320 – 325 mosmol/l (NaCl; $n = 8$) or 5) physiological saline (SHAM; $n = 8$). FITC-Ficoll 70/400 was infused iv for at least 20 min before termination of the experiments, and plasma and urine were collected to determine the glomerular sieving coefficients (θ) for polydisperse Ficoll (molecular radius 15–80 Å) by high-performance size-exclusion chromatography. In G there was a marked increase in θ for Ficoll_{55–80Å} at 20 min, which was completely reversible within 60 min and abrogated by a Rho-kinase (ROCK) inhibitor, while glomerular permeability remained unchanged in MANN and NaCl. In conclusion, acute HG caused rapid, reversible increases in θ for large Ficolls, not related to the concomitant hyperosmolarity, but sensitive to ROCK inhibition. The changes observed were consistent with the formation of an increased number of large pores in the glomerular filter. The sensitivity of the permeability changes to ROCK inhibition strongly indicates that the cytoskeleton of the cells in the glomerular barrier may be involved in these alterations.

microalbuminuria; RhoA-kinase; podocytes; endothelium; hyperosmolarity

CHRONIC HYPERGLYCEMIA (HG), such as in diabetes mellitus, may cause macro- and microangiopathy with microalbuminuria as an early sign, and, eventually, widespread end-organ damage. The pathophysiological changes behind HG-induced microvascular dysfunction and organ damage are partly elusive, but include 1) the formation of advanced glycation end products (AGE), 2) an abnormal glucose metabolism via the polyol pathway, 3) an increase in diacylglycerol production, which in turn activates PKC, and 4) increased RhoA-kinase (ROCK) activity (6, 8, 22, 23, 28, 34). With respect to renal injury, HG-induced hemodynamic alterations leading to hyperfiltration also contribute. The final common step causing vascular dysfunction during HG includes an increase in oxidative stress caused by an increased formation of reactive oxygen species (ROS) and decreased endothelial nitric oxide (NO) production. All these alterations may lead to microalbuminuria.

In *in vitro* studies on cultured endothelial monolayers, acute HG has been shown to produce barrier dysfunction and (reversible) endothelial albumin leakage. Hempel et al. (11) thus demonstrated a marked increase in (porcine) endothelial monolayer permeability, already after 30 min of acute HG, being completely reversible within 100 min of continued HG. Zuurbier et al. (35) demonstrated that acute HG can induce marked increases in the transcapillary escape rate (TER) of high-molecular-weight (70 kDa) dextran in mice. In fact, during acute HG the TER of dextran-70 approached that of dextran-40, which is normally mainly eliminated from the circulation by glomerular filtration (1). These data thus strongly suggest a marked increase in dextran-70 elimination by the urine in acute HG. However, the authors interpreted their findings as solely reflecting a generally increased permeability of the endothelial surface layer (glycocalyx). At any rate, the two mentioned studies indicate that acute HG may alter endothelial and glomerular barrier permeability.

On this background, and since we have recently demonstrated that acute anaphylaxis in rats can rapidly and reversibly increase glomerular permeability to high-molecular-weight Ficoll and to albumin (4), we considered it of interest to investigate whether acute HG, under *in vivo* conditions, can produce similar dynamic increases in glomerular permeability. To exclude the possibility that glomerular barrier function may be altered following increases in plasma osmolarity per se, we also assessed glomerular selectivity following infusions of hypertonic mannitol or NaCl. In addition, to elucidate the dynamics of glomerular permeability changes during HG, glomerular sieving was followed as a function of time during the HG insult. Finally, to find out whether the contractile F-actin cytoskeleton of the cells of the glomerular filter, i.e., the podocytes and the endothelium, may be involved, we investigated the impact of a ROCK inhibitor on HG-induced glomerular barrier alterations.

Glomerular size selectivity was assessed *in vivo* by measuring the glomerular sieving of iv infused FITC-Ficoll (70/400), a neutral, near-spherical, polydisperse polysaccharide, which is not to a significant extent reabsorbed by the proximal tubules (33). The experiments were especially designed so as to detect changes in the sieving patterns of very large Ficoll molecules, by administering predominantly molecules of high molecular weight (MW ~ 400 kDa). Large Ficoll molecules have been shown to exhibit low glomerular permeability properties more or less identical to those of albumin and large native proteins of equivalent chromatographic radii, which are preferentially permeable through “large pores” (shunt pathways) of the glomerular filter (4, 25, 26, 33). Our data demonstrate rapid, reversible increases in glomerular permeability in acute HG, which may have implications for the microalbuminuria seen in diabetic patients with poor glycemic control.

Address for reprint requests and other correspondence: B. Rippe, Dept. of Nephrology, Lund Univ., Univ. Hospital of Lund, S-211 85 Lund, Sweden (e-mail: Bengt.Rippe@med.lu.se).

MATERIALS AND METHODS

Animals

Experiments were performed in 47 male Wistar rats (Møllegaard, Lille Stensved, Denmark), with an average body weight of 273.4 ± 2.4 g. The rats had free access to water and standard chow until the day of the experiment. The animal Ethics Committee at Lund University approved the animal experiments.

Surgery

Anesthesia was induced with pentobarbital sodium (60 mg/kg) intraperitoneally (ip), and body temperature was kept at 37°C by a thermostatically controlled heating pad. The tail artery was cannulated (PE-50 cannula) for continuous monitoring of mean arterial blood pressure (MAP) and heart rate (HR) on a polygraph (model 7B, Grass Instruments, Quincy, MA) and for repeated administration of anesthesia (pentobarbital sodium). The left carotid artery was cannulated (PE-50 cannula) for blood sampling and the left and right jugular veins for infusion purposes. Access to the left ureter was obtained through a small (6–8 mm) abdominal incision. Furosemide (0.375 mg/kg, Furosemid, Recip, Sweden) was administered in the tail artery to increase urine production and facilitate cannulation of the urethra, used for urine sampling. The latter was dissected free, and a PE-10 cannula was inserted and secured by a ligature.

Experimental Protocol

All studies started with an initial resting period of 10–15 min following the cannulation of the left urethra.

Hyperglycemia. Hyperglycemia was induced by iv administration of hypertonic (40%) glucose (D-glucose, K13654437, Merck, Darmstadt, Germany) in saline, given as a bolus (500 μl) followed by an infusion (40% D-glucose in saline; $10 \text{ ml} \cdot \text{kg}^{-1} \cdot \text{h}^{-1}$) throughout the experiment to maintain blood glucose at 20–25 mmol/l. Blood glucose levels were measured approximately every 5 min (Glucometer, Dex 2), and the glucose infusion was adjusted so as to maintain blood glucose at the desired level. Sampling of urine and plasma for Ficoll sieving measurements was performed at 20 min (G; $n = 8$) or, sequentially, at 5, 20, and 60 min (G-5, G-20, and G-60, respectively; $n = 8$) in experiments lasting for (a minimum of) 60 min after induction of HG.

Hyperosmolarity. Hyperosmolarity was induced by iv infusions of either hypertonic NaCl (31434, Sigma-Aldrich Laborchemikalien, Seelze, Germany) or mannitol (M 1425, Sigma, St. Louis, MO) to raise plasma osmolarity by ~ 14 – 15 mosmol/l, as checked by repeated measurements of crystalloid osmotic pressure (π_{crf} ; Fiske Micro-Osmometer, model 210, Fiske Associates, Norwood, MA). For the mannitol experiments (MANN; $n = 7$), a bolus of 500 μl of a 20% solution was given, followed by a constant infusion (20% mannitol; 10 ml/kg/h). For the hypertonic NaCl experiments (NaCl; $n = 8$), a bolus (500 μl) of a 12% NaCl solution was followed by a constant infusion of hyperosmolar NaCl (12% NaCl; $10 \text{ ml} \cdot \text{kg}^{-1} \cdot \text{h}^{-1}$). Besides measuring plasma osmolarity in the NaCl group, the plasma concentration of Na^+ was also determined by indirect potentiometry (i-STAT, Hewlett-Packard, Böblingen, Germany). In the hyperosmolarity groups, sieving measurement for FITC-Ficoll 70/400 was performed at 20 min after the induction of the hyperosmotic insult.

Hyperglycemia and Rho-kinase inhibition (Y-27632). After the initial resting period, an iv administration of a specific Rho-kinase inhibitor, Y-27632 (Mitsubishi Pharma, Osaka, Japan), was initiated, followed (after 5 min) by hypertonic glucose (Rho-G; $n = 8$). Y-27632 was dissolved in physiological saline and given as a bolus (1.5 μl of 10 mg/ml in 200 μl saline) in the left jugular vein, followed by a constant infusion (0.536 mg/ml; 4.5 $\mu\text{l/min}$). Y-27632 was thus given during a period of 5 min before the start of and during the HG period. HG was induced as previously described, and glomerular

sieving measurements occurred at 20 min following the induction of hyperglycemia.

SHAM animals. SHAM animals (SHAM; $n = 8$) were given physiological saline as a bolus and constant infusion in a way mimicking the experimental interventions, and these were followed for 20 min, at which time glomerular sieving measurements were performed.

Glomerular Sieving of FITC-Ficoll-70/400

A mixture of FITC-Ficoll-70 (10 mg/ml) and FITC-Ficoll-400 (10 mg/ml, TdB Consultancy, Uppsala, Sweden) in a 1:24 relationship was administered as a bolus dose together with FITC-inulin (10 mg/ml, TdB Consultancy). The bolus dose (FITC-Ficoll: 70, 40 μg ; FITC-Ficoll: 400 960 μg ; and FITC-inulin: 500 μg) was followed by a constant infusion of $10 \text{ ml} \cdot \text{kg}^{-1} \cdot \text{h}^{-1}$ (FITC-Ficoll-70, 20 $\mu\text{g/ml}$; FITC-Ficoll-400, 0.48 mg/ml; FITC-Inulin, 0.5 mg/ml, and ^{51}Cr -EDTA 0.3 MBq/ml) for at least 20 min before sieving measurements, after which time urine from the left kidney was collected for 5 min, with a midpoint (2.5 min) plasma sample collected.

Glomerular Filtration Rate

Glomerular filtration rate (GFR) was measured in the left kidney during the experiment using ^{51}Cr -EDTA. A priming dose of ^{51}Cr -EDTA (0.3 MBq in 0.2 ml iv, Amersham Biosciences, Buckinghamshire, UK) was administered and followed by a continuous infusion ($10 \text{ ml} \cdot \text{kg}^{-1} \cdot \text{h}^{-1}$) of ^{51}Cr -EDTA (0.3 MBq/ml) throughout the experiment. Urine was collected from the left ureter repeatedly during this period, and blood samples, using microcapillaries, were taken to be able to calculate GFR, every 10 min. Radioactivity in blood and urine was measured in a gamma counter (Wizard 1480, LKP, Wallac, Turku, Finland). Hematocrit was assessed throughout the experiments to convert blood radioactivity into plasma radioactivity. During the FITC-Ficoll sieving period, GFR was also assessed from the urine clearance of FITC-inulin.

High-Performance Size-Exclusion Chromatography

An HPLC system (Waters, Milford, MA) was used to determine size and concentration of the Ficoll samples. Size exclusion was achieved using an Ultrahydrogel-500 column (Waters). The mobile phase was driven by a pump (Waters 1525), and fluorescence was detected with a fluorescence detector (Waters 2475) with an excitation wavelength at 492 nm and an emission wavelength at 518 nm. The samples were loaded to the system with an autosampler (Waters 717 plus), and the system was controlled by Breeze Software 3.3 (Waters). The column was calibrated with Ficoll and protein standards described in a previous paper (2).

Transmission Electron Microscopy of Rat Glomeruli Exposed to HG vs. Control

Biopsies from kidneys were taken using a human (percutaneous) biopsy needle (True Core II Biopsy Instrument, Angiotech Medical Device Technologies, Gainesville, GA). Biopsies were immediately placed in fixative [1.5% glutaraldehyde and 1.5% paraformaldehyde in 0.1 M Sorensen phosphate buffer (pH 7.2)] and left overnight. After fixation, biopsies were rinsed in buffer, postfixed in 1% osmium tetroxide (OsO_4) for 1 h, and dehydrated using graded acetone solutions and embedded in Polarbed 812 (Polaron). Ultrathin sections (60–80 nm) were cut using a LKB Supernova ultramicrotome (Reichert Jung, Vienna, Austria) and placed on thin-bar copper grids and stained with uranyl acetate and lead citrate. The sections were examined using a Philips CM-10 transmission electron microscope (Philips Scientific, Eindhoven, The Netherlands).

Calculations

The urinary excretion of ^{51}Cr -EDTA and FITC-inulin per minute ($U_i \times V_u$) divided by the concentration of tracer in plasma (P_i) was

used to calculate GFR, where U_i represents the tracer concentration in urine, and V_u the flow of urine per minute. Ficoll sieving coefficients (θ) were obtained by analyzing high-performance size-exclusion chromatography (HPSEC) curves from the plasma (C_{PF}) and urine sample for each experiment. The urine concentration vs. the Stokes-Einstein radius (a_c) curve was divided by the inulin concentration to obtain the primary urine concentration (C_{UF}). θ for each a_c was calculated by dividing C_{UF} by C_{PF} . A two-pore model (17, 24, 29) was used to analyze the θ data for Ficoll (molecular radius 15–80 Å). A nonlinear least-squares regression analysis was used to obtain the best curve fit, using scaling multipliers, as described at some length previously (17).

Statistical Analysis

Values are presented as means \pm SE. Differences among groups were tested using nonparametric analysis of variance with the Kruskal-Wallis test and post hoc tested using the Mann-Whitney U -test. Bonferroni corrections for multiple comparisons were made. Significance levels were set at $*P < 0.05$, $**P < 0.01$, and $***P < 0.001$. All statistical calculations were made using SPSS 17.0 for Windows (SPSS, Chicago, IL).

RESULTS

Hemodynamic Parameters

All the experimental groups showed a stable mean arterial pressure (Fig. 1) and heart rate (not shown) over time.

π_{cr} and Blood Glucose

Results from blood glucose and plasma crystalloid osmotic measurements in the various groups as a function of time are listed in Tables 1 and 2, respectively. During HG, blood glucose increased by 14–18 mM, while the hyperosmolar insults (NaCl, MANN) caused an increase in plasma osmolality on the order of 12–14 mosmol/l, which in NaCl matched the measured increase in plasma Na (+7 mmol/l).

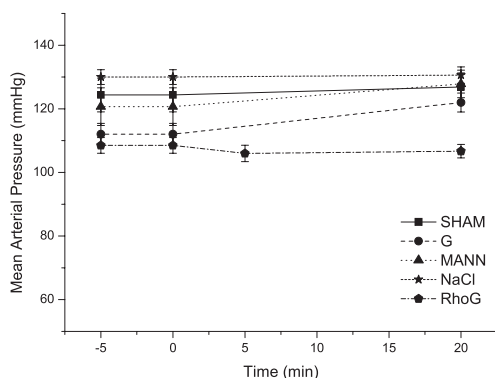


Fig. 1. Mean arterial pressure (MAP) vs. time in the experimental groups and in the SHAM group. During high glucose (HG) and concomitant Rho-kinase inhibition (in Rho-G), there was a fall in MAP, while it was largely unchanged in all other groups. Solid line and squares, SHAM; dashed line and filled circles, G; dotted line and triangles, mannitol (MANN); finely dashed line and stars, NaCl; and dashed-dotted line and pentagons, Rho-G.

Table 1. Blood glucose concentration (mmol/l) as a function of time during 20 min of HG and, sequentially, at G-5, G-20, and G-60, respectively

	G (n = 8)	Rho-G (n = 8)
Time 0	5.26 \pm 0.27	4.86 \pm 0.13
5 min	21.26 \pm 0.89***	21.01 \pm 0.55***
10 min	22.81 \pm 0.87***	21.69 \pm 0.37***
20 min	23.20 \pm 0.90***	21.91 \pm 0.63***
	G-5-G-60 (n = 8)	
Time 0	5.39 \pm 0.19	
5 min	20.49 \pm 0.54***	
10 min	25.07 \pm 1.37***	
20 min	21.23 \pm 0.91***	
30 min	23.16 \pm 0.84***	
45 min	21.13 \pm 0.34***	
60 min	21.82 \pm 0.66***	

Values are means \pm SE. HG, high glucose. Statistical differences are indicated for the test period vs. baseline (time 0). The significance level is $***P < 0.001$.

GFR

GFR (Fig. 2) remained more or less stable in all groups, but tended to slightly increase in SHAM [$0.71 \pm 0.05 \text{ ml} \cdot \text{min}^{-1} \cdot \text{g}$ (kidney) $^{-1}$ to $0.76 \pm 0.06 \text{ ml} \cdot \text{min}^{-1} \cdot \text{g}^{-1}$; not significant].

θ for FITC-Ficoll

Figure 3 demonstrates θ vs. Stokes-Einstein radius (a_c) curves for Ficoll molecules ranging in radius from 15 to 80 Å for G, MANN and NaCl vs. SHAM at 20 min. In the a_c range 55–80 Å, G showed a clearly increased θ , whereas θ for MANN and NaCl remained unchanged compared with SHAM. For Ficoll_{70Å}, θ thus increased from $2.41 \times 10^{-5} \pm 7.57 \times 10^{-6}$ to $1.16 \times 10^{-4} \pm 3.87 \times 10^{-5}$ ($P < 0.01$) in G, whereas θ for Ficoll_{70Å} in MANN and NaCl remained more or less unchanged at $2.88 \times 10^{-5} \pm 7.14 \times 10^{-6}$ and $3.66 \times 10^{-5} \pm 5.14 \times 10^{-6}$, respectively. This was also the case for Rho-G, in which the glomerular Ficoll sieving curve was more or less the same as for SHAM (Fig. 4). For Ficoll_{70Å}, θ was thus $2.84 \times 10^{-5} \pm 6.81 \times 10^{-6}$ at 20 min of HG under Rho-kinase inhibition.

Table 2. Plasma crystalloid osmotic pressure as a function of time in the 2 hyperosmolar groups and plasma Na⁺ concentration

	Plasma Crystalloid Osmotic Pressure, mosmol/l	
Time 0	308.7 \pm 0.61	308.4 \pm 1.08
10 min	320.6 \pm 1.80**	322.6 \pm 2.19***
20 min	322.1 \pm 2.62**	322.8 \pm 2.22***
	Plasma Na ⁺ Concentration, mmol/l (n = 8).	
Time 0	141.4 \pm 0.42	
10 min	147.9 \pm 0.35***	
20 min	148.8 \pm 0.37***	

Values are means \pm SE. Statistical differences are indicated for values after 10 and 20 min versus time 0. Significance levels are $**P < 0.01$ and $***P < 0.001$.

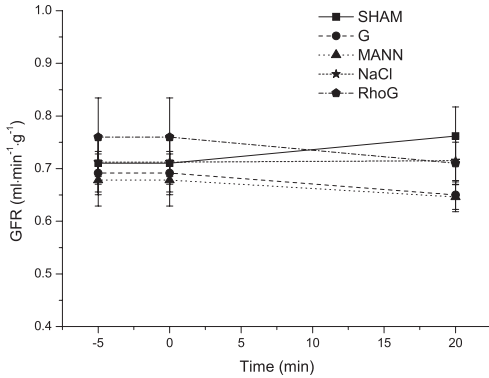


Fig. 2. Glomerular filtration rate (GFR) as a function of time in the experimental groups and in SHAM. No significant alterations occurred in any of the groups. Symbols and lines are as in Fig. 1.

Figure 5 shows θ for Ficoll molecules from 60 to 80 Å in radius during HG as a function of time, i.e., at 5, 20, and 60 min (G-5, G-20, and G-60, respectively). HG caused significant increases in θ for large Ficoll molecules at 20 min, and these changes were completely reversible within 60 min. For Ficoll_{70Å}, G-20 thus showed a sieving coefficient of $2.36 \times 10^{-4} \pm 8.03 \times 10^{-5}$, which was reversed to $1.64 \times 10^{-5} \pm 4.5 \times 10^{-6}$ at G-60 ($P < 0.001$).

Two-Pore Modeling

The best curve fits of θ vs. a_e for Ficoll according to the two-pore model were obtained using the parameters listed in Tables 3 and 4. Data demonstrate that the fractional hydraulic conductance accounted for by the large pores (α_L) had increased almost threefold in G compared with SHAM ($P < 0.05$), indicating the formation of more large pores in the glomerular filter during HG. The fractional fluid flow through the large pores (large-pore volume flow/GFR) was also mark-

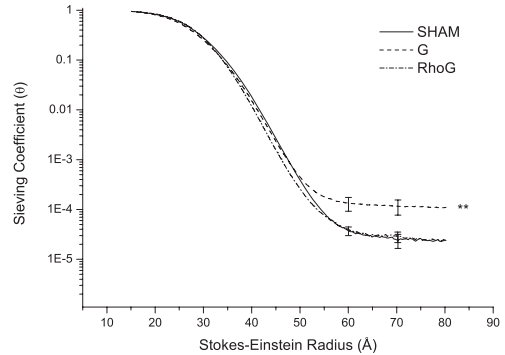


Fig. 4. θ vs. a_e during HG and in Rho-G. Rho-kinase (ROCK) inhibition completely abrogated the HG-induced increase in glomerular permeability. Solid line represents SHAM, while dashed line represents G and dash-dotted line Rho-G. ** $P < 0.01$.

edly increased in G compared with SHAM ($P < 0.05$), which was also the case for the large pore radius ($P < 0.05$).

Transmission Electron Microscopy

Results from transmission electron microscopy (TEM) of samples from HG and SHAM animals are shown in Fig. 6. All structures of the glomerular filtration barrier were investigated at a threefold higher magnification than that demonstrated in Fig. 6. There were no significant morphological alterations observed at this magnification with respect to either endothelial cells, podocytes, or the glomerular basement membrane in G (at 20 min) compared with SHAM, despite the increase in glomerular permeability in G.

DISCUSSION

This is, to our knowledge, the first direct demonstration in vivo that acute HG, independent of the concomitant hyperos-

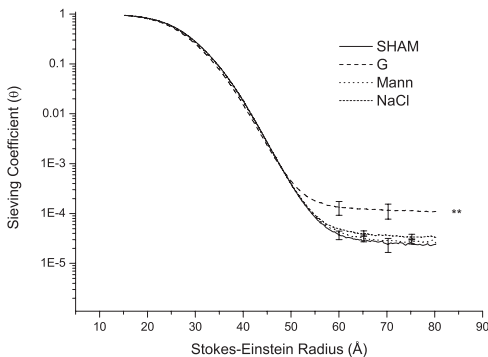


Fig. 3. Sieving coefficients (θ) vs. Stokes-Einstein radii (a_e) at 20 min of HG (G, dashed line) or hyperosmolarity (MANN, dotted line; NaCl, finely dashed line). There was a marked increase in θ for Ficoll_{50–80Å} after 20 min of HG, but not in MANN or NaCl. Solid line represents SHAM. ** $P < 0.01$.

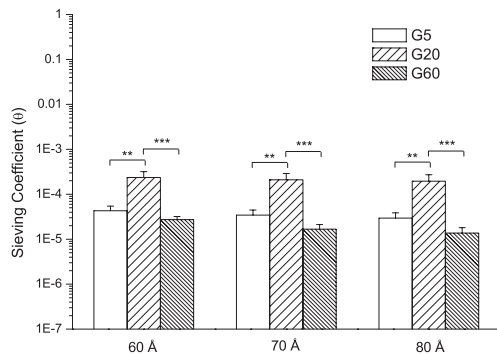


Fig. 5. θ as a function of time (i.e., in G-5, G-20, and G-60, respectively) for Ficoll molecules of 60–80 Å radius. Note the complete reversal of permeability increases noted at 20 min (G-20) after 60 min (G-60). Open bars represent G-5, bars with thick hatch G-20, and bars with thin hatch G-60. ** $P < 0.05$. *** $P < 0.001$.

Table 3. Two-pore parameters

	SHAM (n = 8)	G (n = 8)	MANN (n = 7)	NaCl (n = 8)	Rho-G (n = 8)
r_s , Å	46.6 ± 0.11	45.9 ± 0.18	46.6 ± 0.22	46.6 ± 0.17	45.3 ± 0.18*
r_L , Å	118.4 ± 6.76	164.6 ± 14.62*	119.3 ± 9.16	132.4 ± 4.49	114.2 ± 8.34
$\alpha_L \times 10^5$	3.63 ± 0.59	8.13 ± 1.88*	4.16 ± 1.24	3.48 ± 0.38	4.48 ± 0.76
$J_{VL}/GFR \times 10^5$	9.52 ± 1.70	25.8 ± 6.61*	13.2 ± 3.22	10.0 ± 1.03	11.3 ± 1.59
$A_0/\Delta X$, cm/g $\times 10^{-5}$	2.85 ± 0.13	1.56 ± 0.15	1.85 ± 0.08	2.35 ± 0.16	4.21 ± 0.23*

Values are means \pm SE; n = number of rats. Symbols are given in the text. r_s , Small-pore radius; r_L , large-pore radius; α_L , fractional ultrafiltration coefficient accounted for by large pores; J_{VL}/GFR , fractional fluid flow through large pores; GFR , glomerular filtration rate; $A_0/\Delta X$, effective pore area over unit diffusion path length. Statistical difference between SHAM and experimental groups [G, mannitol (MANN), NaCl, and Rho-G] is * $P < 0.05$.

molarity, can cause rapid, marked, and reversible increases in glomerular permeability to macromolecules. Furthermore, the permeability increases observed were completely abrogated by a ROCK inhibitor. This strongly indicates that the contractile F-actin cytoskeleton of the cells of the glomerular filtration barrier, i.e., the podocytes and/or the fenestrated endothelium, may be directly involved in this acute, dynamic glomerular permeability response. However, from a morphological point of view the permeability alterations were subtle, as electron microscopy of the glomerular filter did not demonstrate any gross alterations of any of the components of the filtration barrier during HG.

These fully reversible permeability changes in response to acute HG in nondiabetic rats should be distinguished from the partly nonreversible glomerular alterations occurring as a consequence of chronic HG in diabetes. In poorly insulin-treated streptozotocin (STZ) diabetic rats, in which blood glucose was maintained at ~ 20 mM for either 3 or 9 wk, we were not able to find any changes in glomerular permeability to albumin after 3 wk of HG, although the animals showed an increased urinary albumin excretion rate (AER) due to a tubular reabsorption defect (27). However, after 9 wk of HG there was a marked reduction in glomerular size selectivity accompanying the large increase in AER, consistent with an increased formation of "large pores" (shunt pathways) in the glomerular filtration barrier. It is likely that the latter changes may be due to (partly) nondynamic structural alterations in the glomerular filter. In recent years, much focus has been on the role of the decline in podocyte number in diabetic nephropathy, largely paralleling the degree of proteinuria and disease progression (15). Hence, although there is evidence that the ultimate filtration barrier to albumin is not at the podocyte slit diaphragm (17, 25), the podocytes are to a very large extent responsible for the maintenance of normal structure and function of the glomerular filter (15). It is thus likely that an important component of the glomerular injury following on chronic HG, besides the well-established changes in the glomerular basement membrane and

the glomerular mesangium, may be related to pathological changes involving the podocytes.

The exact mechanisms of the rapid increases in glomerular permeability observed, and to what extent podocytes or endothelial cells, or both, are involved, are not known. On a longer time scale, i.e., over 1 or several days, there is evidence that HG induces activation of members of the PKC superfamily, especially PKC- α and PKC- β , which may play a role in the pathophysiology of long-term renal diabetic manifestations (20). Hence, in STZ diabetic rats and in the db/db mouse model of type 2 diabetes, PKC- β inhibition using ruboxistaurin was able to prevent albuminuria (12, 13). However, studies in patients with type 2 diabetes have been much less equivocal, suggesting that ruboxistaurin has only little effect on HG-induced albuminuria in humans (5, 31). In monolayers of porcine aortic, i.e., nonrenal, endothelium in vitro, PKC- α seems to be mainly responsible for the permeability actions of HG, and unspecific PKC inhibition completely abrogated the acute endothelial permeability increases induced by HG in this system (11).

Even though PKC activation may be pivotal in the chronic permeability actions of HG, we decided in this study to test whether the cellular F-actin cytoskeleton in podocytes and endothelium be involved in the acute response to HG. There is accumulating evidence that members of the Rho family of small GTPases regulate both the actin cytoskeleton organization and the integrity of the intracellular junctions (21). Rho-A, and its downstream effector ROCK, act, at least in part, by increasing the phosphorylation of myosin light chain, which in nonmuscle cells leads to actomyosin contraction. For example, thrombin-induced endothelial permeability increases have been attributed to stress fiber formation and subsequent actomyosin-mediated contraction of cells (16) as well as changes in the distribution of intercellular adhesion molecules, such as cadherins and catenins (7). Beneficial effects of ROCK inhibition were recently demonstrated in (murine) puromycin aminonucleoside nephrosis, in acute renal failure in rats after ischemia-reperfusion, and in cat skeletal muscle in vivo affected by slight inflammation (18, 30, 32). In the present study, the complete abrogation of HG-induced permeability increases by a ROCK inhibitor strongly indicates that HG causes reversible actomyosin contraction in podocytes and/or endothelial cells and that the RhoA/ROCK system may be directly involved in this process.

As also previously demonstrated (11), the permeability actions of HG were found to be highly transient in nature. This is similar to the action of a number of various permeability substances interacting with the endothelium, such as histamine, substance-P, or thrombin (10, 19), and with the pattern of

Table 4. Two-pore parameters

	G-5 (n = 8)	G-20 (n = 8)	G-60 (n = 8)
r_s , Å	46.3 ± 0.20	46.3 ± 0.16	46.0 ± 0.12
r_L , Å	124.8 ± 5.47	175.6 ± 7.47**	114.3 ± 5.43
$\alpha_L \times 10^5$	3.27 ± 0.60	11.3 ± 3.93*	2.26 ± 0.18
$J_{VL}/GFR \times 10^5$	9.28 ± 1.88	26.1 ± 7.98*	5.8 ± 0.67
$A_0/\Delta X$, cm/g $\times 10^{-5}$	3.30 ± 0.37	2.50 ± 0.36	2.30 ± 0.28

Values are means \pm SE; n = number of rats. Symbols are given in the text. Statistical difference between SHAM and experimental groups (G-5, G-20, and G-60) are * $P < 0.05$ and ** $P < 0.01$.

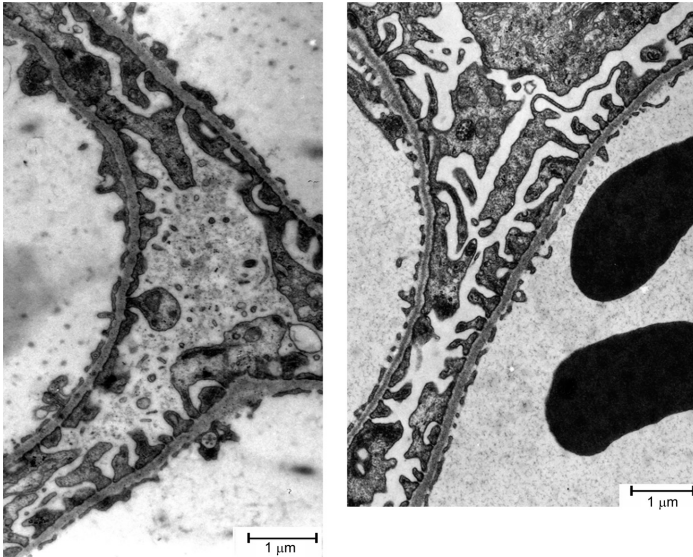


Fig. 6. Transmission electron micrographs of the glomerular filtration barrier in SHAM (*left*) and after 20 min of HG (*right*). No significant alterations were seen regarding endothelial cells, podocytes, or glomerular basement membrane despite marked permeability changes at 20 min of HG.

glomerular response in anaphylactic shock (4). Also, podocytes in culture can undergo rapid, reversible changes in shape due to acute actin reorganization following RhoA and PKB signaling, as recently demonstrated *in vitro* after exposure of podocytes to hemopexin (14). Whether podocytes and/or endothelial cells are affected by acute HG, the clinical implications of rapid bouts of glomerular permeability increases following HG are that repeated episodes of postprandial HG, in e.g., poorly regulated diabetes, may cause increased levels of microalbuminuria. However, as discussed above, continuous long-term HG seems to cause more permanent lesions affecting the structure and function of the glomerular filter, which may occur independently of the phenomena described in this article.

In a number of previous studies, we have been able to simultaneously assess θ for high-molecular-weight Ficoll and θ for radiolabeled albumin (RISA). We have demonstrated a more or less perfect coupling between these two parameters (3, 4, 26, 27). Thus, whenever there was an increase in θ for Ficoll_{50–80Å}, there was a parallel increase in θ for albumin. This is because both native (negatively charged) albumin and high-molecular-weight Ficoll molecules apparently share the same pathways in the glomerular filter, namely, shunt pathways (large pores). In the present study, we chose not to study albumin because of unexpectedly high levels of free iodine and denatured protein forming in the albumin preparation at disposal. The previously established tissue uptake technique (17) requires that the fraction of free iodine be $<0.1\%$, which could not be achieved in the present experiments. So far, however, we have not found an “uncoupling” of increases in θ for Ficoll_{50–80Å} vs. albumin, except during moderate ischemia-reperfusion injury, where θ for Ficoll_{50–80Å} increased slightly less than that for albumin (26). Thus, given the close coupling of θ for albumin and θ for Ficoll_{50–80Å} we have in this study

considered it safe to rely on the latter as an indicator of glomerular permeability.

The absence of gross morphological changes in electron micrographs of glomeruli exposed to HG is intriguing. After all, the observed changes were in the microalbuminuria range, and the normal θ to albumin is only on the order of $1 \cdot 10^{-4}$ (4, 9, 17). According to the two-pore theory of glomerular permeability this implies that there is only one large pore (shunt pathway) per approximately one million of the small pores. Given the very low abundance of shunt pathways, even a three- to fourfold increment in large pore number may be hard to detect by morphological techniques. Alternatively, the changes observed could also be interpreted in terms of an altered endothelial glycocalyx, not visible via routine electron microscopy. If this were the case, then the glycocalyx would have to be rapidly degraded and equally rapidly regenerated to account for the reversible changes in glomerular permeability observed. While this is quite possible, it is less likely, since the permeability changes were abrogated by ROCK inhibition, conceivably affecting the cellular cytoskeleton. Still, to the extent that the glycocalyx may affect intracellular signaling via the RhoA/ROCK system, this possibility cannot be completely ruled out.

In summary, acute hyperglycemia caused marked, reversible increases in glomerular permeability to macromolecules appearing within 20 min in nondiabetic rats. These alterations occurred independently of the concomitant hyperosmolarity and were abrogated by a ROCK inhibitor, interfering with the actin cytoskeleton of the cellular layers of the glomerular filter. The present data may explain the link between poorly controlled diabetes, with repeated episodes of HG on the one hand, and microalbuminuria on the other, even before permanent structural changes in the diabetic glomerular filtration barrier have started to appear.

ACKNOWLEDGMENTS

We gratefully acknowledge Kerstin Wihlborg for the skillful typing of the manuscript and Lina Gefors and Eric Carlemalm (Dept. of Clinical Sciences, Electron Microscopy Unit, Lund University Hospital, Lund, Sweden) for excellent technical assistance with electron microscopic preparation and TEM. We are grateful to Mitsubishi Pharma Corp. (Osaka, Japan) via Per-Olof Grände (Dept. of Anesthesia and Intensive Care, University of Lund and University Hospital of Lund, Lund, Sweden) for the supply of the Rho-kinase inhibitor Y-27632.

GRANTS

This study was supported by the Swedish Research Council, grant no 08285, The Heart and Lung Foundation and the Medical Faculty at Lund University (ALF grant).

DISCLOSURES

No conflicts of interest are declared by the authors.

REFERENCES

- Asgerisson D, Venturoli D, Fries E, Rippe B, Rippe C. Glomerular sieving of three neutral polysaccharides, polyethylene oxide and bikunin in rat. Effects of molecular size and conformation. *Acta Physiol (Oxf)* 191: 237–246, 2007.
- Asgerisson D, Venturoli D, Rippe B, Rippe C. Increased glomerular permeability to negatively charged Ficoll relative to neutral Ficoll in rats. *Am J Physiol Renal Physiol* 291: F1083–F1089, 2006.
- Axelsson J, Mahmutovic I, Rippe A, Rippe B. Loss of size selectivity of the glomerular filtration barrier in rats following laparotomy and muscle trauma. *Am J Physiol Renal Physiol* 297: F577–F582, 2009.
- Axelsson J, Rippe A, Venturoli D, Sward P, Rippe B. Effects of early endotoxemia and dextran-induced anaphylaxis on the size selectivity of the glomerular filtration barrier in rats. *Am J Physiol Renal Physiol* 296: F242–F248, 2009.
- Bakris GL. Protein kinase C-beta inhibition: a promise not yet fulfilled. *Clin J Am Soc Nephrol* 2: 619–620, 2007.
- Dang L, Seale JP, Qu X. High glucose-induced human umbilical vein endothelial cell hyperpermeability is dependent on protein kinase C activation and independent of the Ca^{2+} -nitric oxide signalling pathway. *Clin Exp Pharmacol Physiol* 32: 771–776, 2005.
- Drenckhahn D, Ness W. The endothelial contractile system. In: *Vascular Endothelium: Physiology, Pathophysiology, and Therapeutic Opportunities*, edited by Born GVR and Schwartz CJ. Stuttgart, Germany: Schattauer, 1997, p. 1–25.
- Dronavalli S, Duka I, Bakris GL. The pathogenesis of diabetic nephropathy. *Nat Clin Pract Endocrinol Metab* 4: 444–452, 2008.
- Haraldsson B, Nystrom J, Deen WM. Properties of the glomerular barrier and mechanisms of proteinuria. *Physiol Rev* 88: 451–487, 2008.
- Haraldsson B, Zackrisson U, Rippe B. Calcium dependence of histamine-induced increases in capillary permeability, studied in isolated rat hindlimbs. *Acta Physiol Scand* 128: 247–258, 1986.
- Hempel A, Maasch C, Heintze U, Lindschau C, Dietz R, Luft FC, Haller H. High glucose concentrations increase endothelial cell permeability via activation of protein kinase C alpha. *Circ Res* 81: 363–371, 1997.
- Ishii H, Jirousek MR, Koya D, Takagi C, Xia P, Clermont A, Bursell SE, Kern TS, Ballas LM, Heath WF, Stramm LE, Feener EP, King GL. Amelioration of vascular dysfunctions in diabetic rats by an oral PKC beta inhibitor. *Science* 272: 728–731, 1996.
- Suga D, Haneda M, Nakagawa H, Isshiki K, Sato H, Maeda S, Sugimoto T, Yasuda H, Kashiwagi A, Ways DK, King GL, Kikkawa R. Amelioration of accelerated diabetic mesangial expansion by treatment with a PKC beta inhibitor in diabetic db/db mice, a rodent model for type 2 diabetes. *FASEB J* 14: 439–447, 2000.
- Lennon R, Singh A, Welsh GI, Coward RJ, Satchell S, Ni L, Mathieson PW, Bakker WW, Saleem MA. Hemopexin induces nephrin-dependent reorganization of the actin cytoskeleton in podocytes. *J Am Soc Nephrol* 19: 2140–2149, 2008.
- Lewko B, Stepinski J. Hyperglycemia and mechanical stress: targeting the renal podocyte. *J Cell Physiol* 221: 288–295, 2009.
- Lum H, Malik AB. Mechanisms of increased endothelial permeability. *Can J Physiol Pharmacol* 74: 787–800, 1996.
- Lund U, Rippe A, Venturoli D, Tenstad O, Grubb A, Rippe B. Glomerular filtration rate dependence of sieving of albumin and some neutral proteins in rat kidneys. *Am J Physiol Renal Physiol* 284: F1226–F1234, 2003.
- Lundblad C, Bentzer P, Grande PO. The permeability-reducing effects of prostacyclin and inhibition of Rho kinase do not counteract endotoxin-induced increase in permeability in cat skeletal muscle. *Microvasc Res* 68: 286–294, 2004.
- McDonald DM. Endothelial gaps and permeability of venules in rat tracheas exposed to inflammatory stimuli. *Am J Physiol Lung Cell Mol Physiol* 266: L61–L83, 1994.
- Meier M, Menne J, Haller H. Targeting the protein kinase C family in the diabetic kidney: lessons from analysis of mutant mice. *Diabetologia* 52: 765–775, 2009.
- Narumiya S, Ishizaki T, Watanabe N. Rho effectors and reorganization of actin cytoskeleton. *FEBS Lett* 410: 68–72, 1997.
- Nitta K, Horiba N, Uchida K, Horita S, Hayashi T, Kawashima A, Yumura W, Nihei H. High glucose modulates albumin permeability across glomerular endothelial cells via a protein kinase C-dependent mechanism. *Nippon Jinzo Gakkai Shi* 37: 317–322, 1995.
- Peng F, Wu D, Gao B, Ingram AJ, Zhang B, Chorneyko K, McKenzie R, Krepsinsky JC. RhoA/Rho-kinase contribute to the pathogenesis of diabetic renal disease. *Diabetes* 57: 1683–1692, 2008.
- Rippe B, Haraldsson B. Transport of macromolecules across microvascular walls. The two-pore theory. *Physiol Rev* 74: 163–219, 1994.
- Rippe C, Asgerisson D, Venturoli D, Rippe A, Rippe B. Effects of glomerular filtration rate on Ficoll sieving coefficients (theta) in rats. *Kidney Int* 69: 1326–1332, 2006.
- Rippe C, Rippe A, Larsson A, Asgerisson D, Rippe B. Nature of glomerular capillary permeability changes following acute renal ischemia-reperfusion injury in rats. *Am J Physiol Renal Physiol* 291: F1362–F1368, 2006.
- Rippe C, Rippe A, Torffvit O, Rippe B. Size and charge selectivity of the glomerular filter in early experimental diabetes in rats. *Am J Physiol Renal Physiol* 293: F1533–F1538, 2007.
- Salameh A, Zinn M, Dhein S. High D-glucose induces alterations of endothelial cell structure in a cell-culture model. *J Cardiovasc Pharmacol* 30: 182–190, 1997.
- Tencer J, Frick IM, Öqvist BW, Alm P, Rippe B. Size-selectivity of the glomerular barrier to high molecular weight proteins: upper size limitations of shunt pathways. *Kidney Int* 53: 709–715, 1998.
- Teraishi K, Kurata H, Nakajima A, Takaoka M, Matsumura Y. Preventive effect of Y-27632, a selective Rho-kinase inhibitor, on ischemia/reperfusion-induced acute renal failure in rats. *Eur J Pharmacol* 505: 205–211, 2004.
- Tuttle KR, Bakris GL, Toto RD, McGill JB, Hu K, Anderson PW. The effect of ruboxistaurin on nephropathy in type 2 diabetes. *Diabetes Care* 28: 2686–2690, 2005.
- Wang L, Ellis MJ, Fields TA, Howell DN, Spurney RF. Beneficial effects of the Rho kinase inhibitor Y27632 in murine puromycin aminonucleoside nephrosis. *Kidney Blood Press Res* 31: 111–121, 2008.
- Venturoli D, Rippe B. Ficoll and dextran vs. globular proteins as probes for testing glomerular permselectivity: effects of molecular size, shape, charge, and deformability. *Am J Physiol Renal Physiol* 288: F605–F613, 2005.
- Yamashita T, Mimura K, Umeda F, Kobayashi K, Hashimoto T, Nawata H. Increased transendothelial permeation of albumin by high glucose concentration. *Metabolism* 44: 739–744, 1995.
- Zuurbier CJ, Demirci C, Koeman A, Vink H, Ince C. Short-term hyperglycemia increases endothelial glycocalyx permeability and acutely decreases lineal density of capillaries with flowing red blood cells. *J Appl Physiol* 99: 1471–1476, 2005.

Paper IV

Transient and sustained increases in glomerular permeability following ANP infusion in rats

Josefin Axelsson, Anna Rippe, and Bengt Rippe

Department of Nephrology, Lund University, Lund, Sweden

Submitted 14 June 2010; accepted in final form 6 October 2010

Axelsson J, Rippe A, Rippe B. Transient and sustained increases in glomerular permeability following ANP infusion in rats. *Am J Physiol Renal Physiol* 300: F24–F30, 2011. First published October 13, 2010; doi:10.1152/ajprenal.00347.2010.—The present study was performed to investigate the effects of systemic atrial natriuretic peptide (ANP) infusion on the glomerular permeability to macromolecules in rats. In anesthetized Wistar rats (250–280 g), the left ureter was cannulated for urine collection while simultaneously blood access was achieved. Rats were continuously infused intravenously with ANP [$30 \text{ ng} \cdot \text{kg}^{-1} \cdot \text{min}^{-1}$ (Lo-ANP; $n = 8$) or $800 \text{ ng} \cdot \text{kg}^{-1} \cdot \text{min}^{-1}$ (Hi-ANP; $n = 10$)] or 0.9% NaCl (SHAM; $n = 16$), respectively, and with polydisperse FITC-Ficoll-70/400 (molecular radius 13–90 Å) and ^{51}Cr -EDTA for 2 h. Plasma and urine samples were taken at 5, 15, 30, 60, and 120 min of ANP infusion and analyzed by high-performance size-exclusion chromatography (HPLC) for determination of glomerular sieving coefficients (θ) for Ficoll. GFR was also assessed (^{51}Cr -EDTA). In Hi-ANP, there was a rapid (within 5 min), but bimodal, increase in glomerular permeability. θ to high-molecular-weight Ficoll thus reached a maximum at 15 min, after which θ returned to near control at 30 min, to again increase moderately at 60 and 120 min. In Lo-ANP, there was also a rapid, reversible increase in glomerular θ , returning to near control at 30 min, followed by just a tendency of a sustained increase in permeability, but with a significant increase in “large-pore” radius. In conclusion, in Hi-ANP there was a rapid increase in glomerular permeability, with an early, partly reversible permeability peak, followed by a (moderate) sustained increase in permeability. In Lo-ANP animals, only the initial permeability peak was evident. In both Lo-ANP and Hi-ANP, the glomerular sieving pattern observed was found to mainly reflect an increase in the number and radius of large pores in the glomerular filter.

capillary permeability; Ficoll; glomerular filtration; glomerular sieving coefficient

common feature during exercise, posttrauma (4, 14) or after surgery (21), and in systemic inflammation (6), but also in congestive heart failure and following myocardial infarction (15, 23). In the latter conditions, microalbuminuria has been attributed to permeability effects mediated via ANP. Intravenous (iv) infusion of ANP in anesthetized rats thus resulted in moderate increases in urinary albumin/Inulin concentration ratios for the dose of $0.5 \mu\text{g} \cdot \text{min}^{-1} \cdot \text{kg}^{-1}$ body wt (BW) and in marked albuminuria for a dose of $1 \mu\text{g} \cdot \text{min}^{-1} \cdot \text{kg}^{-1}$ (22). The exact (patho)physiology of ANP-induced albuminuria is not known. Some of the proteinuric actions of ANP have been attributed to reductions in the proximal tubular reabsorption of albumin, but whether, or to what extent, glomerular permeability per se is affected, either via charge-selective or size-selective glomerular changes, needs to be further elucidated.

On that background, we investigated the functional behavior of the glomerular filtration barrier in response to continuous iv infusion of ANP in rats. A low, “physiological” (Lo-ANP) and a high, “supraphysiological” ANP (Hi-ANP) dose were investigated. Glomerular size selectivity was assessed *in vivo* using FITC-Ficoll 70/400, a neutral polysaccharide which is not significantly reabsorbed by the proximal tubules, to assess the glomerular sieving coefficient (θ), i.e., the filtrate-to-plasma concentration ratio, for a broad spectrum of molecular radii, with emphasis on the glomerular sieving pattern of molecules of high molecular weight (MW $\sim 400,000$). A rapid, reversible increase in glomerular permeability was noted for both Lo-ANP and Hi-ANP animals, in the latter followed by a moderate, but sustained increase in glomerular permeability.

MATERIALS AND METHODS

Animals and surgery. Experiments were performed in 34 male Wistar rats (Møllegaard, Lille Stensved, Denmark) with an average BW of 267.7 ± 2.8 g. The rats were kept on standard chow and had free access to water until the day of the experiment. The animal Ethics Committee at Lund University approved the animal experiments. The rats were anesthetized with an intraperitoneal injection of pentobarbital sodium, 60 mg/kg, and the animals were placed on a thermostatically controlled heating pad to keep body temperature at 37°C . A tracheotomy was performed to facilitate breathing. The tail artery was cannulated (PE-50 cannula) for blood pressure monitoring and registration of heart rate (HR) on a polygraph (model 7B; Grass Instruments, Quincy, MA) and for repeated injections of maintenance anesthesia (pentobarbital sodium). The left carotid artery and the left and right external jugular veins were cannulated (PE-50 cannulas) for blood sampling and infusion purposes, respectively. Access to the left ureter was obtained through a small (6–8 mm) abdominal incision. Furosemide (0.375 mg/kg , Furosemid, Recip, Sweden) was administered in the tail artery to increase urine production and facilitate cannulation of the ureter, which was used for urine sampling. The latter was dissected free, and a PE-10 (connected to a PE-50) cannula was inserted and secured by a ligature.

PLASMA VOLUME OVERLOAD, in conjunction with e.g., congestive heart failure, induces an increased secretion to the circulation of atrial natriuretic peptide (ANP) from the heart upon atrial stretch. By its natriuretic, diuretic, and vasodilating properties, ANP is believed to act physiologically as a compensatory hormone protecting against plasma volume expansion (9, 11, 29). Furthermore, in extrarenal tissues ANP induces a fluid shift from the vascular to the extravascular space, causing increases in hematocrit and plasma protein concentration in nephrectomized rats (2). Although these effects can be related to vasodilatation, and hence, to increases in capillary surface area and in microvascular pressure, there is now good evidence that ANP directly affects capillary permeability to proteins (11, 12, 25, 29, 34) and microvascular hydraulic conductance (16).

Microalbuminuria (i.e., moderately elevated albumin excretion rates, ranging from 20 to 200 $\mu\text{g/min}$ in humans) is a

Address for reprint requests and other correspondence: B. Rippe, Dept. of Nephrology, Lund University, University Hospital of Lund, S-211 85 Lund, Sweden (e-mail: Bengt.Rippe@med.lu.se).

Experimental procedures: ANP infusion. All experiments started with an initial resting period of 10–15 min following the cannulation of the left ureter. ANP (A8208, lot no. 049K4809, Sigma-Aldrich, St. Louis, MO) was infused iv by either a low dose ($30 \text{ ng} \cdot \text{kg}^{-1} \cdot \text{min}^{-1}$; Lo-ANP; $n = 8$) (34) or a high dose ($800 \text{ ng} \cdot \text{kg}^{-1} \cdot \text{min}^{-1}$; Hi-ANP; $n = 10$). The Lo-ANP dose, chosen not to affect mean arterial pressure (MAP) or glomerular filtration rate (GFR), was selected based mainly on two previous studies (30, 34). Tucker et al. (34) found that $20 \text{ ng} \cdot \text{kg}^{-1} \cdot \text{min}^{-1}$ infused iv in rats resulted in a plasma concentration of 190 pg/ml , which caused moderate increases in the extravasation of radiolabeled albumin to the gut (colon and jejunum), while MAP remained unaltered, despite a reduction in heart rate. Salazar et al. (30) found in dogs that $50 \text{ ng} \cdot \text{kg}^{-1} \cdot \text{min}^{-1}$ of ANP infusion iv was the highest dose that could be given without a drop in MAP or an increase in GFR. In a pilot study, we found that 50 and $60 \text{ ng} \cdot \text{kg}^{-1} \cdot \text{min}^{-1}$ of ANP iv slightly reduced MAP. We therefore chose a moderately lower dose, $30 \text{ ng} \cdot \text{kg}^{-1} \cdot \text{min}^{-1}$, for the Lo-ANP group, yielding a calculated plasma ANP level of 200 pg/ml , which is approximately twice the physiological plasma ANP level. From the data of Tucker et al. (34), we could calculate that an iv ANP infusion rate of $800 \text{ ng} \cdot \text{kg}^{-1} \cdot \text{min}^{-1}$ would produce a plasma concentration of $1,740 \text{ pg/ml}$, which is in the (lower) range of $2,000$ – $3,000 \text{ pg/ml}$, which have been observed after 25% blood volume expansion in rats with experimental heart failure (10), but higher than observed after 20% plasma volume expansion in rats by another group (24). Furthermore, $800 \text{ ng} \cdot \text{kg}^{-1} \cdot \text{min}^{-1}$ is about intermediate between the medium and the high doses of ANP infused in rats for studies of ANP-induced albuminuria by Nielsen et al. (22).

For the Lo-ANP dose, an initial bolus ($4.75 \text{ } \mu\text{l}$ of a $0.04 \text{ } \mu\text{g}/\mu\text{l}$ ANP solution) was given iv followed by a constant infusion ($2.5 \text{ } \mu\text{l}/\text{min}$ of a $0.0033 \text{ } \mu\text{g}/\mu\text{l}$ solution) throughout the experiment (2 h). Also for the Hi-ANP dose, an initial bolus ($75 \text{ } \mu\text{l}$ of a $0.04 \text{ } \mu\text{g}/\mu\text{l}$ solution) was given followed by a continuous infusion ($5 \text{ } \mu\text{l}/\text{min}$ of a $0.04 \text{ } \mu\text{g}/\mu\text{l}$ solution). For Ficoll sieving experiments, sampling of urine and blood ($2 \times 70 \text{ } \mu\text{l}$ at a time for Ficoll determinations, using hematocrit capillaries, plus $25 \text{ } \mu\text{l}$ for ^{51}Cr -EDTA assessments, using precision Micro-caps) was performed sequentially, at 5, 15, 30, 60, and 120 min, respectively. The blood sampling in hematocrit tubes allowed for simultaneous plasma retrieval and hematocrit determination. In SHAM ($n = 16$), 0.9% NaCl in a bolus and infusion, mimicking the volume load of the ANP experiments, was given during 2 h with measurements performed at the start (0–5 min; SHAM-5) and at 60 min (SHAM-60) and 120 min (SHAM-120). The total blood volume withdrawn during 120 min was $825 \text{ } \mu\text{l}$ (4% of total blood volume) for ANP animals and $495 \text{ } \mu\text{l}$ for SHAM animals.

GFR. GFR was measured in the left kidney during the experiment, using ^{51}Cr -EDTA. A priming dose of ^{51}Cr -EDTA (0.3 MBq in 0.2 ml iv, Amersham Biosciences, Buckinghamshire, UK) was administered and followed by a continuous infusion ($10 \text{ ml} \cdot \text{kg}^{-1} \cdot \text{h}^{-1}$) of ^{51}Cr -EDTA (0.37 MBq/ml in 0.9% NaCl) throughout the experiment, which yielded a stable plasma concentration of ^{51}Cr -EDTA over time. Urine was collected from the left ureter repeatedly during the experiment, and blood samples, using microcapillaries, $25 \text{ } \mu\text{l}$ at a time (see above), were taken to be able to assess GFR, approximately every 20 min. Radioactivity in blood and urine was measured in a gamma counter (Wizard 1480, LKP, Wallac, Turku, Finland). Hematocrit (see above) was assessed throughout the experiments to be able to convert blood radioactivity into plasma radioactivity. During the FITC-Ficoll sieving periods (see below), GFR was also assessed from the urine clearance of FITC-Inulin. The urinary excretion of ^{51}Cr -EDTA and FITC-Inulin per minute ($U_i \times V_u$) divided by the concentration of tracer in plasma (P_i) was used to calculate GFR where U_i represents the tracer concentration in urine, and V_u the flow of urine per minute. Since the variability (coefficient of variation) for FITC-Inulin-assessed GFR was slightly higher than that for ^{51}Cr -EDTA-assessed GFR, we have presented the latter consistently throughout this study.

Glomerular sieving of FITC-Ficoll. A mixture of FITC-Ficoll-70 (10 mg/ml) and FITC-Ficoll-400 (10 mg/ml) (TdB Consultancy, Uppsala, Sweden) in a 1:24 relationship was administered as a bolus dose together with FITC-Inulin (10 mg/ml , TdB Consultancy). The bolus dose [$40 \text{ } \mu\text{g}$ (FITC-Ficoll-70); $960 \text{ } \mu\text{g}$ (FITC-Ficoll-400); and $500 \text{ } \mu\text{g}$ (FITC-Inulin)] was followed by a constant infusion of $10 \text{ ml} \cdot \text{kg}^{-1} \cdot \text{h}^{-1}$ (FITC-Ficoll-70, $20 \text{ } \mu\text{g/ml}$; FITC-Ficoll-400, 0.48 mg/ml ; FITC-Inulin, 0.5 mg/ml ; and ^{51}Cr -EDTA, 0.3 MBq/ml) for at least 20 min before sieving measurements, after which urine from the left kidney was collected for 5 min, with a midpoint (2.5 min) plasma sample collected. During the constant infusion of FITC-Ficoll 70/400, Ficoll molecules $>50 \text{ } \text{\AA}$ in radius slightly increased their concentration, while Ficoll molecules $<30 \text{ } \text{\AA}$ decreased their concentrations over the course of the infusion. During a 5-min period, however, these changes were $<1\%$. The midpoint plasma sample taken during the 5 min of urine collection would thus rather accurately reflect the average plasma concentration of Ficoll during each urine sampling period.

High-performance size-exclusion chromatography. Plasma and urine samples were assessed on a size-exclusion high-performance chromatography system (Waters, Milford, MA) with an Ultrahydrogel 500 column (Waters) and calibrated as described in detail previously (5). The mobile phase was driven by a pump (Waters 1525), and fluorescence was detected with a fluorescence detector (Waters 2475) with an excitation wavelength at 492 nm and an emission wavelength at 518 nm . The samples were loaded to the system with an autosampler (Waters 717 plus), and the system was controlled by Breeze Software 3.3 (Waters).

Glomerular Ficoll θ vs. Stokes-Einstein radius. The θ is defined as the concentration of solute in the ultrafiltrate over that in plasma, i.e., a filtrate-to-plasma concentration ratio. Ficoll θ were obtained by analyzing HPLC-curves, i.e., Ficoll concentration vs. elution time (translated into the relative distribution volumes in the column of the different size Ficoll molecules) from the plasma (C_{PF}) and urine samples for each experiment. The urine Ficoll concentration vs. the Stokes-Einstein radius (a_c) curve was divided by the Inulin concentration to obtain the primary urine concentration of Ficoll (C_{UF}). For each a_c , θ was then calculated by dividing C_{UF} by C_{PF} .

Two-pore analysis. A two-pore model (19, 26, 28) was used to analyze the θ data for Ficoll (molecular radius 15 – $80 \text{ } \text{\AA}$). A nonlinear least-squares regression analysis was used to obtain the best curve fit, using scaling multipliers, as described at some length previously (27). The major parameters of the two-pore model are 1) the small-pore radius (r_s), 2) the large-pore radius (r_L), 3) the unrestricted pore area over unit diffusion path-length ($A_0/\Delta X$), and 4) the fraction of the glomerular ultrafiltration-coefficient accounted for by the large pores (α_L). The latter parameter reflects the abundance of “large pores” in the glomerular filter and is calculated from the fractional GFR diverted through the large pores, i.e., J_{VL}/GFR . For stable GFRs, this parameter may be regarded as a more “robust” parameter than α_L . α_L and J_{VL}/GFR are mathematically obtained by extrapolating the “flat” portion of the Ficoll sieving curve for molecules $>50 \text{ } \text{\AA}$ in radius, i.e., the r_L curve, back to the ordinate scale (i.e., to $0 \text{ } \text{\AA}$). This imparts some uncertainty to α_L , especially if r_L is markedly altered. After a large increment in r_L , α_L (J_{VL}/GFR) may tend to be slightly underestimated. By contrast, if r_L is reduced, then α_L and J_{VL}/GFR may be overestimated. The parameter, r_s , is mainly dependent on sieving data (θ) close to the inflection point between the r_s curve and the r_L curve, i.e., for θ values for a_c ranging between ~ 40 and $\sim 46 \text{ } \text{\AA}$. $A_0/\Delta X$ is a diffusive parameter reflecting the surface area of the small pores. A high $A_0/\Delta X$ (or a low GFR) will displace the sieving curve for Ficoll radii between 20 and $40 \text{ } \text{\AA}$ to the right, thereby causing a “steeper” r_s curve with a sharp cut-off. A low $A_0/\Delta X$ (or a high GFR) will displace the r_s curve to the left, creating a more “shallow” r_s curve (27).

Statistical analysis. Values are presented as medians and ranges (25th–75th percentile). Differences among groups were tested using nonparametric analysis of variance with the Kruskal-Wallis test and

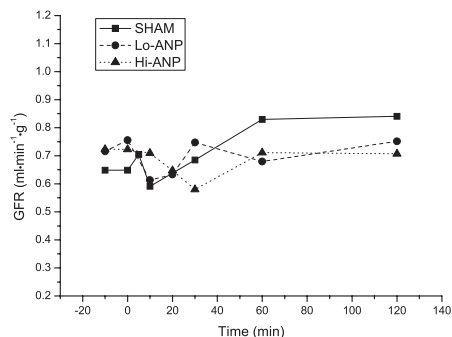


Fig. 1. Glomerular filtration rate (GFR) as a function of time in control (SHAM), low-dose atrial natriuretic peptide (ANP; Lo-ANP)-, and high-dose ANP (Hi-ANP)-treated animals. Values are given as medians. Medians and ranges are given in Table 1. There was a tendency toward an increase in GFR in SHAM, which, however, was not statistically significant (at 60 and 120 min).

post hoc tested using the Mann-Whitney *U*-test. Bonferroni corrections for multiple comparisons were made. Significance levels were set at $*P < 0.05$, $**P < 0.01$ and $***P < 0.001$. All statistical calculations were made using SPSS 18.0 for Windows (SPSS, Chicago, IL).

RESULTS

MAP and HR. SHAM and Lo-ANP animals showed a stable MAP and HR (not shown) throughout the experiment. Hi-ANP animals showed an early decrease in MAP just after start of the infusion of ANP from 97.5 (85–111.3) to 77.5 (73.8–87.5) mmHg, the MAP remaining depressed during the rest of the experiment, reaching 65.0 (65–75) mmHg at 120 min. A decrease in HR from 340 (320–385) to 275 (248–303) beats/min; $P < 0.01$ was also seen in the Hi-ANP group at 120 min of the experiment.

GFR. GFR (Fig. 1 and Table 1) remained more or less stable in all groups, but tended to slightly increase in SHAM from 0.65 (0.62–0.82) to 0.84 (0.73–0.93) ml·min⁻¹·g (kidney)⁻¹; not significant.

θ of FITC-Ficoll. Figure 2 shows the θ for Ficoll_{70Å} in Hi-ANP (top), Lo-ANP (middle), and SHAM (bottom), respectively, as a function of time, i.e., at 5, 15, 30, 60, and 120 min. There was a bimodal permeability response with an early permeability peak, i.e., an increase in θ for Ficoll_{70Å} vs. SHAM

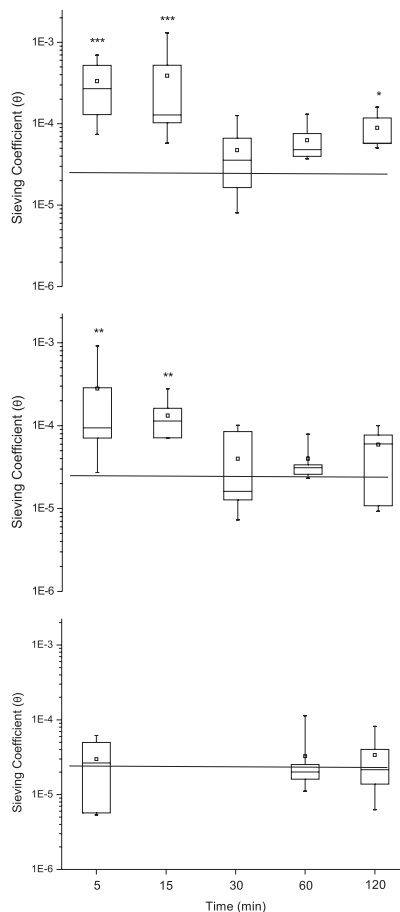


Fig. 2. Sieving coefficients (θ) for Ficoll_{70Å} for Hi-ANP (top), Lo-ANP (middle), and SHAM (bottom) as a function of time. Values are given as medians and ranges (1st–4th quartile) within the boxes, whereas whiskers indicate highest and lowest values. Arithmetic averages are given as small quadrates. A bimodal permeability pattern is evident, especially for Hi-ANP. SHAM (nonstimulated) θ as a function of time are represented by the horizontal line.

Table 1. Median and 1st–4th quartile ranges for GFR as a function of time in Fig. 1

Time, min	SHAM	Time, min	Lo-ANP	Hi-ANP
0	0.65 (0.62–0.82)	0	0.72 (0.43–0.92)	0.72 (0.64–0.80)
5	0.70 (0.63–0.73)	10	0.62 (0.57–0.73)	0.71 (0.55–0.85)
10	0.59 (0.57–0.76)	20	0.63 (0.45–0.71)	0.65 (0.52–0.79)
30	0.69 (0.59–0.87)	30	0.74 (0.53–0.84)	0.58 (0.49–0.69)
60	0.83 (0.78–0.87)	60	0.68 (0.54–0.79)	0.71 (0.61–0.79)
120	0.84 (0.73–0.93)	120	0.74 (0.54–0.84)	0.71 (0.60–0.78)

GFR, glomerular filtration rate; ANP, atrial natriuretic peptide; SHAM, control animals; Lo-ANP and Hi-ANP, low-dose ANP- and high-dose ANP-treated animals, respectively.

(horizontal line) at 5 and 15 min, reversing to near SHAM values at 30 min. This was later followed by a more sustained, low-grade increase in θ for Ficoll_{70Å} at 60 and 120 min, which was statistically significant in Hi-ANP (at 60 min).

Figure 3 and Table 2 demonstrate the median θ vs. a_e curves for Ficoll molecules ranging in radius from 15 to 80 Å for Lo-ANP and Hi-ANP vs. SHAM at the (first) permeability peak at 15 min. Median and ranges for Ficoll_{60Å}, Ficoll_{70Å}, and Ficoll_{80Å}, are shown in Table 2. In the a_e range 50–80 Å, both Lo-ANP and Hi-ANP showed a clearly increased θ . For Ficoll_{70Å}, θ thus increased from 2.19×10^{-5} [1.67×10^{-5} – 3.09×10^{-5} (SHAM-60 min) to 1.14×10^{-4} ($7.15 \times$

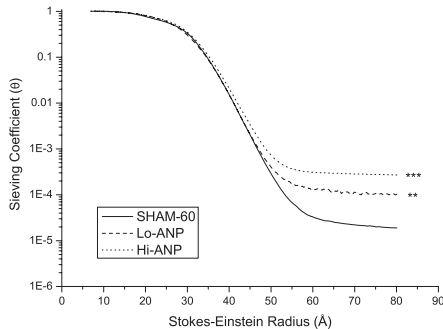


Fig. 3. Median curves depicting θ vs. Stokes-Einstein radius (a_e) for SHAM-60 and Lo-ANP and Hi-ANP, respectively, at 15 min after start of the ANP infusion. Medians and ranges of θ values for Ficoll_{60A}, Ficoll_{70A}, and Ficoll_{80A}, respectively, are given in Table 2. The increase in glomerular permeability to ANP occurred in a more or less dose-dependent fashion during the initial (0–30 min) permeability peak.

10^{-5} – 1.62×10^{-4}) ($P < 0.01$)] and to 2.86×10^{-4} (9.93×10^{-5} – 5.49×10^{-4}) ($P < 0.001$) at 15 min for Lo-ANP and Hi-ANP, respectively.

Two-pore modeling. The best curve fits of θ vs. a_e for Ficoll according to the two-pore model were obtained using the parameters listed in Table 3 (Lo-ANP) and Table 4 (Hi-ANP). The fractional fluid flow through the large pores (large-pore volume flow/GFR) was markedly increased, nearly 10-fold at 15 min, in Hi-ANP and then remained elevated compared with SHAM-60 even at 30 min ($P < 0.05$). For Lo-ANP, the fractional volume flow through the large pores was seen to be increased (more than doubled) at 5 ($P < 0.05$) and 15 min ($P < 0.05$), but not thereafter. The fractional hydraulic conductance accounted for by the large pores (α_L) increased almost threefold in Hi-ANP at 5 and 15 min compared with SHAM-60 ($P < 0.01$), clearly indicating the formation of more large pores in the glomerular filter during infusion of high doses of ANP. Furthermore, there was an increase in r_L in Hi-ANP at 5 and 15 min. In Lo-ANP, such an increment was actually significant at all time points ($P < 0.05$) except at 30 min.

DISCUSSION

This is the first direct assessment of the dynamics of glomerular permeability alterations occurring during infusions of ANP in the rat. The essential result of the study is that both low (34) and high ANP concentrations caused a rapid (within 5 min), partly reversible increase in glomerular permeability. This was followed by a very moderate, sustained increase in barrier permeability, which was significant for the high ANP dose. Even though the second, more sustained increase in permeability did not reach statistical significance in Lo-ANP

animals, there were indications of increases in r_L throughout the intervention in this group. Thus, according to a two-pore model of glomerular permeability, the sieving patterns observed during the first and second phase of ANP infusion were compatible with an increase in the number and/or radius of large pores in the glomerular filter without any primary alterations in glomerular charge selectivity. Furthermore, a dose dependence of ANP action on glomerular permeability was evident.

ANP is a small peptide secreted by the heart upon atrial stretch and/or myocardial ischemia. The acute effects of ANP are both renal and nonrenal. The renal effects include an increased GFR and an increased renal excretion of sodium and water, preferentially in the distal part of the nephron (9). The nonrenal effects of ANP include vasodilation, by relaxation of vascular smooth muscle, and an acute increase in vascular permeability via receptors in the microvascular endothelium (25). Due to the diuretic and natriuretic effects of ANP, it would cause plasma protein upconcentration and increases in plasma oncotic pressure that would mobilize fluid from the interstitium, counteracting any reductions in plasma volume. However, due to the nonrenal effects of ANP, mainly the increases in vascular permeability, plasma volume overload is counteracted by permitting an increased flux of fluid and proteins to the interstitium. Both ANP and the closely related B-type natriuretic peptide (BNP) act on the ANP/BNP receptor guanylyl cyclase-A (GC-A) signaling via a guanylyl cyclase pathway. Deletion of this receptor has been found to result in various degrees of hypertension, plasma volume expansion, and cardiac hypertrophy. In endothelial cell-specific GC-A knockout mice, iv ANP failed to increase endothelial permeability and failed to cause a hypovolemic and hypotensive response, despite intact renal responses to ANP (29). This strongly indicates that increases in endothelial permeability are critically involved in ANP-induced reductions of plasma volume during volume overload.

While the rationale for systemic ANP actions on vascular permeability is logical, the effects on glomerular permeability are more enigmatic. Previous studies have indeed demonstrated that systemic ANP infusion in anesthetized rats can markedly increase urinary albumin excretion, although the exact mechanisms of this proteinuric action have not been elucidated (22). The direct assessment of glomerular permeability in the present study supports the concept that ANP-induced albuminuria is a consequence of a direct effect on the glomerular filtration barrier, leading to a partly reversible increase in the radius and number of large glomerular pores without any primary effects on glomerular charge selectivity.

We have previously demonstrated that anaphylaxis (8) and hyperglycemia (7) can induce rapid, reversible changes in glomerular permeability similar to those induced by ANP. The hyperglycemic permeability response could be abrogated by a

Table 2. Median and ranges of θ for Ficoll_{60A}, Ficoll_{70A}, and Ficoll_{80A} in SHAM, Lo-ANP, and Hi-ANP, respectively

	SHAM 60 min	Lo-ANP	Hi-ANP
60 Å	3.28×10^{-5} (2.94×10^{-5} – 4.03×10^{-5})	1.35×10^{-4} * (8.11×10^{-5} – 1.75×10^{-4})	3.10×10^{-4} † (1.29×10^{-4} – 5.85×10^{-4})
70 Å	2.19×10^{-5} (1.67×10^{-5} – 3.09×10^{-5})	1.14×10^{-4} * (7.15×10^{-5} – 1.62×10^{-4})	2.86×10^{-4} † (9.93×10^{-5} – 5.49×10^{-4})
80 Å	1.91×10^{-5} (1.71×10^{-5} – 2.97×10^{-5})	9.98×10^{-5} * (6.83×10^{-5} – 1.49×10^{-4})	2.72×10^{-4} † (9.43×10^{-5} – 5.33×10^{-4})

Statistical difference between SHAM and experimental groups: * $P < 0.01$, † $P < 0.001$.

Table 3. Two-pore parameters, Lo-ANP

	Lo-ANP				
	SHAM 60 min	5 min	15 min	30 min	120 min
Small-pore radius (r_s), Å	45.96 (45.66–46.29)	46.02 (45.79–46.18)	45.94 (45.81–46.31)	45.79 (45.28–45.86)	45.73 (45.73–45.73)
Large-pore radius (r_L), Å	122.36 (116.59–128.37)	192.78‡ (150.74–205.44)	183.03‡ (163.79–203.59)	108.63 (103.24–139.54)	159.74‡ (158.10–164.49)
$\alpha_L \times 10^5$	4.31 (3.21–5.66)	5.81 (3.86–12.1)	5.69 (2.98–7.77)	3.34 (2.61–5.04)	2.05* (2.01–2.10)
$J_{ul}/GFR \times 10^5$	6.87 (6.05–8.85)	22.5‡ (13.54–68.57)	18.6‡ (10.3–26.5)	8.05 (6.09–16.9)	6.67 (6.54–6.82)
$A_0/\Delta X$, cm/g $\times 10^{-5}$	3.95 (3.70–4.84)	3.67 (2.93–4.13)	4.59 (2.84–5.76)	3.21 (2.66–4.94)	3.98 (3.61–5.95)

Median values are given together with ranges (1st–4th quartile); n = no. of rats. α_L , Fractional ultrafiltration coefficient accounted for by large pores; J_{ul}/GFR , fractional fluid flow through large pores; $A_0/\Delta X$, effective pore area over unit diffusion path length. Statistical difference between SHAM and experimental groups: * $P < 0.05$, † $P < 0.01$, ‡ $P < 0.001$.

Table 4. Two-pore parameters, Hi-ANP

	Hi-ANP				
	SHAM 60 min	5 min	15 min	30 min	120 min
Small-pore radius (r_s), Å	45.96 (45.66–46.29)	46.40 (46.37–46.61)	46.84 (46.58–47.07)	46.56 (46.47–46.97)	46.35 (46.02–46.46)
Large-pore radius (r_L), Å	122.36 (116.59–128.37)	146.66‡ (140.01–163.02)	154.72‡ (135.55–172.12)	128.94 (113.59–141.78)	125.78 (128.39–131.78)
$\alpha_L \times 10^5$	4.31 (3.21–5.66)	18.10‡ (9.97–34.07)	18.48‡ (7.96–30.49)	4.69 (3.38–10.4)	7.96* (6.26–13.5)
$J_{ul}/GFR \times 10^5$	6.87 (6.05–8.85)	56.1‡ (29.3–114.2)	58.3‡ (23.8–102.3)	14.3* (9.39–29.5)	22.6‡ (17.7–38.3)
$A_0/\Delta X$, cm/g $\times 10^{-5}$	3.95 (3.70–4.84)	3.39 (3.12–4.19)	3.30 (3.07–4.21)	2.94 (2.48–4.20)	3.86 (3.57–5.12)

Median values are given together with ranges (1st–4th quartile); n = no. of rats. Statistical difference between SHAM and experimental groups: * $P < 0.05$, † $P < 0.01$, ‡ $P < 0.001$.

Rho-kinase inhibitor, influencing the contractile F-actin cytoskeleton in podocytes and endothelial cells. Even though previous studies from this group have indicated that the ultimate sieving barrier to proteins is not at the podocyte slit diaphragm (19, 27), podocyte interactions with the rest of the glomerular filtration barrier seem crucial for its integrity. It is thus speculated that the rapid alterations in glomerular permeability observed in this study may actually be a consequence of actions on podocyte actin dynamics. Endothelial cells may also be involved, in a way similar to how they react to, for example, histamine, substance P, or thrombin, or in anaphylaxis in nonfenestrated endothelium (20, 26). The first permeability peak induced by ANP actually showed a time cycle which is similar to that following massive histamine release in anaphylactic shock (0–30 min) (8).

On podocytes there are ANP binding receptors, which have been localized mostly to the foot processes (32). ANP receptors signal through a family of particulate guanylate cyclases (pGC) (18), which can induce cGMP formation in a dose-dependent fashion (3). The functional consequences of increases in cGMP in podocytes are, however, poorly understood. In undifferentiated rat podocytes, $1 \mu\text{M}$ ANP (3×10^6 ng/ml) produced a decreased intensity of F-actin fluorescence and rearrangements of actin in sparse, parallel bundles (31). This suggests that ANP might produce podocyte relaxation (31). It is thus speculated that such changes in the F-actin cytoskeleton may alter the shape of the podocytes, and hence, the tension they exert on the glomerular basement membrane, thereby affecting glomerular permeability.

In the present study, the Hi-ANP animals showed a clear-cut second steady-state phase of increased glomerular permeability, but in the Lo-ANP group this phase was less evident. However, Lo-ANP animals still seemed to have been moderately affected by ANP over 2 h, because the r_L had actually increased significantly at both 60 ($P < 0.05$) and 120 min ($P < 0.01$) in this group. Therefore, also low concentrations of ANP seemed to have produced sustained alterations in glomerular size selectivity, which may partly explain the microproteinuria occurring in states of plasma volume expansion.

In Hi-ANP ($800 \text{ ng} \cdot \text{kg}^{-1} \cdot \text{min}^{-1}$ of ANP infusion), there was a marked fall in systemic MAP, but despite that, there was a well-maintained GFR. ANP has been shown to be able to stimulate unmyelinated vagal receptors in the myocardium to induce vagal afferent and efferent excitation, leading to reductions in heart rate and contractility (1). In the present animal model, reductions in MAP would normally cause reductions in GFR, but this was completely prevented in the Hi-ANP group. Dunn et al. (13) found in rats infused with $500 \text{ ng} \cdot \text{kg}^{-1} \cdot \text{min}^{-1}$ of ANP that MAP was only moderately affected. In this situation, GFR increased, which resulted from relaxation of the afferent arteriole and a slight contraction of the efferent arteriole by ANP, raising the capillary glomerular pressure. In the present study, any reductions in glomerular capillary pressure seem to have been counteracted by such mechanisms, despite the reduction in MAP. In fact, it has been shown that infusions of human ANP at moderate supraphysiological doses positively affect renal dysfunction (GFR reductions) after complicated cardiac surgery and decreases the probability of dialysis (33), although this is slightly controversial (17). In the Lo-ANP group ($30 \text{ ng} \cdot \text{kg}^{-1} \cdot \text{min}^{-1}$), systemic MAP was not affected, and the intrarenal hemodynamic effects were not large enough

to produce any significant increments in GFR. This is consistent with data of Salazar et al. (30), who found that intrarenal infusion of ANP at a dose of $50 \text{ ng} \cdot \text{kg}^{-1} \cdot \text{min}^{-1}$ in anesthetized dogs did not produce any changes in either GFR or MAP, while the natriuretic effect was similar to that of higher doses of ANP ($300 \text{ ng} \cdot \text{kg}^{-1} \cdot \text{min}^{-1}$). Due to the rather unchanging levels of GFR throughout the study for all animal groups, the experimental conditions in the present experiment, at least during the assessment of glomerular Ficoll sieving curves, should have been similar among the groups.

In the present study, we chose not to assess θ for albumin, because of unexpectedly high levels of free iodine and denatured protein in the radiolabeled albumin preparation (^{125}I -albumin) at our disposal. Especially, the high concentrations of free label yielded abnormally high θ values in tissue uptake studies under control (SHAM) conditions. However, we have previously demonstrated a near-perfect coupling between alterations in θ for high-molecular-weight Ficoll and θ for radiolabeled albumin under conditions of increased permeability (6, 8, 28). Thus, given the high correlation between θ for albumin and θ for Ficoll_{50–80Å}, we considered it quite safe in this study to rely upon the glomerular sieving of high-molecular-weight Ficoll as an indicator of glomerular permeability.

In conclusion, the present study, especially designed to assess θ for large Ficoll molecules, demonstrated a rapid, reversible increase in glomerular permeability for both low-dose and high-dose ANP infusions in rats. A more sustained action of ANP following the initial peak of permeability was especially noted for the high ANP dose. Also, for low ANP concentrations, there were indications of a sustained phase of changes in glomerular selectivity, manifested by an increase in the glomerular r_L . The early permeability peak, especially in Hi-ANP animals, can be explained by an increase in glomerular large pore number and r_L without invoking any changes in glomerular charge selectivity. The actions of ANP on the glomerular filter may be responsible for the microalbuminuria observed in plasma volume overload associated with e.g., congestive heart failure.

ACKNOWLEDGMENTS

The skillful typing of the manuscript by Kerstin Wihlborg is gratefully acknowledged.

GRANTS

This study was supported by Swedish Medical Research Council Grant 08285, the Heart and Lung Foundation, and the Medical Faculty at Lund University (ALF grant).

DISCLOSURES

No conflicts of interest, financial or otherwise, are declared by the authors.

REFERENCES

- Allen DE, Gellai M. Cardioinhibitory effect of atrial peptide in conscious rats. *Am J Physiol Regul Integr Comp Physiol* 252: R610–R616, 1987.
- Almeida FA, Suzuki M, Maack T. Atrial natriuretic factor increases hematocrit and decreases plasma volume in nephrectomized rats. *Life Sci* 39: 1193–1199, 1986.
- Ardaillou N, Lelongt B, Turner N, Piedagnel R, Baudouin B, Estrade S, Cassingena R, Ronco PM. Characterization of a simian virus 40-transformed human podocyte cell line producing type IV collagen and exhibiting polarized response to atrial natriuretic peptide. *J Cell Physiol* 152: 599–616, 1992.

4. Asgeirsson D, Axelsson J, Rippe C, Rippe B. Similarity of permeabilities for Ficoll, pullulan, charge-modified albumin and native albumin across the rat peritoneal membrane. *Acta Physiol (Oxf)* 196: 427–433, 2009.
5. Asgeirsson D, Venturoli D, Rippe B, Rippe C. Increased glomerular permeability to negatively charged Ficoll relative to neutral Ficoll in rats. *Am J Physiol Renal Physiol* 291: F1083–F1089, 2006.
6. Axelsson J, Mahmutovic I, Rippe A, Rippe B. Loss of size selectivity of the glomerular filtration barrier in rats following laparotomy and muscle trauma. *Am J Physiol Renal Physiol* 297: F577–F582, 2009.
7. Axelsson J, Rippe A, Rippe B. Acute hyperglycemia induces rapid, reversible increases in glomerular permeability in nondiabetic rats. *Am J Physiol Renal Physiol* 298: F1306–F1312, 2010.
8. Axelsson J, Rippe A, Venturoli D, Swärd P, Rippe B. Effects of early endotoxemia and dextran-induced anaphylaxis on the size selectivity of the glomerular filtration barrier in rats. *Am J Physiol Renal Physiol* 296: F242–F248, 2009.
9. Brenner BM, Ballermann BJ, Gunning ME, Zeidel ML. Diverse biological actions of atrial natriuretic peptide. *Physiol Rev* 70: 665–699, 1990.
10. Chien YW, Barbee RW, MacPhee AA, Frohlich ED, Trippodo NC. Increased ANF secretion after volume expansion is preserved in rats with heart failure. *Am J Physiol Regul Integr Comp Physiol* 254: R185–R191, 1988.
11. Curry FR. Atrial natriuretic peptide: an essential physiological regulator of transvascular fluid, protein transport, and plasma volume. *J Clin Invest* 115: 1458–1461, 2005.
12. Curry FR, Rygh CB, Karlsen T, Wiig H, Adamson RH, Clark JF, Lin YC, Gassner B, Thorsen F, Moen I, Tenstad O, Kuhn M, Reed RK. Atrial natriuretic peptide modulation of albumin clearance and contrast agent permeability in mouse skeletal muscle and skin: role in regulation of plasma volume. *J Physiol* 588: 325–339, 2010.
13. Dunn BR, Ichikawa I, Pfeffer JM, Troy JL, Brenner BM. Renal and systemic hemodynamic effects of synthetic atrial natriuretic peptide in the anesthetized rat. *Circ Res* 59: 237–246, 1986.
14. Gosling P, Sanghera K, Dickson G. Generalized vascular permeability and pulmonary function in patients following serious trauma. *J Trauma* 36: 477–481, 1994.
15. Gosling P, Hughes EA, Reynolds TM, Fox JP. Microalbuminuria is an early response following acute myocardial infarction. *Eur Heart J* 12: 508–513, 1991.
16. Huxley VH, Tucker VL, Verburg KM, Freeman RH. Increased capillary hydraulic conductivity induced by atrial natriuretic peptide. *Circ Res* 60: 304–307, 1987.
17. Lewis J, Salem MM, Chertow GM, Weisberg LS, McGrew F, Marbury TC, Allgren RL. Atrial natriuretic factor in oliguric acute renal failure. Anaritide Acute Renal Failure Study Group. *Am J Kidney Dis* 36: 767–774, 2000.
18. Lewko B, Stepinski J. Cyclic GMP signaling in podocytes. *Microsc Rev Tech* 57: 232–235, 2002.
19. Lund U, Rippe A, Venturoli D, Tenstad O, Grubb A, Rippe B. Glomerular filtration rate dependence of sieving of albumin and some neutral proteins in rat kidneys. *Am J Physiol Renal Physiol* 284: F1226–F1234, 2003.
20. McDonald DM. Endothelial gaps and permeability of venules in rat tracheas exposed to inflammatory stimuli. *Am J Physiol Lung Cell Mol Physiol* 266: L61–L83, 1994.
21. Nergelius G, Vinge E, Grubb A, Lidgren L. Renal impairment after hip or knee arthroplasty. Urinary excretion of protein markers studied in 59 patients. *Acta Orthop Scand* 68: 34–40, 1997.
22. Nielsen SH, Magid E, Spannow J, Christensen S, Lam HR, Petersen JS. Renal function after myocardial infarction and cardiac arrest in rats: role of ANP-induced albuminuria? *Acta Physiol Scand* 160: 301–310, 1997.
23. Nielsen SH, Petersen JS, Magid E. Albuminuria in ischemic heart disease. *Scand J Clin Lab Invest* 230: 143–152, 1999.
24. Paul RV, Ferguson T, Navar LG. ANF secretion and renal responses to volume expansion with equilibrated blood. *Am J Physiol Renal Fluid Electrolyte Physiol* 255: F936–F943, 1988.
25. Renkin EM, Tucker VL. Atrial natriuretic peptide as a regulator of transvascular fluid balance. *News Physiol Sci* 11: 138–141, 1996.
26. Rippe B, Haraldsson B. Transport of macromolecules across microvascular walls. The two-pore theory. *Physiol Rev* 74: 163–219, 1994.
27. Rippe C, Asgeirsson D, Venturoli D, Rippe A, Rippe B. Effects of glomerular filtration rate on Ficoll sieving coefficients (theta) in rats. *Kidney Int* 69: 1326–1332, 2006.
28. Rippe C, Rippe A, Larsson A, Asgeirsson D, Rippe B. Nature of glomerular capillary permeability changes following acute renal ischemia-reperfusion injury in rats. *Am J Physiol Renal Physiol* 291: F1362–F1368, 2006.
29. Sabrane K, Kruse MN, Fabritz L, Zetsche B, Mitko D, Skryabin BV, Zwiener M, Baba HA, Yanagisawa M, Kuhn M. Vascular endothelium is critically involved in the hypotensive and hypovolemic actions of atrial natriuretic peptide. *J Clin Invest* 115: 1666–1674, 2005.
30. Salazar FJ, Fiksen-Olsen MJ, Oppenorth TJ, Granger JP, Burnett JC Jr, Romero JC. Renal effects of ANP without changes in glomerular filtration rate and blood pressure. *Am J Physiol Renal Fluid Electrolyte Physiol* 251: F532–F536, 1986.
31. Sharma R, Lovell HB, Wiegmann TB, Savin VJ. Vasoactive substances induce cytoskeletal changes in cultured rat glomerular epithelial cells. *J Am Soc Nephrol* 3: 1131–1138, 1992.
32. Shimonaka M, Saheki T, Hagiwara H, Hagiwara Y, Sono H, Hirose S. Visualization of ANP receptor on glomeruli of bovine kidney by use of a specific antiserum. *Am J Physiol Renal Fluid Electrolyte Physiol* 253: F1058–F1062, 1987.
33. Swärd K, Valsö F, Odencrants P, Samuelsson O, Ricksten SE. Recombinant human atrial natriuretic peptide in ischemic acute renal failure: a randomized placebo-controlled trial. *Crit Care Med* 32: 1310–1315, 2004.
34. Tucker VL, Simanok KE, Renkin EM. Tissue-specific effects of physiological ANP infusion on blood-tissue albumin transport. *Am J Physiol Regul Integr Comp Physiol* 263: R945–R953, 1992.

